Characterization of Mammalian Hyaluronidase-2 Activity and Identification of Inhibitors of *Streptococcal* Hyaluronan Lyase

Dissertation

Zur Erlangung des Doktorgrades der Naturwissenschaften (Dr. rer. nat.)

der Fakultät für Chemie und Pharmazie

der Universität Regensburg

vorgelegt von

Janina Hamberger

aus Stephansposching

2012

Die vorliegende Arbeit entstand in der Zeit von April 2008 bis April 2012 unter der Leitung von Herrn Prof. Dr. A. Buschauer und Herrn Prof. Dr. G. Bernhardt am Institut für Pharmazie der Naturwissenschaftlichen Fakultät IV – Chemie und Pharmazie – der Universität Regensburg

Das Promotionsgesuch wurde eingereicht im April 2012

Tag der mündlichen Prüfung: 21.05.2012

Prüfungsausschuss:	Prof. Dr. S. Elz	(Vorsitzender)
	Prof. Dr. A. Buschauer	(Erstgutachter)
	Prof. Dr. G. Bernhardt	(Zweitgutachter)
	Prof. Dr. J. Wegener	(Drittprüfer)

Für Roberto

“Verstehen kann man das Leben nur rückwärts, leben muss man es vorwärts.”

Sören Kierkegaard

Danksagung

An dieser Stelle möchte ich mich bedanken bei:

Herrn Prof. Dr. A. Buschauer für die Gelegenheit an diesem interessanten Projekt arbeiten zu dürfen, seine wissenschaftlichen Anregungen und seine konstruktive Kritik bei der Durchsicht der Arbeit;

Herrn Prof. Dr. G. Bernhardt für seine fachliche Anleitung, seine sehr hilfreichen Anregungen bei experimentellen Problemen und seine konstruktive Kritik bei der Durchsicht der Arbeit;

Herrn Prof. B. Flamion (Universität Namur, Belgien) und seinen Mitarbeitern/-innen für die Bereitstellung der Blutproben von Wildtyp- und Hyal-2 KO- Mäusen und für seine fachlichen Anregungen;

Herrn Prof. Dr. R. Stern, UCSF, für die Bereitstellung des anti Hyal-1 Serums und seine fachlichen Anregungen;

Herrn Prof. Dr. J. Heilmann und seinen Mitarbeitern/-innen für die Bereitstellung der humanen Endothelzellen HMEC-1 und des Kapillarviskosimeters;

Herrn Prof. Dr. A. Göpferich und seinen Mitarbeitern/-innen für die Gelegenheit, Versuche am Lehrstuhl für pharmazeutische Technologie der Universität Regensburg durchführen zu können und die Einführung in die Benutzung der HPLC-Anlage;

Herrn Dr. M. J. Jedrzejas (Children's Hospital Oakland Research Institute, Oakland, USA) für die Bereitstellung der transformierten *E. coli*;

Der Origenis GmbH, Martinsried für die Bereitstellung der Deep-Well-Platten für das Screening;

Herrn C. Textor für die gute Zusammenarbeit, die Expression von *Spn*Hyl im Großmaßstab, die Bereitstellung der Deep-Well-Platten und der Substanz UR-CT-619;

Frau Dr. N. Pop für die Hilfe beim Erlernen der SDS-Page und des Western Blots;

Herrn M. Rothenhöfer für die Durchführung der HPAEC-PAD;

Frau M. Kaske für die Einführung am Durchflußzytometer;

Frau E. Schreiber für die Einführung am Flourimeter;

Frau C. Meyer für die Hilfe bei der Aufreinigung von *Spn*Hyl;

Frau M. Wechler, Frau S. Heinrich, Frau U. Hasselmann, Frau K. Reindl und Herrn P. Richthammer für die Unterstützung bei technischen und organisatorischen Problemen;

meinen Wahlpflichtstudenten Bettina Hafenmair, Dominik Katarzynski und Recep Ünver für ihre engagierte Mitarbeit im Labor;

Julia und Stephanie Söldner für die Durchführung einiger Zytotoxizitätstests;

allen aktuellen und ehemaligen Mitgliedern des Lehrstuhls für die gute Kollegialität, Arbeitsatmosphäre und die schönen Momente auch außerhalb der Universität;

meinen Freunden aus Greifswalder Zeiten Jana, Lars, Carina, Jens, Uta, Arne, Tobi, Julia, Moritz, Franzi, Christiane, Kai, Doro und Matze für die jährlichen Treffen und den Zusammenhalt;

meinen Freunden Judith, Ina, Vroni, Johanna, Anja, Denny, Daniela und Christian für alles;

und insbesondere meinen Eltern und meinen Geschwistern, auf die ich mich immer verlassen kann. Danke!

Poster presentations and short lecture

Poster presentations:

Hamberger J., Howe, Th, Bernhardt G., Buschauer A.; *"Determination of Hyal-2 activity in blood platelets by viscosimetry and polyacrylamide gel electrophoresis"*; Annual meeting of the German Pharmaceutical Society (DPhG), Jena, Germany, September 28 – October 1, 2009

Hamberger J. Onclinx C., Hofinger E., Bernhardt G., Flamion B., Buschauer A.; *"Detection of enzymatic Hyal-2 activity in human and murine platelets"*; 8th International Conference on Hyaluronan, Kyoto, Japan, June 6 – 11, 2010

Hamberger J., Onclinx C., Hofinger E., Bernhardt G., Flamion B., Buschauer A.; *"Hyaluronidase-2 (Hyal-2): Proof of hydrolytic activity"*; 5th Summer School Medicinal Chemistry, University of Regensburg, Germany, September 13 – 15, 2010

Hamberger J., Hofinger E., Onclinx C., Bernhardt G., Flamion B., Buschauer A.; *"Expression, Purification and Characterization of Hyaluronidase-2"*; Frontiers in Medicinal Chemistry, Saarbrücken, Germany, March 20 – 23, 2011

Short lecture:

"Detection of enzymatic Hyal-2 activity in human and murine platelets"

8th International Conference on Hyaluronan, Kyoto, Japan, June 6 – 11, 2010

Contents

List of abbreviations

2-D	two dimensional
η_{rel}	relative viscosity
ν	kinematic viscosity
ADP	adenosine diphosphate
AM-ester	acetoxymethylester
APS	ammonium peroxodisulfate
BCA	2,2‘-biquinoline-4,4‘-dicarboxylic acid
BPB	bromophenol blue
BRCA1	breast cancer susceptibility gene 1
BSA	bovine serum albumin
BTH	bovine testicular hyaluronidase
CD	cluster of differentiation
CTAB	cetyltrimethylammonium bromide
CV	column volume
DMEM	Dulbecco´s Modified Eagle Medium
DMSO	dimethylsulfoxide
DRSP	drug resistant *S. pneumoniae* strains
DS-2	*Drosophila* Schneider-2
DTT	dithiothreitol
EC	endothelial cell
ECL	enhanced chemiluminescence
ECM	extracellular matrix
EDTA	ethylene diamine tetraacetate
ER	estrogen receptor
FACS	fluorescence activated cell sorter

FCS	fetal calf serum
FPLC	fast protein liquid chromatography
GAG	glycosaminoglycan
GPC	gel permeation chromatography
GPI-anchor	glycosylphosphatidylinositol-anchor
HA	hyaluronan
HAS	hyaluronan synthase
HER2	human epidermal growth factor receptor receptor 2
HMW	high molecular weight
HPAEC-PAD	High Performance Anion Exchange Chromatography with pulsed amperometric detection
HRP	horseradish peroxidase
IBD	inflammatory bowel disease
IEF	isoelectric focusing
IgG	immunoglobulin G
IMAC	immobilized metal affinity chromatography
IPG	immobilized pH gel
IPTG	isopropylthiogalactoside
LMW	low molecular weight
MW	molecular weight
MWCO	molecular weight cutoff
NAG	N-acetyl-D-glucosamine
NHE1	Na^+-H^+-exchanger 1
PAGE	polyacrylamide gel electrophoresis
PAR	proteinase activated receptor
PDGF	platelet derived growth factor
pI	isoelectric point

PMP	platelet microparticle
PR	progesterone receptor
PRP	platelet rich plasma
RBC	red blood cells
RHAMM	receptor for hyaluronan mediated motility
ROK	RhoA-binding kinase
RT	room temperature
*Sag*Hyal$_{4755}$	*S. agalactiae* hyaluronate lyase
SDS	sodium dodecyl sulfate
SEM	standard error of the mean
*Spn*Hyl	*S. pneumoniae* hyaluronate lyase
TEMED	N,N,N′,N′-tetramethylethylenediamine
TN	triple-negative
Tris	tris(hydroxymethyl)aminomethane
UV	ultra violet
VEGF	vascular endothelial growth factor

Chapter 1

General Introduction

1.1. Hyaluronan

1.1.1. Structure and physicochemical properties

In 1934 Karl Meyer and his assistant John Palmer were the first to isolate hyaluronic acid from bovine vitreous humor; the name was composed of hyaloid (vitreous) and uronic acid, a component of the molecule (Meyer and Palmer, 1934). Nowadays, the nonsulfated glycosaminoglycan (GAG) is called hyaluronan, respecting the fact that the macromolecule exists as a polyanion *in vivo*, as the carboxyl groups of the glucuronic acid residues ($pK_a = 3 – 4$) are predominantly charged (Hascall and Laurent, 1997).

Hyaluronan was shown to be an acidic, negatively charged, linear polysaccharide consisting of long chains that are made up of disaccharide units comprising *D*-glucuronic acid and *D*-N-acetylglucosamine, linked by alternating ß-1,4 and ß-1,3 glycosidic bonds (Laurent and Fraser, 1992; Weissmann and Meyer, 1954) (**Fig. 1.1**).

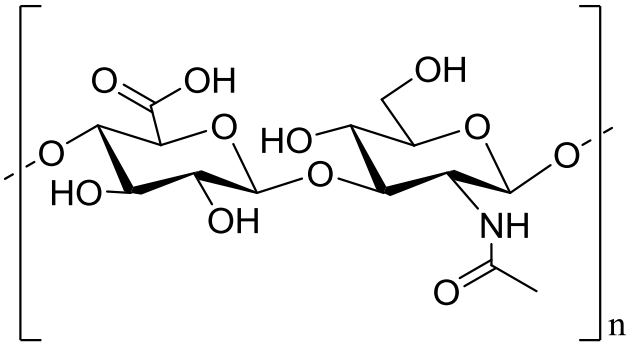

Fig. 1.1: The chemical structure of hyaluronan. The polysaccharide is made up of alternating units of glucuronic acid and N-acetylglucosamine. n= 2000 – 25000.

Usually, the polysaccharide consists of 2000 – 25000 disaccharide units, resulting in molecular masses from $10^6 – 10^7$ Da and lengths of 2 – 25 µm.

In aqueous solution hyaluronan has been considered as a twofold helix, stabilized by internal hydrogen bonds (Atkins et al., 1980; Scott and Heatley, 2002). This conformation was hypothesized to be the basis of tertiary organization in solution. Recent structural work has led to a locally dynamic structure that is on average a contracted fourfold helix in aqueous solution (Almond et al., 2006).

Dissolved hyaluronan chains have been shown to behave like typical semi-flexible polymer molecules (Cowman and Matsuoka, 2005). Therefore, hyaluronan is a space-filling molecule that can undergo deformation as required during rapid growth and tissue remodeling. It can move unhindered into vacant spaces where it can keep cells stationary and give them a substrate on which to move (Almond, 2007).

1.1.2. Occurrence, synthesis and physiological roles

Hyaluronan is present in all vertebrates and in the capsule of some strains of *Streptococci*. It is an essential component of the embryonic extracellular matrix in which cells differentiate and that of mature tissues (Hascall and Laurent, 1997). The highest concentrations of the polysaccharide are found in typical connective tissues e. g. in the skin (7 – 8 g, ca. 50 % of the total hyaluronan in the body), the umbilical cord as well as a constituent of synovial fluid and the vitreous body, but notable amounts are also present in the lung, the heart valves, the kidney, the brain and in muscle (Fraser et al., 1997).

Unlike other extracellular polysaccharides, synthesized in the Golgi apparatus, hyaluronan is produced on the inner face of the plasma membrane by hyaluronan synthases (HAS) and is extruded into the extracellular space. This simultaneous extrusion of the growing chain allows unconstrained polymer growth, thereby achieving the exceptionally large size of the molecule. Currently, three HAS isoforms have been identified in mammals (Weigel et al., 1997) and there is evidence that the chain length depends on the individual HAS protein. While HAS1 and HAS2 catalyze the biosynthesis of chain lengths of up to $2 \cdot 10^6$ Da, the product polymerized by HAS3 is significantly shorter ($< 2 \cdot 10^5 – 1 \cdot 10^6$ Da) (Itano et al., 1999). Hyaluronan chains of different lengths are supposed to exert various effects on cell behavior to be discussed later.

Hyaluronan fulfills several physiological functions that contribute both, to structural tissue properties and to cell behavior during tissue formation and remodeling. Because of its hydrodynamic characteristics in terms of viscosity and the ability to retain water, it plays an important role in tissue homeostasis and biomechanical integrity. These properties form the basis of the widespread use of hyaluronan in tissue engineering (Allison and Grande-Allen, 2006; Toole, 2004). The GAG also forms a multivalent template for interactions with proteoglycans and other extracellular molecules, which is important for the formation of the pericellular coat found for some cell types. During tissue formation and remodeling such matrices provide a hydrated fluid pericellular environment in which assembly of other matrix components and presentation of growth and differentiation factors can readily occur; without interference from the highly structured fibrous matrix usually found in fully differentiated tissues. In some cases, for instance in cartilage, the pericellular matrix is a unique structural component that protects cells and contributes to the characteristic properties of the differentiated tissue (Toole, 2001). Furthermore, hyaluronan interacts with cell surfaces and can mediate intracellular signals through binding to specific

receptors like CD44 or the receptor for hyaluronan mediated motility (RHAMM). The hyaluronan-binding receptors are described in the following section.

In the early response to tissue injury, a temporary matrix rich in hyaluronan and fibrin is formed that supports the influx of fibroblasts and endothelial cells into the wound. The formation of granulation tissue is also supported (Oksala et al., 1995; Weigel et al., 1988; Weigel et al., 1986). Some studies showed that there is a beneficial effect of exogenous hyaluronan applied to chronic wounds (Ortonne, 1996; Vazquez et al., 2003), where tissue damage is one of the consequences of prolonged inflammation mediated by free oxygen radicals and matrix degrading enzymes. Therefore, the formation of granulation tissue is inhibited during these pathological conditions.

Moreover, scarless fetal wound healing has been associated with a prolonged presence of high molecular weight hyaluronan, which led to the suggestions that the polysaccharide may inhibit fetal platelet function and reduce collagen deposition, precluding overshooting scar formation (Longaker et al., 1991; Olutoye et al., 1997).

1.2. Hyaluronan receptors and signalling

There are several cell surface receptors that have been identified for hyaluronan binding, namely CD44, RHAMM, the lymphatic vascular endothelial hyaluronan receptor (LYVE-1), the toll-like receptor 4 (TLR-4) and the human hyaluronan receptor for endocytosis (HARE, also designated Stabilin-2).

CD44, considered as the major receptor for hyaluronan, comprises a group of multifunctional type-I transmembrane glycoproteins, which are all encoded by a highly conserved gene. The heterogeneity of the gene products is due to alternative splicing of multiple variant exons and is in part generated by post-translational modifications (Ponta et al., 2003). All CD44 isoforms contain a hyaluronan-binding site on the link module in their extracellular domain, but binding properties are determined by the isoform and the cell type on which it is expressed (Day and Prestwich, 2002). Through interaction of the intracellular domain of CD44 with cytoskeletal proteins and specific signaling, there is an association between hyaluronan binding and cell behavior (Bourguignon et al., 1998). For example, hyaluronan–CD44 interactions contribute to cell–cell aggregation, matrix–cell and cell–matrix signaling, receptor-mediated degradation/internalization of hyaluronan and retention of the pericellular matrix (Girish and Kemparaju, 2007). Upon hyaluronan

binding the cytoplasmatic domain of CD44 binds to c-Src kinase, which leads to increasing tyrosine phosphorylation of the cytoskeletal protein cortactin which in turn attenuates cross-linking of filamentous actin *in vitro* (Bourguignon et al., 2001). Moreover, CD44 interacts with the membrane linker proteins ezrin/radixin/moesin (ERM) and another member of the membrane-associated cytoskeletal protein family, ankyrin, which promotes hyaluronan-dependent and CD44-specific tumor cell migration (Turley et al., 2002).

RHAMM is also alternatively spliced and is distributed to multiple compartments (mitochondria and the cell nucleus) as well as to the cell surface and to the cytoskeleton. This receptor has been shown to promote cell motility via different pathways. The binding of hyaluronan to RHAMM on the cell surface mediates transient activation of c-Src, focal adhesion kinase (FAK) , the MAP kinases Erk-1 and -2 and protein kinase C (Hall et al., 1994; Turley et al., 2002). Furthermore, hyaluronan-induced increase in cell motility is accompanied by a rapid formation and then disassembly of focal adhesions and spreading of cell lamellae, which is also mediated by binding to cell-surface RHAMM (Hall et al., 1994).

Like CD44, LYVE-1 is a member of the link protein superfamily and is expressed in lymphatic vessels. The role of this receptor has not been elucidated so far. It has been speculated about its involvement in the uptake of hyaluronan for its catabolism or in cell adhesion, either in promoting or blocking the interaction of leukocytes with the endothelium (Jackson, 2004).

Hyaluronan oligosaccharides induce maturation of dentritic cells (DC) via the TLR-4 pathway, where phosphorylation of MAP-kinases and the nuclear translocation of NF-κB take place. TLRs belong to the IL-1 receptor family and participate in the innate defense against bacterial infection through activation of immunocompetent cells like macrophages and DCs (Termeer et al., 2002).

HARE exists in two isoforms and mediates the endocytotic clearance of hyaluronan and other GAGs from lymph and blood. It is highly expressed by the sinusoidal cells of the liver and the endothelial cells of the spleen and the lymph nodes (Zhou et al., 2000). Hyaluronan bound to HARE is internalized and degraded in lysosomes, completing the physiological turnover process described in the next section.

1.3. Hyaluronan turnover

1.3.1. Hyaluronidases

Hyaluronidases are enzymes that degrade hyaluronan for catabolism; to produce small fragments with signaling character or in case of venoms and bacterial hyaluronidases they serve as spreading factor to facilitate distribution in the host. Hyaluronidases have been identified in a number of organisms, such as mammals, bacteria and pathogenic fungi (e. g. *Candida*) and in the venom of snakes, lizards and insects (e. g. bee venom hyaluronidase). The isolated enzymes differ in their substrate specificity, pH optimum and their catalytic mechanism of hyaluronan degradation (Csoka et al., 1997b; Frost et al., 1996; Meyer, 1971).

1.3.1.1. Bacterial hyaluronidases

Many pathogenic bacteria produce hyaluronidases (hyaluronate lyases), which serve as virulence factors. Since hyaluronan is a major constituent of the ground substance of most connective tissues, hyaluronidase may be an essential factor in enabling the spread of the pathogens from an initial site of infection. Moreover, the end products of hyaluronan degradation are disaccharides, which may be internalized and metabolized to supply nutrients for the bacterium (Hynes and Walton, 2000).

The best known and characterized bacterial hyaluronate lyases are those from *Streptococcus agalactiae* and *Streptococcus pneumoniae*, respectively. The degradative process of both enzymes is thought to proceed via a sequential mode initialized by a random cut in the hyaluronan chain. Subsequently, degradation precedes toward the nonreducing end until the whole substrate is degraded by a ß-elimination reaction, resulting in the unsaturated disaccharide 2-acetamido-2-deoxy-3-O-(ß-D-gluco-4-ene-pyranosyluronic acid)-D-glucose (ΔDiHA) (Li et al., 2000; Pritchard et al., 1994) (**Fig. 1.2**).

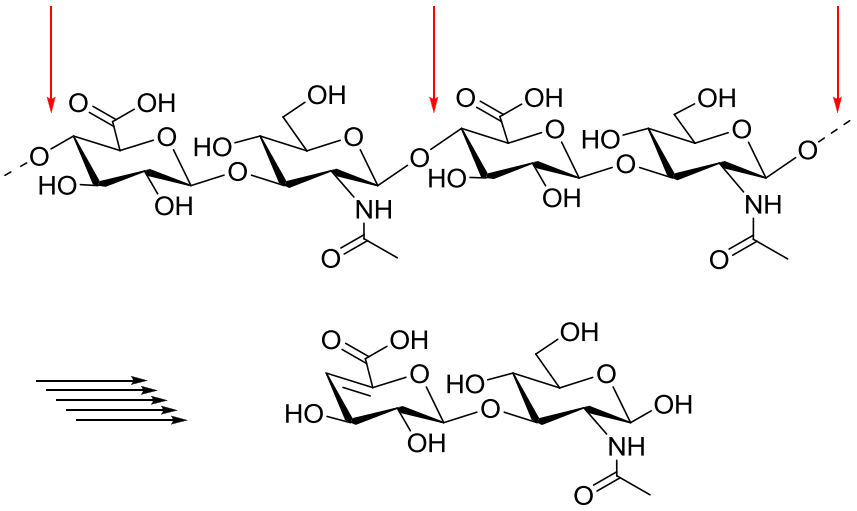

Fig. 1.2: Cleavage of hyaluronan to unsaturated disaccharides by hyaluronate lyase. Red arrows mark bonds which are cleaved.

1.3.1.2. Human Hyaluronidases

There are six hyaluronidase-like sequences with about 40 % identity to each other encoded in the human genome. Those of HYAL1, HYAL2 and HYAL3 are clustered on chromosome 3p21.3, the other three genes encoding HYAL4, PH-20 and HYALP1 on chromosome 7q31.3 (Csoka et al., 2001).

Hyaluronidase-1 (Hyal-1) was first isolated from human plasma and is the predominant hyaluronidase in human plasma and urine. It has also been found at high levels in the kidney, liver, spleen and heart. The enzyme is localized in lysosomes and works at acidic pH (Csoka et al., 1997a; Frost et al., 1997). In addition to its function in normal hyaluronan turnover, Hyal-1 is implicated in cancer cell proliferation, angiogenesis and inflammation. For example, the expression of the enzyme is up-regulated in high grade bladder and prostate cancers (Lokeshwar et al., 2000; Lokeshwar et al., 2001). Presumably, Hyal-1 degrades hyaluronan into angiogenic fragments (see 1.4), which might promote the growth of hyaluronidase overexpressing cancer types. Furthermore, the hereditary disease mucopolysaccharidosis IX, a lysosomal storage disorder, has been associated with inactivating mutations of Hyal-1 (Triggs-Raine et al., 1999).

Besides Hyal-1, hyaluronidase-2 (Hyal-2) is one of the major hyaluronidases in somatic tissues. Hyal-2 has been proposed to act in concert with Hyal-1 in the catabolism of hyaluronan (Stern, 2004), but its enzymatic activity is a matter of controversial discussion, further described in Chapter 3.

Hyaluronidase-3 (Hyal-3) is still a mystery. It is expressed in several tissues, especially in testis and bone marrow (Csoka et al., 1999), but until now, its enzymatic activity or physiological relevance are totally unclear. Recently, a possible role in fertilization was suggested, as Hyal-3 may contribute to acidic hyaluronidase activity in mouse sperm (Reese et al., 2010).

Hyaluronidase-4 was shown to display only chondroitinase, not hyaluronidase activity (Kaneiwa et al., 2010).

PH-20, also known as SPAM 1 (spam adhesion molecule 1) is located on the membrane, bound to a GPI-anchor and in the lysosome-derived acrosome of mammalian sperm and plays an important role during fertilization. It degrades the hyaluronan-enriched cumulus of the oocyte during sperm penetration and then serves as receptor for the sperm binding to the zona pellucida inducing hyaluronan-associated sperm signaling (Cherr et al., 2001; Lin et al., 1994; Primakoff et al., 1985). Membrane-bound PH-20 shows hyaluronidase activity only at neutral pH, whereas acrosomal PH-20 was found to be active at both acidic and neutral pH. These different activities appear to involve two different domains of the protein; acidic hyaluronidase activity may be evoked after the acrosome reaction, where the enzyme is endoproteolytically cleaved, but held together by a disulfide bond. This cleavage may alter the three-dimensional structure of PH-20 resulting in an activation of the domain responsible for activity at acidic pH (Cherr et al., 2001).

HYALP1 is a pseudogene and does not encode for an active enzyme in humans.

1.3.2. Model of hyaluronan turnover

It is estimated that 5 g out of 15 g of hyaluronan in a 70 kg individual are replaced daily. Turnover rates vary widely between tissues; the half-life of the macromolecule is about 1 day in the skin and 1–3 weeks in relatively inert cartilage (Stern, 2003). In the blood stream, the turnover of hyaluronan is very rapid with a half life of 2–5 min (Fraser et al., 1981).

However, the catabolic pathways responsible for the clearance of hyaluronan have not been elucidated completely until now. CD44 is known to bind hyaluronan and it is also thought to contribute to internalization of the polysaccharide (Culty et al., 1992; Hua et al., 1993; Kaya et al., 1997), but the molecular mechanisms of endocytosis are largely unknown. However, it is likely that high molecular weight hyaluronan is tethered to the

cell surface by CD44 and that it is degraded by membrane-bound Hyal-2 to a certain extent. This could take place in specialized microdomains, so-called caveolae. The truncated hyaluronan chains may then be internalized, delivered to endosomes and ultimately to lysosomes, where they are degraded by Hyal-1, and the lysosomal exoglycosidases ß-glucuronidase and ß-N-acetylglucosaminidase to the final catabolism products (Stern, 2004). The possible metabolic scheme is depicted in **Fig. 1.3**.

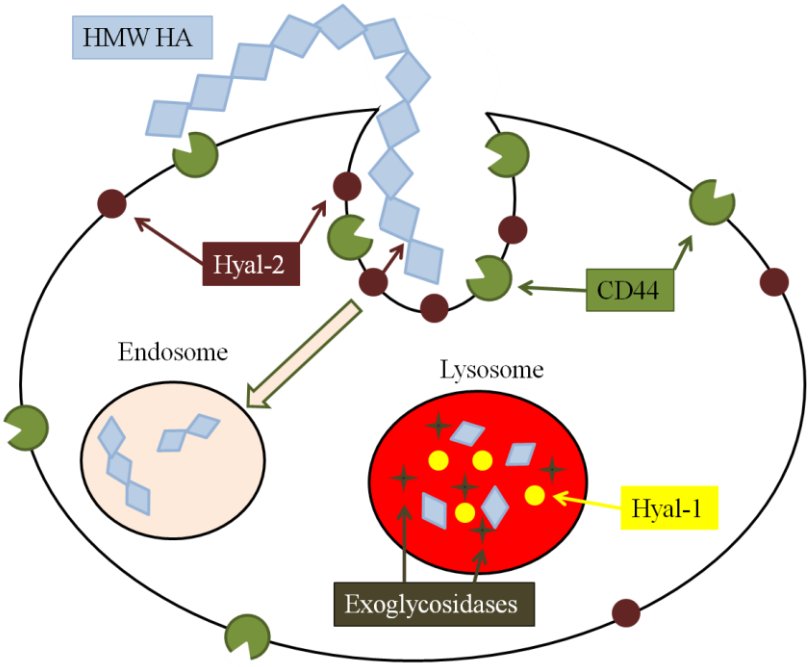

Fig. 1.3: Possible metabolic scheme of hyaluronan degradation through concerted action of CD44, Hyal-2 and Hyal-1. Modified from Csoka et al. (2001).

1.4. Size-dependent functions of hyaluronan fragments

Hyaluronan chains of different lengths resulting from HAS-catalyzed synthesis and degradation by hyaluronidase, respectively, show very different biological functions. High (HMW) and low (LMW) molecular weight chains seem to have opposing cellular effects. The extracellular HMW polysaccharides inhibit angiogenesis (Feinberg and Beebe, 1983) and also show anti-inflammatory and immune-suppressive effects (Delmage et al., 1986; McBride and Bard, 1979). LMW hyaluronan fragments are involved in a number of physiological and pathophysiological processes, like induction of inflammatory cytokines, angiogenesis and tumor cell migration. During the inflammatory stage of wound healing, LMW hyaluronan, having a polydisperse mass distribution with an average around $2.5 \cdot 10^5$ Da, accumulates and induces the expression of inflammatory cytokines in monocytes, such as macrophage inflammatory protein 1 alpha (MIP-1 alpha), MIP-1 beta, IL-12, IL-1

beta, tumor necrosis factor alpha (TNF-α) and insulin-like growth factor-1 (IGF-1) (Hodge-Dufour et al., 1997; Horton et al., 1998; Noble et al., 1993). Moreover, LMW fragments with a size of 8–32 disaccharide units were shown to stimulate angiogenesis by enhancing endothelial cell migration and induction of multiple signaling pathways (Sattar et al., 1994; Slevin et al., 2002). LMW hyaluronan fragments are also found in cancers, where tumor cell motility and invasion are facilitated. For example, highly invasive bladder cancers produce angiogenic hyaluronan fragments, which may contribute to the invasiveness (Stern et al., 2006).

1.5. References

Allison, D.D., Grande-Allen, K.J., 2006. Review. Hyaluronan: A powerful tissue engineering tool. Tissue Eng. 12, 2131-2140.

Almond, A., 2007. Hyaluronan. Cell. Mol. Life Sci. 64, 1591-1596.

Almond, A., Deangelis, P.L., Blundell, C.D., 2006. Hyaluronan: the local solution conformation determined by NMR and computer modeling is close to a contracted left-handed 4-fold helix. J. Mol. Biol. 358, 1256-1269.

Atkins, E.D.T., Meader, D., Scott, J.E., 1980. Model for Hyaluronic-Acid Incorporating 4 Intramolecular Hydrogen-Bonds. Int. J. Biol. Macromol. 2, 318-319.

Bourguignon, L.Y., Zhu, D., Zhu, H., 1998. CD44 isoform-cytoskeleton interaction in oncogenic signaling and tumor progression. Front. Biosci. 3, d637-649.

Bourguignon, L.Y., Zhu, H., Shao, L., Chen, Y.W., 2001. CD44 interaction with c-Src kinase promotes cortactin-mediated cytoskeleton function and hyaluronic acid-dependent ovarian tumor cell migration. J. Biol. Chem. 276, 7327-7336.

Cherr, G.N., Yudin, A.I., Overstreet, J.W., 2001. The dual functions of GPI-anchored PH-20: hyaluronidase and intracellular signaling. Matrix Biol. 20, 515-525.

Cowman, M.K., Matsuoka, S., 2005. Experimental approaches to hyaluronan structure. Carbohydr. Res. 340, 791-809.

Csoka, A.B., Frost, G.I., Stern, R., 2001. The six hyaluronidase-like genes in the human and mouse genomes. Matrix Biol. 20, 499-508.

Csoka, A.B., Frost, G.I., Wong, T., Stern, R., 1997a. Purification and microsequencing of hyaluronidase isozymes from human urine. FEBS Lett. 417, 307-310.

Csoka, A.B., Scherer, S.W., Stern, R., 1999. Expression analysis of six paralogous human hyaluronidase genes clustered on chromosomes 3p21 and 7q31. Genomics 60, 356-361.

Csoka, T.B., Frost, G.I., Stern, R., 1997b. Hyaluronidases in tissue invasion. Invasion Metastasis 17, 297-311.

Culty, M., Nguyen, H.A., Underhill, C.B., 1992. The hyaluronan receptor (CD44) participates in the uptake and degradation of hyaluronan. J. Cell Biol. 116, 1055-1062.

Day, A.J., Prestwich, G.D., 2002. Hyaluronan-binding proteins: tying up the giant. J. Biol. Chem. 277, 4585-4588.

Delmage, J.M., Powars, D.R., Jaynes, P.K., Allerton, S.E., 1986. The selective suppression of immunogenicity by hyaluronic acid. Ann. Clin. Lab. Sci. 16, 303-310.

Feinberg, R.N., Beebe, D.C., 1983. Hyaluronate in vasculogenesis. Science 220, 1177-1179.

Fraser, J.R., Laurent, T.C., Pertoft, H., Baxter, E., 1981. Plasma clearance, tissue distribution and metabolism of hyaluronic acid injected intravenously in the rabbit. Biochem. J. 200, 415-424.

Fraser, J.R.E., Laurent, T.C., Laurent, U.B.G., 1997. Hyaluronan: its nature, distribution, functions and turnover. J. Intern. Med. 242, 27-33.

Frost, G.I., Csoka, A.B., Stern, R., 1996. The Hyaluronidases: A Chemical, Biological and Clinical Overview. Trends Glycosci Glycotechnol 8, 419-434.

Frost, G.I., Csoka, T.B., Wong, T., Stern, R., 1997. Purification, cloning, and expression of human plasma hyaluronidase. Biochem. Biophys. Res. Commun. 236, 10-15.

Girish, K.S., Kemparaju, K., 2007. The magic glue hyaluronan and its eraser hyaluronidase: a biological overview. Life Sci. 80, 1921-1943.

Hall, C.L., Wang, C., Lange, L.A., Turley, E.A., 1994. Hyaluronan and the hyaluronan receptor RHAMM promote focal adhesion turnover and transient tyrosine kinase activity. J. Cell Biol. 126, 575-588.

Hascall, V.C., Laurent, T.C., 1997. Hyaluronan: structure and physical properties. http://www.glycoforum.gr.jp/science/hyaluronan/HA01/HA01E.html.

Hodge-Dufour, J., Noble, P.W., Horton, M.R., Bao, C., Wysoka, M., Burdick, M.D., Strieter, R.M., Trinchieri, G., Pure, E., 1997. Induction of IL-12 and chemokines by hyaluronan requires adhesion-dependent priming of resident but not elicited macrophages. J. Immunol. 159, 2492-2500.

Horton, M.R., Burdick, M.D., Strieter, R.M., Bao, C., Noble, P.W., 1998. Regulation of hyaluronan-induced chemokine gene expression by IL-10 and IFN-gamma in mouse macrophages. J. Immunol. 160, 3023-3030.

Hua, Q., Knudson, C.B., Knudson, W., 1993. Internalization of hyaluronan by chondrocytes occurs via receptor-mediated endocytosis. J. Cell Sci. 106 (Pt 1), 365-375.

Hynes, W.L., Walton, S.L., 2000. Hyaluronidases of Gram-positive bacteria. FEMS Microbiol. Lett. 183, 201-207.

Itano, N., Sawai, T., Yoshida, M., Lenas, P., Yamada, Y., Imagawa, M., Shinomura, T., Hamaguchi, M., Yoshida, Y., Ohnuki, Y., Miyauchi, S., Spicer, A.P., McDonald, J.A.,

Kimata, K., 1999. Three isoforms of mammalian hyaluronan synthases have distinct enzymatic properties. J Biol Chem 274, 25085-25092.

Jackson, D.G., 2004. The Lymphatic Endothelial Hyaluronan Receptor LYVE-1. http://www.glycoforum.gr.jp/science/hyaluronan/HA28/HA28E.html.

Kaneiwa, T., Mizumoto, S., Sugahara, K., Yamada, S., 2010. Identification of human hyaluronidase-4 as a novel chondroitin sulfate hydrolase that preferentially cleaves the galactosaminidic linkage in the trisulfated tetrasaccharide sequence. Glycobiology 20, 300-309.

Kaya, G., Rodriguez, I., Jorcano, J.L., Vassalli, P., Stamenkovic, I., 1997. Selective suppression of CD44 in keratinocytes of mice bearing an antisense CD44 transgene driven by a tissue-specific promoter disrupts hyaluronate metabolism in the skin and impairs keratinocyte proliferation. Genes Dev. 11, 996-1007.

Laurent, T.C., Fraser, J.R., 1992. Hyaluronan. FASEB J. 6, 2397-2404.

Li, S., Kelly, S.J., Lamani, E., Ferraroni, M., Jedrzejas, M.J., 2000. Structural basis of hyaluronan degradation by Streptococcus pneumoniae hyaluronate lyase. EMBO J. 19, 1228-1240.

Lin, Y., Mahan, K., Lathrop, W.F., Myles, D.G., Primakoff, P., 1994. A hyaluronidase activity of the sperm plasma membrane protein PH-20 enables sperm to penetrate the cumulus cell layer surrounding the egg. J. Cell Biol. 125, 1157-1163.

Lokeshwar, V.B., Obek, C., Pham, H.T., Wei, D., Young, M.J., Duncan, R.C., Soloway, M.S., Block, N.L., 2000. Urinary hyaluronic acid and hyaluronidase: markers for bladder cancer detection and evaluation of grade. J. Urol. 163, 348-356.

Lokeshwar, V.B., Rubinowicz, D., Schroeder, G.L., Forgacs, E., Minna, J.D., Block, N.L., Nadji, M., Lokeshwar, B.L., 2001. Stromal and epithelial expression of tumor markers hyaluronic acid and HYAL1 hyaluronidase in prostate cancer. J. Biol. Chem. 276, 11922-11932.

Longaker, M.T., Chiu, E.S., Adzick, N.S., Stern, M., Harrison, M.R., Stern, R., 1991. Studies in fetal wound healing. V. A prolonged presence of hyaluronic acid characterizes fetal wound fluid. Ann. Surg. 213, 292-296.

McBride, W.H., Bard, J.B., 1979. Hyaluronidase-sensitive halos around adherent cells. Their role in blocking lymphocyte-mediated cytolysis. J. Exp. Med. 149, 507-515.

Meyer, K., 1971. Hyaluronidases, in: Boyer, P.D. (Ed.), The Enzymes. Academic Press, New York, pp. 307-320.

Meyer, K., Palmer, J.W., 1934. The Polysaccharide of the Vitreous Humor. J. Biol. Chem. 107, 629-634.

Noble, P.W., Lake, F.R., Henson, P.M., Riches, D.W., 1993. Hyaluronate activation of CD44 induces insulin-like growth factor-1 expression by a tumor necrosis factor-alpha-dependent mechanism in murine macrophages. J. Clin. Invest. 91, 2368-2377.

Oksala, O., Salo, T., Tammi, R., Hakkinen, L., Jalkanen, M., Inki, P., Larjava, H., 1995. Expression of proteoglycans and hyaluronan during wound healing. J. Histochem. Cytochem. 43, 125-135.

Olutoye, O.O., Barone, E.J., Yager, D.R., Uchida, T., Cohen, I.K., Diegelmann, R.F., 1997. Hyaluronic acid inhibits fetal platelet function: implications in scarless healing. J. Pediatr. Surg. 32, 1037-1040.

Ortonne, J., 1996. A controlled study of the activity of hyaluronic acid in the treatment of venous leg ulcers. Journal of Dermatological Treatment 7, 75-81.

Ponta, H., Sherman, L., Herrlich, P.A., 2003. CD44: from adhesion molecules to signalling regulators. Nat. Rev. Mol. Cell Biol. 4, 33-45.

Primakoff, P., Hyatt, H., Myles, D.G., 1985. A role for the migrating sperm surface antigen PH-20 in guinea pig sperm binding to the egg zona pellucida. J. Cell Biol. 101, 2239-2244.

Pritchard, D.G., Lin, B., Willingham, T.R., Baker, J.R., 1994. Characterization of the Group B Streptococcal Hyaluronate Lyase. Arch. Biochem. Biophys. 315, 431-437.

Reese, K.L., Aravindan, R.G., Griffiths, G.S., Shao, M., Wang, Y., Galileo, D.S., Atmuri, V., Triggs-Raine, B.L., Martin-Deleon, P.A., 2010. Acidic hyaluronidase activity is present in mouse sperm and is reduced in the absence of SPAM1: evidence for a role for hyaluronidase 3 in mouse and human sperm. Mol. Reprod. Dev. 77, 759-772.

Sattar, A., Rooney, P., Kumar, S., Pye, D., West, D.C., Scott, I., Ledger, P., 1994. Application of angiogenic oligosaccharides of hyaluronan increases blood vessel numbers in rat skin. J. Invest. Dermatol. 103, 576-579.

Scott, J.E., Heatley, F., 2002. Biological properties of hyaluronan in aqueous solution are controlled and sequestered by reversible tertiary structures, defined by NMR spectroscopy. Biomacromolecules 3, 547-553.

Slevin, M., Kumar, S., Gaffney, J., 2002. Angiogenic oligosaccharides of hyaluronan induce multiple signaling pathways affecting vascular endothelial cell mitogenic and wound healing responses. J. Biol. Chem. 277, 41046-41059.

Stern, R., 2003. Devising a pathway for hyaluronan catabolism: are we there yet? Glycobiology 13, 105R-115R.

Stern, R., 2004. Hyaluronan catabolism: a new metabolic pathway. Eur. J. Cell Biol. 83, 317-325.

Stern, R., Asari, A.A., Sugahara, K.N., 2006. Hyaluronan fragments: an information-rich system. Eur. J. Cell Biol. 85, 699-715.

Termeer, C., Benedix, F., Sleeman, J., Fieber, C., Voith, U., Ahrens, T., Miyake, K., Freudenberg, M., Galanos, C., Simon, J.C., 2002. Oligosaccharides of Hyaluronan activate dendritic cells via toll-like receptor 4. J. Exp. Med. 195, 99-111.

Toole, B.P., 2001. Hyaluronan in morphogenesis. Semin. Cell Dev. Biol. 12, 79-87.

Toole, B.P., 2004. Hyaluronan: from extracellular glue to pericellular cue. Nat. Rev. Cancer 4, 528-539.

Triggs-Raine, B., Salo, T.J., Zhang, H., Wicklow, B.A., Natowicz, M.R., 1999. Mutations in HYAL1, a member of a tandemly distributed multigene family encoding disparate hyaluronidase activities, cause a newly described lysosomal disorder, mucopolysaccharidosis IX. Proc. Natl. Acad. Sci. U. S. A. 96, 6296-6300.

Turley, E.A., Noble, P.W., Bourguignon, L.Y., 2002. Signaling properties of hyaluronan receptors. J. Biol. Chem. 277, 4589-4592.

Vazquez, J.R., Short, B., Findlow, A.H., Nixon, B.P., Boulton, A.J.M., Armstrong, D.G., 2003. Outcomes of hyaluronan therapy in diabetic foot wounds. Diabetes Res. Clin. Pract. 59, 123-127.

Weigel, P.H., Frost, S.J., McGary, C.T., LeBoeuf, R.D., 1988. The role of hyaluronic acid in inflammation and wound healing. Int. J. Tissue React. 10, 355-365.

Weigel, P.H., Fuller, G.M., Leboeuf, R.D., 1986. A Model for the Role of Hyaluronic-Acid and Fibrin in the Early Events during the Inflammatory Response and Wound-Healing. J. Theor. Biol. 119, 219-234.

Weigel, P.H., Hascall, V.C., Tammi, M., 1997. Hyaluronan synthases. J Biol Chem 272, 13997-14000.

Weissmann, B., Meyer, K., 1954. The Structure of Hyalobiuronic Acid and of Hyaluronic Acid from Umbilical Cord1,2. J. Am. Chem. Soc. 76, 1753-1757.

Zhou, B., Weigel, J.A., Fauss, L., Weigel, P.H., 2000. Identification of the hyaluronan receptor for endocytosis (HARE). J. Biol. Chem. 275, 37733-37741.

Chapter 2

Scope and objectives

Hyaluronan and its catabolic products are increasingly gaining attention with respect to embryonic development, cell biology, oncology and immunology. For a more detailed insight into the pathways of hyaluronan catabolism, the enzymological characterization of the individual hyaluronidases is a prerequisite. Particularly, the enzymatic activity of hyaluronidase-2 is still a matter of controversial discussion. Recently, hyaluronidases 1 and 2 were suggested to be the major hyaluronidases in somatic tissues and to act in concert in the degradation of hyaluronan. However, supposed that Hyal-2 plays a crucial role in the turnover of hyaluronan, enzymatic activity is a prerequisite. Therefore, the major goal of this thesis was to prove that Hyal-2 is a catalytically active protein, and to explore its biological role in platelets and red blood cells.

The first part of this thesis aimed at the investigation of the enzymatic activity of Hyal-2, using a purified recombinant enzyme expressed in insect cells, and native enzyme expressed by blood platelets and red blood cells. Viscosimetry was previously shown to be the most sensitive method to show hyaluronan degrading activity, compared to other conventional hyaluronidase assays, such as turbidimetry and the Morgan-Elson reaction. Additionally, an electrophoretic method had to be established and optimized to allow the determination of the size distribution of possibly formed hyaluronan fragments. Moreover, proliferation studies with human endothelial cells were intended in order to investigate, if Hyal-2 is able to produce signalling hyaluronan fragments.

The design and synthesis of hyaluronidase inhibitors is subject of several doctoral projects pursued in parallel with the present work. Hyaluronidases represent a heterogeneous group of enzymes of different origin. For example, pathogenic strains of *Streptococci* produce hyaluronate lyases, which have been suggested virulence factors. *S. pneumoniae*, a bacterial respiratory pathogen, produces such a hyaluronate lyase (*Spn*Hyl). Hence, another goal of this thesis was to find drug-like small molecules as lead structures of inhibitors of *Spn*Hyl, which might be useful as adjuvants in antibiotic therapy.

Consequently, a library of small molecules, prepared by multicomponent reactions, was provided by Christian Textor, to be screened in a turbidimetric assay in order to investigate inhibitory activities on *Spn*Hyl. For this purpose, the enzyme had to be expressed in *E. coli* strain BL21 (DE 3).

Chapter 3

Expression, purification and characterization of recombinant human Hyal-2

3.1. Introduction

The m-RNA of Hyaluronidase-2 (Hyal-2), also termed LUCA-2, has been found in many somatic tissues except the adult brain. It was initially described as an enzyme, which is active at acidic pH and located in lysosomes (Lepperdinger et al., 1998). However, Hyal-2 is still not characterized very well and the few publications dealing with its localization and activity have been rather contradictory.

Several authors published that Hyal-2 is a protein, which is bound to the cell membrane via a glycosylphosphatidylinositol (GPI) anchor (Miller, 2003; Mullegger and Lepperdinger, 2002; Rai et al., 2001). In other publications a lysosomal localization is proposed (Chow et al., 2006a, b; Lepperdinger et al., 1998). To explain the different findings, Chow et al. speculated about a primary localization of Hyal-2 in lysosomes with a fraction being transferred to the cell membrane (Chow et al., 2006b), whereas Lepperdinger et al. suggested that Hyal-2 is transported to lysosomes via secretion and re-uptake at the plasma membrane (Lepperdinger et al., 2001).

The comparison of publications regarding catalytic activity of Hyal-2 raises even more questions. Lepperdinger et al. were the first who reported that Hyal-2 is enzymatically active at pH 3.8 and that substrate degradation stops with fragments of a molecular weight of approximately 20 kDa (Lepperdinger et al., 1998). Thereby, Hyal-2 was expressed by means of a recombinant vaccinia virus containing human Hyal-2 cDNA in C6 glioma cells. By contrast, Rai et al. could not detect any hyaluronidase activity using HEK293 cells transfected with human Hyal-2 (Rai et al., 2001). Moreover, Vigdorovich et al. investigated a soluble form of Hyal-2 (sHyal-2) and reported on enzymatic activity at a broad pH range from 4.5 – 8.6 (Vigdorovich et al., 2005). However, this activity was found to be due to a contaminating hyaluronidase present in the used expression system. A re-investigation with purified sHyal-2 revealed little hyaluronidase activity at pH 5.6 (Vigdorovich et al., 2007).

Hyal-2 has been supposed to have different physiological roles. It serves as cell entry receptor for the Jaagsiekte sheep retro virus (JSRV) (Miller, 2003; Rai et al., 2001) and is therefore responsible for the strong oncogenic potential of the retrovirus. Furthermore, this hyaluronidase has been proposed to act in concert with Hyal-1 in the catabolism of hyaluronan in the ECM (Csoka et al., 2001). It also plays a role in HA fragmentation in the airway lumen in inflammatory conditions associated with oxidative stress (Monzon et al.). Aside from these functions, Duterme et al. found a relation between Hyal-2 expression and

the formation of the glycocalyx and a regulation of CD44-ERM interactions by Hyal-2 (Duterme et al., 2009).

E. Hofinger transfected *Drosophila* Schneider-2 cells (DS-2) with His-tagged recombinant human Hyal-2 (rhHyal-2) (Hofinger, 2007). DS-2 cells are a suitable expression system for hyaluronidases because of the absence of hyaluronan (Toyoda et al., 2000) and hyaluronidase-like genes. By these stably transfected DS-2 cells rhHyal-2 was excreted into the medium as a soluble protein and purified by Ni-IMAC or a simplified purification protocol. In this work, purified Hyal-2 was characterized with respect to catalytic activity and supplied to a cooperation partner for antibody production.

3.2. Materials and methods

3.2.1. Cultivation and storage of stably transfected DS-2/pMTHygro/Hyal-2 cells

DS-2/pMTHygro/Hyal-2 cells were grown in serum-free Insect-XPRESS™ medium (Lonza Cologne AG, Cologne, Germany) containing 300 µg/mL hygromycin B (A.G. Scientific Inc., San Diego, USA) at 27 °C. For sub-culturing, adherent cells were grown in 25-cm² culture flasks (Sarstedt, Nürnbrecht, Germany) and serially passaged every 4 – 5 days. Confluent cells were removed from the bottom of the culture flask by tapping, and the suspension was diluted 5 – 6 fold with fresh medium.

For long term storage, cells were grown to a density of $1 – 2 \cdot 10^7$ cells per mL and centrifuged at 1000 g for 3 min at 4 °C. Cells were re-suspended in the same volume of sterile PBS and centrifuged again. After re-suspension in the same volume of freezing medium (45 % fresh medium, 45 % conditioned medium, 10 % DMSO), the cell suspension was split into aliquots of 1 mL and cooled down slowly for the storage in liquid nitrogen. For revival an aliquot of frozen cells was quickly thawed and diluted 5 – 6 fold with fresh medium. After attachment of the cells to the bottom of the culture flask, medium was exchanged with fresh medium to remove residual DMSO.

3.2.2. Expression of rhHyal-2 in DS-2 cells

For expression of His-tagged rhHyal-2, suspension cultures with initially $1 – 2 \cdot 10^6$ of DS-2/pMTHygro/Hyal-2 cells per mL in Insect-XPRESS™ medium supplemented with 300 µg/mL hygromycin were used and shaken at 135 rpm at 27 °C for 10 days. Cells were then harvested by centrifugation at 1500 g for 15 min at 4 °C. The medium was used for isolation of rhHyal-2.

3.2.3. Isolation and purification of rhHyal-2 by Ni-IMAC

Imidazole and triton X-100 were added to the collected rhHyal-2 containing cell culture medium at a final concentration of 20 mM and 0.1 %, respectively, and the pH was carefully adjusted to 7.4. After the solution was clarified by centrifugation at 8000 g for 30 min at 4 °C, the sample was loaded onto a HisTrap™ HP Ni-IMAC column (column volume (CV) 5 mL, GE Healthcare, Munich, Germany). Before loading the sample, the column was equilibrated with binding buffer (20 mM Na_2HPO_4, 0.5 M NaCl, 20 mM imidazole, 0.1 % Triton X-100, pH 7.4). After washing with 15 CV of binding buffer, the

immobilized His-tagged Protein was eluted with 10 CV of elution buffer (20 mM Na_2HPO_4, 0.5 M NaCl, 0.5 M imidazole, 0.1 % triton X-100, pH 7.4). Protein purification was performed with an ÄKTA FPLC device with a Frac-950 fraction collector using UNICORN™ v5.10 software (GE Healthcare Bio-Sciences AB, Uppsala, Sweden) at a flow rate of 5 mL/min and a pressure limit of 0.3 MPa. The chromatography was monitored by UV detection at 280 nm. The protein content of the collected elution fractions (6 mL) was determined using the BCA assay and plotted against the respective elution volume. Then, the elution fractions were pooled, dialyzed against 0.1 M ammonium acetate and lyophilized.

3.2.4. Bicinchoninic acid (BCA) protein assay

For the determination of the protein content using the BCA assay, three stock solutions were prepared. Reagent A: 4.0 g Na_2CO_3, 0.8 g NaOH and 0.08 g K-Na-tartrate were dissolved in 50 mL of water and the pH was adjusted to 11.25; reagent B: 1.0 g of BCA was dissolved in 25 mL of water; reagent C: 4 % $CuSO_4$ x 5 H_2O in water. For preparation of the working solution 1 volume of reagent C was mixed with 25 volumes of reagent B and 26 volumes of reagent C. A BSA standard curve from 5 – 200 µg/mL was prepared from a 1 mg/mL stock solution (BSA in elution buffer). 70 µL of working solution were added to 70 µL of sample or standard and incubated in a 96-well microtiter plate for 1 h at 60 °C. After cooling, the absorbance at 540 nm was measured using a Tecan Genios Pro microtiter plate reader (Tecan, Crailsheim, Germany) with XFluor Genios Pro software version V.4.55. The standard curve was plotted as absorbance versus µg/mL of BSA and the protein concentration of the samples was determined.

3.2.5. Simplified purification protocol for rhHyal-2

To simplify the purification procedure, Ni Sepharose™ 6 FF (GE Healthcare, Munich, Germany) was used and the purification was performed according to the manufacturer´s instructions for gravity-flow purification with minimal changes. In brief, 2 mL of Ni Sepharose slurry were sedimented by centrifugation at 1000 g for 3 min and then washed with 5 mL of Millipore water. After gentle shaking for 30 min and centrifugation, the water was discarded and replaced with 5 mL of binding buffer (20 mM Na_2HPO_4, 0.5 M NaCl, 20 mM imidazole, pH 7.4). The shaking and centrifugation procedure was repeated, subsequently a 50 % slurry of Ni Sepharose and binding buffer was made and allowed to

equilibrate for 5 min. 4 mL of clarified DS-2/pMTHygro/Hyal-2 medium, containing 20 mM imidazole were added per mL of slurry and the resulting loading suspension was gently shaken for 1 h at RT. The incubated loading suspension was transferred to empty gravity flow columns and washed 3 times with 2 mL of binding buffer. Bound protein was detached from the chromatography material with 2 mL of elution buffer (20 mM Na_2HPO_4, 0.5 M NaCl, 0.5 M imidazole) added in four 0.5 mL portions. A buffer exchange of the elution fractions was achieved with PD-10 columns (Sigma-Aldrich, Munich, Germany) using 0.1 M ammonium acetate. Samples were lyophilized, and their protein content was determined. Purity of the received protein was controlled by SDS-PAGE.

3.2.6. SDS-Polyacrylamide gel electrophoresis

Proteins were analyzed by sodium dodecyl sulfate polyacrylamide gel electrophoresis (SDS-PAGE) under reducing conditions. The composition of all required buffers is summarized in **Tab. 3.1**. 12 % polyacrylamide separating gels contained 2.2 mL of water, 2 mL of buffer A and 3.2 mL of acrylamide/bisacrylamide 30 % solution (acrylamide/bisacrylamide 29/1; Sigma-Aldrich, Munich, Germany). Polymerization was initiated by adding 3.5 µL N,N,N′,N′-tetramethylethylenediamine (TEMED, Serva, Heidelberg, Germany) and 35 µL of ammonium peroxodisulfate (APS, 10 % solution in water, Serva, Heidelberg, Germany). The mixture was filled into gel chambers (10 x 10 x 0.8 cm) and overlaid with water saturated isobutyl alcohol. After complete polymerization, the isobutyl alcohol layer was discarded and a 5 % stacking gel was casted. The stacking gel contained 3.25 mL of water, 1.25 mL of buffer B and 0.5 mL of acrylamide/bisacrylamide 30 % solution. 3.5 µL of TEMED and 50 µL of APS were added to start polymerization. Electrophoresis was performed in a PerfectBlue gel electrophoresis system Twin S (Peqlab, Erlangen, Germany) with the electrode chambers filled with 1 x running buffer at 150 V for approximately 2 h. Protein samples were mixed with a one-third volume of sample buffer and heated for 5 min at 100 °C.

Tab. 3.1: Composition of buffers for SDS-PAGE.

Buffer and additives	Buffer A	Buffer B	Running buffer 10 x	Sample buffer
Tris (M)	1.5	0.5	0.25	0.075

Glycin (M)	-	-	2	0.5
SDS (%, m/v)	0.4	0.4	1	0.3
Glycerol (%, v/v)	-	-	-	4.5
Bromophenol blue (%, m/v)	-	-	-	0.05
Mercaptoethanol (%, v/v)	-	-	-	1
pH	8.8	6.8	8.3	6.8

3.2.7. Western Blot analysis

After SDS-PAGE, the proteins were transferred to a nitrocellulose membrane (0.2 µm, Peqlab, Erlangen, Germany) in a PerfectBlue "Semi-Dry" electro blot apparatus (Peqlab, Erlangen, Germany). The gel was equilibrated in transfer buffer (186 mM glycine, 25 mM tris, 20 % (v/v) methanol), placed on top of the membrane between 6 filter slides soaked in transfer buffer and blotted for 45 min at 2.5 mA/cm^2. The membrane was subsequently blocked by washing with 5 % (w/v) fat-free milk-powder dissolved in a mixture of 1 x tris buffered saline (10 x buffer: 1.4 M NaCl, 0.2 M tris, pH 7.6) and 0.1 % tween-20 (v/v) (TBST) for 2 h at room temperature. After washing with TBST three times for 5 min, the primary antibody (anti-Hyal-2 from Abcam, Cambridge, UK) diluted 1000-fold in 25 mL of TBST was incubated overnight at 4 °C with the membrane. After washing, the secondary antibody (donkey anti-rabbit IgG-HRP from Santa Cruz Biotechnology, Santa Cruz, USA), diluted 10000-fold in 25 mL of TBST, was added and shaken with the membrane at RT for 1 h. Immunoreactive bands were visualized by enhanced chemiluminescence with the Pierce® ECL detection kit (Thermo Fisher scientific, Bonn, Germany) according to the manufacturer´s instructions. Blots and gels were analyzed in a Bio-Rad gel detection system (GS-710 Imaging Densitometer) using Quantity One quantification software, version 4.0.3. (Bio-Rad, Munich, Germany).

3.2.8. Viscosimetric hyaluronidase activity assay

The decrease in viscosity of the substrate solution was determined in a micro Ubbelohde capilllary viscosimeter (Schott Instruments, Mainz, Germany). The viscosimeter was

clamped into an AVS measurement tripod connected to an AVS automated measuring device (Schott Instruments, Mainz, Germany). Sample mixtures containing 1 mL of McIlvaine´s buffer (pH 4.0), 1 mL of BSA (0.2 mg/mL), 3 mL of HA-solution (5 mg/mL) and 1 mL of sample solution were incubated at 37 °C for 24 – 96 h and viscosity was measured at various time points. Due to the negligibly short time of viscosity measurement compared with the long time period required for the incubation of the substrate with the enzyme, outflow times were not added to incubation periods.

The relative viscosities η_{rel} were calculated according to the following equations:

$$\eta_{rel} = \frac{\nu}{\nu_{ref}} = \frac{K \cdot t}{K \cdot t_{ref}} = \frac{t_M - t_{HC}}{t_{ref} - t_{HC}}$$

Eq. 3.1

with ν being the kinematic viscosity of the sample and ν_{ref} that of the reference. K is the viscosimeter constant (0.03126 mm^2/s^2). The outflow time t_M, measured for the sample and t_{ref} for the reference were both corrected by the Hagen-Couette correction time (t_{HC}) according to the manufacturer´s recommendation. References were prepared by replacing HA with H_2O in the sample mixture.

To compare changes in viscosity, η_{rel} (%) was plotted versus incubation time. η_{rel} (%) was calculated according to the following equation:

$$\eta_{rel}\ (\%) = \frac{\eta_{rel}(t_n)}{\eta_{rel}(t_0)} \cdot 100$$

Eq. 3.2

with η_{rel} (t_n) and η_{rel} (t_0) being the relative viscosities at time point n and at the beginning of the incubation period, respectively.

3.2.9. Polyacrylamide gel electrophoresis followed by combined alcian blue silver staining

Polyacrylamide gel electrophoresis was performed by analogy with a previously described protocol (Ikegami-Kawai and Takahashi, 2002; Min and Cowman, 1986). 10 % polyacrylamide gels contained 5 mL of tris/borate/EDTA (TBE) buffer (89 mM tris; 82 mM boric acid; 2 mM EDTA, pH 8.3) and 2.5 mL of acrylamide/bisacrylamide 30 % solution. Polymerization was started by adding 3.5 µL of TEMED and 35 µL of 10 % APS. The mixture was filled into gel chambers (10 x 10 x 0.8 cm) and overlaid with water

saturated isobutyl alcohol. After complete polymerization, the isobutyl alcohol layer was discarded and a 5 % stacking gel was casted. The stacking gel contained 4.1 mL of TBE buffer and 0.85 mL of acrylamide/bisacrylamide 30 % solution. Polymerization was again initiated with 3.5 µL of TEMED and 35 µL of 10 % APS. Hyaluronan digest samples and sulphonated polystyrenes in water, respectively, were mixed with a one-fifth volume of 2 M sucrose in TBE buffer and 2 µL thereof were applied directly to the gel. Bromophenol blue (BPB) was used as a tracking dye. For electrophoresis, the electrode chambers were filled with TBE buffer and the gels were run first at 250 V for 20 min, then at 500 V for 10 min, and, additionally, at 400 V for approximately 15 min until the BPB tracking dye reached the gel bottom. After electrophoresis, a combined alcian blue and silver staining protocol was used for the detection of oligosaccharides, similar to that of Ikegami-Kawai and Takahashi (Ikegami-Kawai and Takahashi, 2002). Firstly the gel was soaked in alcian-blue solution (0.5 % alcian-blue in 2 % acetic acid) for 30 min and under light protection. Afterwards, destaining was achieved by shaking in 2 % acetic acid for 30 min. The subsequent silver staining protocol was performed according to Merril et al (Merril et al., 1981). In brief: after destaining the gel was soaked in oxidation solution (3.4 mM $K_2Cr_2O_7$, 3.2 mM HNO_3) for 5 min and then it was washed for 3 x 5 min in water before putting the gel in 12 mM $AgNO_3$ solution for another 20 min. Then, the gel was washed in water for 3 min and soaked in developing solution (5 g Na_2CO_3, 100 µL of formaldehyde in 200 mL of water) until bands of appropriate intensity became visible. Development was stopped by soaking the gel in 5 % acetic acid for 15 min. Gels were stored in water until they were analyzed.

3.3. Results and discussion

3.3.1. Purification of rhHyal-2 from DS-2 cell medium

The medium from rhHyal-2 expression was first purified using Ni-IMAC. The purity of the lyophilized elution fractions was sufficiently high, though the yield of the protein was very low. **Fig. 3.1 A** shows a typical profile of the FPLC purification, the protein content of the elution fractions was plotted against the respective elution volume. SDS-PAGE of 5 µg of the purified, lyophilized protein revealed a protein band with a molecular mass of 54 kDa, which is consistent with the calculated mass of Hyal-2. Another band with a molecular mass of 40 kDa was detected, which represents either non-glycosylated Hyal-2, or it may be speculated about an artefactual protein degradation product, originated from sample

preparation (Cookson and Beynon, 1987). The former protein was identified as rhHyal-2 by Western Blot analysis, showing an immunoreactive band at approximately 60 kDa (**Fig. 3.1, B**).

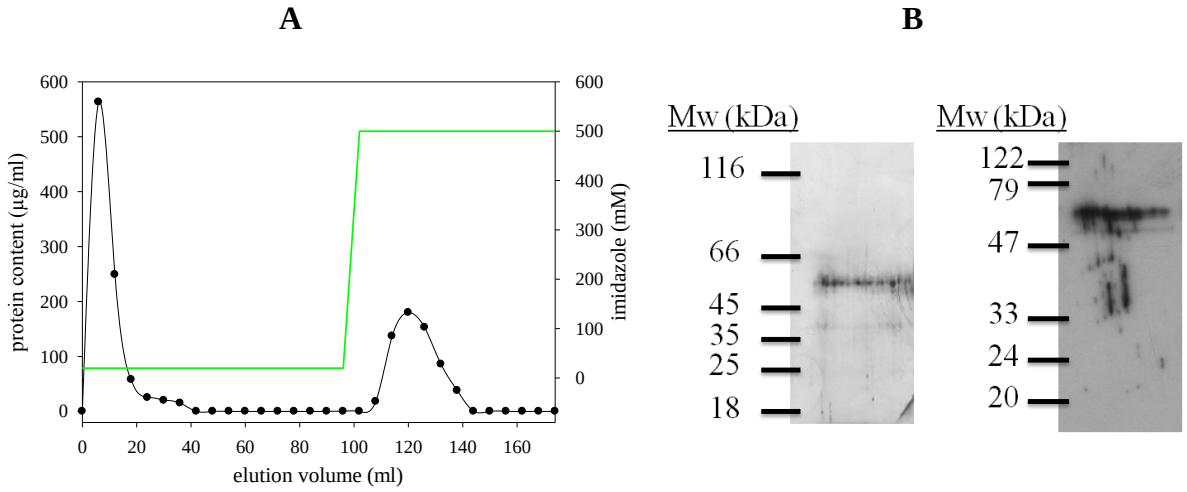

Fig. 3.1: A: Elution profile of rhHyal-2 purification using Ni-IMAC, protein content of the elution fractions was plotted against the respective elution volume; B: silver stained SDS-PAGE (left) and Western Blot analysis (right) of 5 µg of purified, lyophilized rhHyal-2. A polyclonal anti-Hyal-2 antibody was used as primary antibody, HRP-conjugated anti-rabbit-IgG as secondary antibody and detection was achieved by ECL.

3.3.2. Purification of rhHyal-2 according to a simplified protocol using Ni Sepharose™ 6 FF

As the protein content after FPLC purification was rather low and the protein containing elution fractions had been pooled anyway, a simplified and faster method for purification was used. This procedure gave similar qualitative results to the chromatographic purification. Silver stained SDS-PAGE of 5 µg lyophilized protein showed two bands with molecular weights of 54 and 42 kDa, respectively. Identification as rhHyal-2 was again achieved by Western Blot analysis, which revealed two immunoreactive bands with molecular weights of approximately 60 and 45 kDa, respectively (**Fig. 3.2**). The rhHyal-2 was still very low, but neither a longer expression time, nor thawing of another batch of transfected cells increased the protein yield.

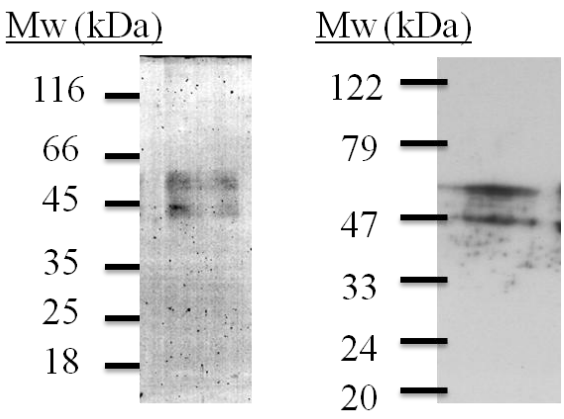

Fig. 3.2: SDS-PAGE (left) and Western Blot analysis (right) of purified, lyophilized rhHyal-2. Gels were loaded with 5 µg of protein and silver stained. Immunoreactive bands were visualized by ECL.

A total amount of 430 µg of purified, lyophilized rhHyal-2 was obtained, from which 200 µg were sent to our collaboration partners in Namur, Belgium for monoclonal antibody production. Moreover, obtained rhHyal-2 was characterized with respect to hyaluronan degrading activity.

3.3.3. Determination of enzymatic activity of purified rhHyal-2 by viscosimetry

Hyaluronidase activity, if any, of the purified protein was expected to be rather low. For this reason, viscosimetry, the most sensitive method of the classical hyaluronidase assays with a limit of quantitation of 0.1 IE/mL (bovine testicular hyaluronidase, hyaluronan from *S. zooepidemicus*, 37 °C, period of incubation: 24 h) was used for the investigations. For comparison, the limits of quantitation for the Morgan-Elson and the turbidity assay at the same conditions were 2 IE/mL and 5 IE/mL, respectively (Hofinger, 2007).

Viscosimetric measurements were performed at pH 4 as acidic conditions were used in the majority of studies suggesting Hyal-2 to be an enzymatically active protein. Dependency of Hyal-2 activity on pH is described in the next chapter. Decrease in viscosity was compared to that triggered by rhHyal-1 (Hofinger et al., 2007) and to incubation mixture without enzyme, respectively. Error bars presented in **Fig. 3.3** are SEM of three independent experiments.

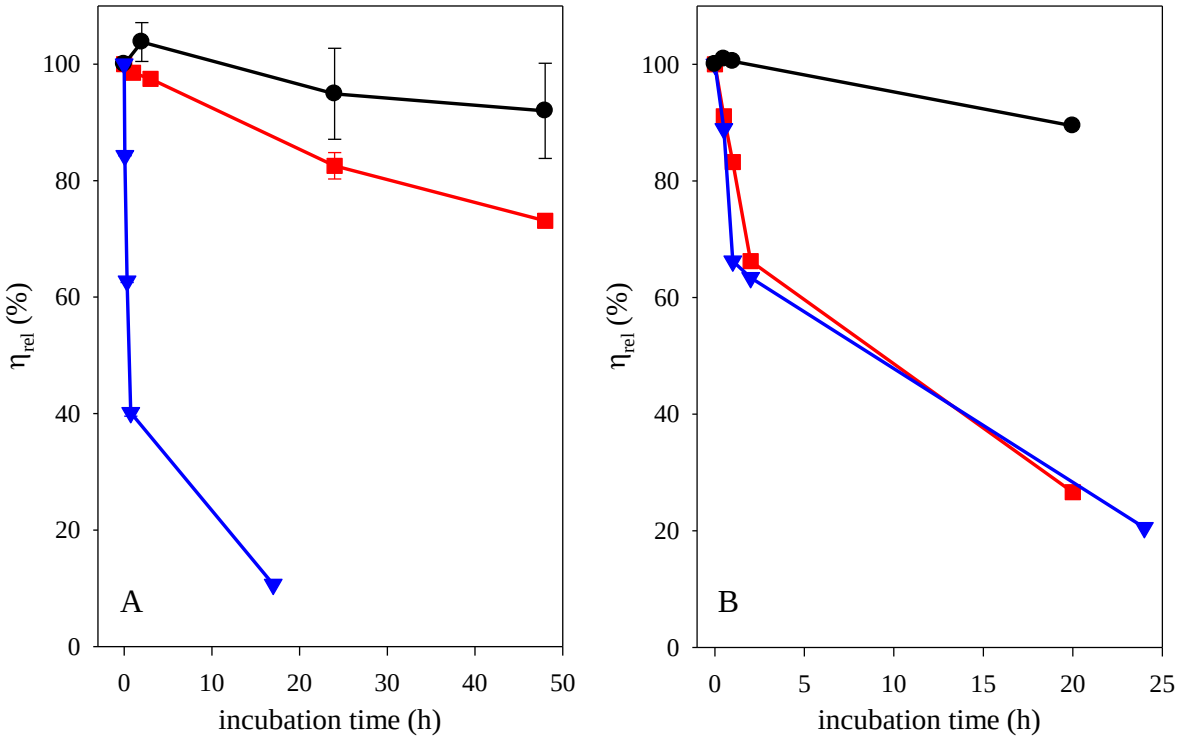

Fig. 3.3: Viscosimetric analysis of enzymatic activity of purified lyophilized rhHyal-2. Incubation of HA (circles) with rhHyal-2 (squares), compared to rhHyal-1 (triangles) using hyaluronan from different sources. A: HA from S. zooepidemicus; B: HA from human umbilical cord.

The viscosimetric analyses revealed that purified, lyophilized rhHyal-2 is able to degrade hyaluronan. The viscosity of the control slightly decreased over time. This can be explained by degradation of hyaluronan by reactive oxygen species (Soltes et al., 2006), which can be present in the environment during the long incubation time needed. By contrast, there was a pronounced decrease in viscosity of samples containing rhHyal-2.

Strikingly, the enzymatic activity depended on the source of hyaluronan used in the assay. Hyaluronan from human umbilical cord (**Fig. 3.3 B**) was degraded faster and apparently to a higher extent than hyaluronan from *S. zooepidemicus* (**Fig. 3.3 A**). As described previously, HA from human umbilical cord possesses shorter chain lengths than the bacterial HA (Hoechstetter, 2005). Possibly, the activity of rhHyal-2 is hampered by the formation of secondary and tertiary structures of HA through intramolecular interactions, which would be facilitated with increasing chain length, decreasing the probability of an endolytic attack at the hyaluronan from *S. zooepidemicus*.

3.3.4. Determination of enzymatic activity of rhHyal-2 by electrophoresis

In order to verify the results of the viscosimetric analyses and to get a hint regarding the HA fragment size distribution resulting from Hyal-2 activity, electrophoretic investigations were performed. For this purpose, rhHyal-2 mediated hyaluronan degradation was compared with the action of rhHyal-1, and the approximate size of the generated fragments was determined by comparing the migration of the fragments with these of different sulphated polystyrenes of known average molecular mass.

The electrophoresis was performed after viscosimetry using both types of hyaluronan as substrates to substantiate the differences in the degradation pattern. In **Fig. 3.4** lanes of a PAA gel electrophoresis loaded with hyaluronidase incubation mixtures (HA from *S. zooepidemicus)* is shown. Degradation catalyzed by rhHyal-2 stops at chain lengths of about 20 kDa as already described by Lepperdinger et al. (Lepperdinger et al., 1998).

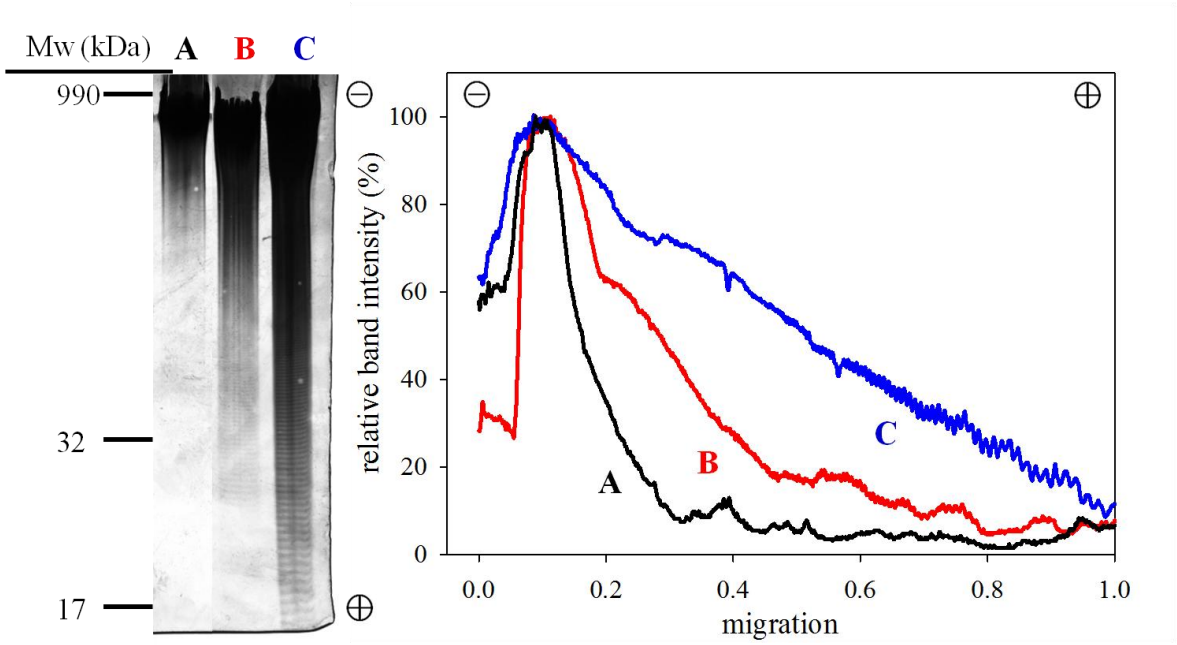

Fig. 3.4: Polyacrylamide gel electrophoresis and corresponding densitometric scans of HA derived from S. zooepidemicus (lane A) incubated with 20 µg lyophilized rhHyal-2 for 48 h (lane B) and 0.0042 U/mL rhHyal-1 for 24 h (lane C).

In case of HA from human umbilical cord, incubated with rhHyal-2, clear differences in the degradation pattern compared to HA from *S. zooepidemicus* became obvious. The degradation did not stop at hyaluronan chain lengths of 20 kDa. Unfortunately, the end product of enzymatic digestion could not be identified, as the limit of detection was approximately 10 – 15 kDa (**Fig. 3.5**).

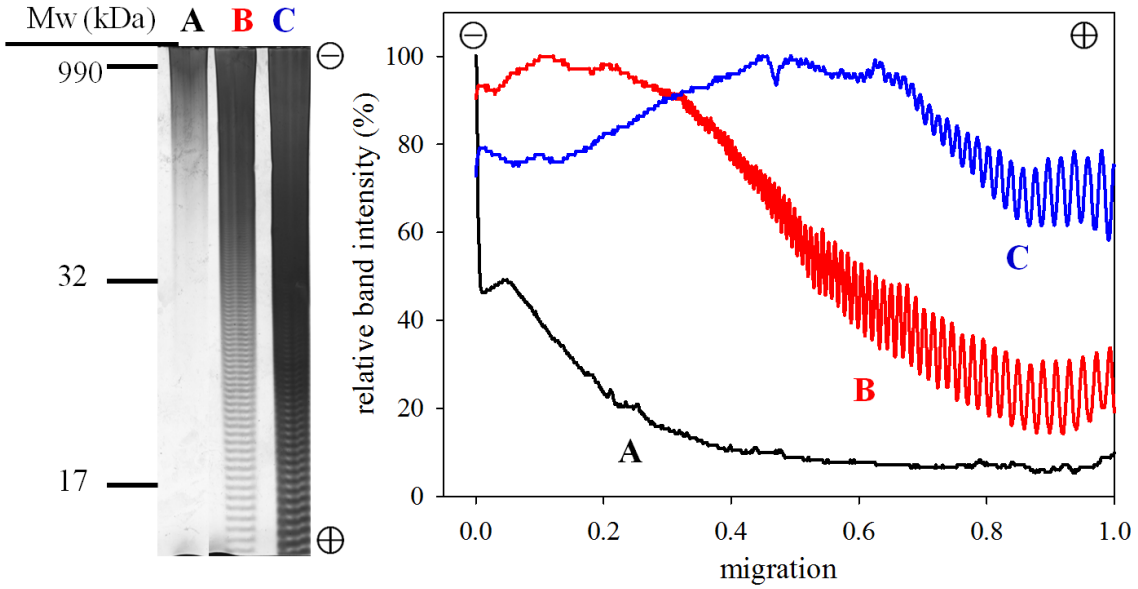

Fig. 3.5: Polyacrylamide gel electrophoresis and corresponding densitometric scan of HA from human umbilical cord (lane A) incubated with 20 µg lyophilized rhHyal-2 for 48 h (lane B) and 0.0041 U/mL of rhHyal-1 for 24 h (lane C).

These findings confirm the results from the viscosimetric measurements with respect to the suggestion, that there is a substrate dependency of enzymatic digestion by rhHyal-2.

3.4. Summary and conclusions

Recombinant human hyaluronidase-2 was expressed in DS-2 cells by analogy with the procedure reported by E. Hofinger (Hofinger, 2007). The protein was isolated from conditioned insect cell medium and purified by Ni-IMAC, which led to a product of sufficiently high purity. Since the reported method gave only rather low yields, a simplified and faster purification protocol was established. After dialysis and lyophilization of the elution fractions the presence of rhHyal-2 was proven by Western Blot analysis and the protein was characterized with respect to hyaluronan degrading activity. Moreover, a portion of the obtained purified protein was provided for monoclonal antibody production.

As enzymatic activity was expected to be very low, a viscosimetric assay was set up. This method was favored for detection of Hyal-2 activity because of the significant decrease in viscosity, especially at the beginning of the hyaluronan degradation (Hoechstetter, 2005). Furthermore, viscosimetry was previously shown to be the most sensitive method among

the common hyaluronidase assays (Hofinger, 2007), and the colorimetric assay was reported by Lepperdinger et al. (1998) to apparently unveil inactivity of Hyal-2.

The viscosimetric measurements clearly showed hyaluronan degrading activity of rhHyal-2 at acidic conditions. The rather low activity is in agreement with previous publications, which suggested low, if any Hyal-2 activity in an acidic environment (Lepperdinger et al., 1998; Vigdorovich et al., 2007). Strikingly, enzymatic activity of rhHyal-2 was dependent on the source of hyaluronan used. High molecular weight HA from *S. zooepidemicus* was digested slowly and to a lesser extent compared to HA from human umbilical cord, which is composed of shorter chain lengths. The latter was degraded pretty fast. This finding was confirmed by analytical investigations using polyacrylamide gel electrophoresis combined with alcian blue silver staining. With this method, the molecular weight of the generated HA fragments was estimated by comparing the migration of the fragments with those of sulphonated polystyrenes of known median sizes. Differences between both HA types were also detected using the electrophoresis method. By analogy with the results from viscosimetry, HA from human umbilical cord was degraded into smaller fragments by rhHyal-2 than HA from *S. zooepidemicus*. It may be speculated that these results reflect differences in the secondary and tertiary structure of both types of HA. Possibly the longer chains of the bacterial hyaluronan facilitates intramolecular interactions protecting against rhHyal-2 digestion to a certain extent.

In summary, enzymatic activity of purified, lyophilized rhHyal-2, which is dependent on the source of hyaluronan used, was unequivocally demonstrated. Nevertheless, the physiological role of the rather weak activity is still totally unclear.

It cannot be excluded that Hyal-2 has a preferential substrate other than HA, although Lepperdinger et al. found no enzymatic cleavage of structurally related carbohydrates such as chondroitin sulfates A, B and C, heparan sulfate or heparin (Lepperdinger et al., 1998).

3.5. References

Chow, G., Knudson, C.B., Knudson, W., 2006a. Expression and cellular localization of human hyaluronidase-2 in articular chondrocytes and cultured cell lines. Osteoarthritis Cartilage 14, 849-858.

Chow, G., Knudson, C.B., Knudson, W., 2006b. Human hyaluronidase-2 is localized intracellularly in articular chondrocytes and other cultured cell lines. Osteoarthritis Cartilage 14, 1312-1314.

Cookson, E.J., Beynon, R.J., 1987. Degradation Artifacts during Sample Preparation for Sodium Dodecyl-Sulfate Polyacrylamide-Gel Electrophoresis. Biosci. Rep. 7, 209-215.

Csoka, A.B., Frost, G.I., Stern, R., 2001. The six hyaluronidase-like genes in the human and mouse genomes. Matrix Biol. 20, 499-508.

Duterme, C., Mertens-Strijthagen, J., Tammi, M., Flamion, B., 2009. Two Novel Functions of Hyaluronidase-2 (Hyal2) Are Formation of the Glycocalyx and Control of CD44-ERM Interactions. J. Biol. Chem. 284, 33495-33508.

Hoechstetter, J., 2005. Characterisation of bovine testicular hyaluronidase and a hyaluronate lyase from Streptococcus agalactiae, Doctoral thesis, University of Regensburg.

Hofinger, E., 2007. Recombinant expression, purification and characterization of human hyaluronidases, Doctoral thesis, University of Regensburg.

Hofinger, E.S.A., Spickenreither, M., Oschmann, J., Bernhardt, G., Rudolph, R., Buschauer, A., 2007. Recombinant human hyaluronidase Hyal-1: insect cells versus Escherichia coli as expression system and identification of low molecular weight inhibitors. Glycobiology 17, 444-453.

Ikegami-Kawai, M., Takahashi, T., 2002. Microanalysis of hyaluronan oligosaccharides by polyacrylamide gel electrophoresis and its application to assay of hyaluronidase activity. Anal. Biochem. 311, 157-165.

Lepperdinger, G., Mullegger, J., Kreil, G., 2001. Hyal2 - less active, but more versatile? Matrix Biol. 20, 509-514.

Lepperdinger, G., Strobl, B., Kreil, G., 1998. HYAL2, a human gene expressed in many cells, encodes a lysosomal hyaluronidase with a novel type of specificity. J. Biol. Chem. 273, 22466-22470.

Merril, C.R., Goldman, D., Sedman, S.A., Ebert, M.H., 1981. Ultrasensitive Stain for Proteins in Polyacrylamide Gels Shows Regional Variation in Cerebrospinal-Fluid Proteins. Science 211, 1437-1438.

Miller, A.D., 2003. Identification of Hyal2 as the cell-surface receptor for jaagsiekte sheep retrovirus and ovine nasal adenocarcinoma virus. Jaagsiekte Sheep Retrovirus and Lung Cancer 275, 179-199.

Min, H., Cowman, M.K., 1986. Combined alcian blue and silver staining of glycosaminoglycans in polyacrylamide gels: application to electrophoretic analysis of molecular weight distribution. Anal. Biochem. 155, 275-285.

Monzon, M.E., Fregien, N., Schmid, N., Falcon, N.S., Campos, M., Casalino-Matsuda, S.M., Forteza, R.M., Reactive Oxygen Species and Hyaluronidase 2 Regulate Airway Epithelial Hyaluronan Fragmentation. J. Biol. Chem. 285, 26126-26134.

Mullegger, J., Lepperdinger, G., 2002. Hyaluronan is an abundant constituent of the extracellular matrix of Xenopus embryos. Mol. Reprod. Dev. 61, 312-316.

Rai, S.K., Duh, F.M., Vigdorovich, V., Danilkovitch-Miagkova, A., Lerman, M.I., Miller, A.D., 2001. Candidate tumor suppressor HYAL2 is a glycosylphosphatidylinositol (GPI)-anchored cell-surface receptor for jaagsiekte sheep retrovirus, the envelope protein of which mediates oncogenic transformation. Proc. Natl. Acad. Sci. U. S. A. 98, 4443-4448.

Soltes, L., Mendichi, R., Kogan, G., Schiller, J., Stankovska, M., Arnhold, J., 2006. Degradative action of reactive oxygen species on hyaluronan. Biomacromolecules 7, 659-668.

Toyoda, H., Kinoshita-Toyoda, A., Selleck, S.B., 2000. Structural Analysis of Glycosaminoglycans inDrosophila and Caenorhabditis elegans and Demonstration That tout-velu, a Drosophila Gene Related to EXT Tumor Suppressors, Affects Heparan Sulfate in Vivo. J. Biol. Chem. 275, 2269-2275.

Vigdorovich, V., Miller, A.D., Strong, R.K., 2007. Ability of hyaluronidase 2 to degrade extracellular hyaluronan is not required for its function as a receptor for jaagsiekte sheep retrovirus. J. Virol. 81, 3124-3129.

Vigdorovich, V., Strong, R.K., Miller, A.D., 2005. Expression and characterization of a soluble, active form of the jaagsiekte sheep retrovirus receptor, Hyal2 (vol 79, pg 79, 2005). J. Virol. 79, 3228-3228.

Chapter 4

Enzymatic activity of Hyal-2 in blood platelets

4.1. Introduction

Platelets are anucleated cells derived from megakaryocytes and are the second most numerous corpuscles circulating in the blood. They are involved in several patho-/physiological processes, namely haemostasis and thrombosis, inflammation, host defense and maintenance and regulation of the vascular tone (Harrison, 2005). Likely, the most important function of platelets is to seal openings in the vascular network. Upon vessel wall damage, platelets play a central role in a functional sequence, beginning with adhesion to collagen, which leads to activation and subsequent shape change from discoid to spiny spheres with filopodia. The change in shape goes along with secretion of protein (e.g. fibrinogen, plasminogen, PDGF, VEGF) and nonprotein mediators (ADP, Ca^{2+}, serotonin), which are responsible for further platelet activation and stimulation of wound healing. In the past few years, the role of platelets in inflammatory conditions has been acknowledged, but this needs to be elucidated further. Platelets have been shown to contribute to inflammatory processes, for instance, in inflammatory bowel disease (IBD) (Danese et al., 2004), cardiovascular diseases (Lindemann et al., 2007) and neuroinflammatory disorders (Horstman et al., 2010).

Previously, an association between platelet fractions and hyaluronidase activity was documented (Fiszer-Szafarz et al., 2000), but it remained unclear, which hyaluronidase isoform is responsible for the displayed activity.

Recently, de la Motte et al. detected Hyal-2 as the only hyaluronidase expressed on platelet membranes and suggested that this isoenzyme is capable of cleaving hyaluronan into signalling fragments (de la Motte et al., 2009). The hyaluronan degrading activity was detected at neutral pH, which is in contrast to other published data on Hyal-2 activity (Lepperdinger et al., 1998; Vigdorovich et al., 2007; Vigdorovich et al., 2005). However, this result has been linked to inflammatory diseases, as HA fragment formation is observed under inflammatory conditions, such as arthritis (Poole and Dieppe, 1994) and in the intestinal mucosa of patients with IBD (de la Motte et al., 2003). Moreover, IBD is associated with reactive thrombocytosis (Shen et al., 2009) and increased leukocyte-platelet interactions have been described (Irving and Rampton, 2007).

Inspired by the results of de la Motte et al., in this work human platelet preparations were used as source of Hyal-2 to explore the enzymatic activity at different pH-values, the approximate size of generated fragments, differences in the degradation of HA from different sources and differences in enzymatic activity between non-activated and activated

platelets. The results from human platelets were compared to those obtained from investigations on murine platelets from Hyal-2 knockout and wildtype mice and to rhHyal-2, respectively.

4.2. Materials and methods

4.2.1. Isolation of human platelets

Blood was collected from a forearm vein of a 28 year-old female, healthy volunteer into syringes containing citrate – citric acid – dextrose (CCD) (2.5 % trisodium citrate; 1.37 % citric acid monohydrate; 2.0 % glucose). The ratio of anticoagulant to blood was 2:8. After centrifugation at 200 g for 20 min at room temperature (RT), platelet-rich plasma (PRP) was carefully collected. Platelets were isolated from PRP by additional centrifugation at 2000 g for 12 min at RT. The supernatant was discarded and the resulting platelet pellet was washed three times with the assay buffer (see 3.2.8).

4.2.2. Isolation of murine platelets

Murine blood was collected in ketamine/xylazine anesthesia by cardiac puncture into 200 µL of Alsever´s buffer (0.8 % trisodium citrate; 0.05 % citric acid monohydrate; 2.0 % glucose; 0.42 % NaCl). Blood samples were centrifuged at 70 g for 15 min to collect the PRP. PRPs were centrifuged a second time to reduce contamination by red and white blood cells. After washing with hepes-buffer (20 mM hepes; 138 mM NaCl; 2.9 mM KCl; 1 mM $MgCl_2$; 0.36 mM NaH_2PO_4), pH 7.4, platelets were used for investigations.

4.2.3. Preparation of human platelet membranes

Isolated platelets from 5 mL of PRP were resuspended in 5 mL of hypotonic buffer (5 mM EDTA; 5 mM tris in Millipore water, pH 7.4). The resulting suspension was dispersed in 1.5 mL polypropylene tubes and frozen in liquid nitrogen. Platelets were allowed to thaw at room temperature, pooled and disrupted by ten manual strokes of a Potter Elvehjem model Potter S (B. Braun Melsungen AG, Melsungen, Germany). After repeating this step, the platelet homogenate was centrifuged for 30 min at 25000 rpm using a TGA-45 ultracentrifuge, equipped with a TFT 45.94 rotor (Kontron Analytical, Zürich, Switzerland). The supernatant was removed and the pellet was re-suspended in 10 mL of hypotonic buffer and centrifuged again for 30 min at 25000 rpm. The resulting platelet membrane pellet was re-suspended in 5 mL of 1 mM $KHCO_3$ solution. Protein content was determined using the Bio-Rad protein assay (Bio-Rad, Munich, Germany) based on the method of Bradford (Bradford, 1976). 100 µL aliquots of the membrane suspension were stored at -80 °C until use.

4.2.4. SDS-PAGE and Western Blot

Electrophoresis and Western Blot analyses were performed as described in Chapter 3.

4.2.5. 2-D gel electrophoresis

Samples for 2-D electrophoresis were diluted with sample buffer (7 M urea, 2 M thiourea, 2 % chaps, 0.5 % Bio-Lyse 3/10 ampholytes (100 x), 1 % Serdolit MB-1™ and 100 mM DTDE) and solubilized for 1 h at room temperature. After centrifugation at 13000 g for 30 min at 15 °C, immobilized pH gel strips (IPG, ReadyStrip™ 7 cm, pH 3 – 10, Bio-Rad, Munich, Germany) were loaded with the sample and an IEF marker mix (pH 3.6 – 9.3, Sigma-Aldrich, Munich, Germany), respectively, and were re-hydrated for 11-16 h. Isoelectric focusing (IEF) was performed with a Bio-Rad Protean IEF cell (Bio-Rad, Munich, Germany) for 16.2 kWh at 20 °C. The IPG strips were soaked with equilibration buffer I for 15 min and subsequently transferred to equilibration buffer II (buffer compositions see **Tab. 4.1**) for another 15 min. The strips were loaded onto a 12% polyacrylamide gel (gel composition see **Tab. 3.1**) and SDS-PAGE was performed at 200 V.

Tab. 4.1: Composition of equilibration buffers for 2-D electrophoresis.

	Urea (M)	SDS (%)	Tris/HCl pH 8.8 (M)	Glycerol (%)	DTT (%)	Iodoacetamide (%)
Buffer I	6	2	0.375	20	2	-
Buffer II	6	2	0.375	20	-	2.5

The gel was blotted on a nitrocellulose membrane or fixed in a solution containing 30 % (v/v) methanol, 10 % (v/v) acetic acid for silver staining. Western Blot analysis was performed as described above. For analysis of glycosylation the membrane was incubated with peroxidase conjugated lectin from *Helix pomatia* (Sigma-Aldrich, Munich, Germany). The chemiluminescence detection of peroxidase activity was carried out as described in **3.2.7.** Silver staining was performed as described in **3.2.9**.

4.2.6. Gel permeation chromatography (GPC)

Gel permeation chromatography was carried out using a Shimadzu (Shimadzu, Tokyo, Japan) LD-10 liquid chromatograph equipped with degasser, pump, auto-injector and column oven in combination with a TDA-300 triple detector (Viscotek, Malvern Instruments Ltd., Malvern, UK) operated in dual mode (refractive index, UV detection at 210 nm). A BioSep-SEC-S 4000 column (Phenomenex Ltd., Aschaffenburg, Germany) was used as stationary phase and water and incubation buffer (see above) as mobile phase, respectively. The amount of HA in the injection volume of 10 µL was 25 ng. Column and detector were operated at 40 °C and the flow rate was 0.7 mL/min. To determine the size of HA fragments, dextrane standards with average molecular wheights of 5.2, 11.6, 20, 48 and 148 kDa were used (Malvern Instruments Ltd., Malvern, UK).

4.2.7. Viscosimetric and electrophoretic hyaluronidase activity assays

Viscosimetry and polyacrylamide gel electrophoresis followed by combined alcian blue silver staining were performed as described in Chapter 3.

4.2.8. Zymography

Hyaluronan gel electrophoresis was performed as described by Cherr et al (Cherr et al., 1996). SDS polyacrylamide gels were prepared as described in section **3.2.6** with additional 67 µg/mL hyaluronan (5 mg/mL stock solution) in the separation gel. Samples for zymography were mixed with sample buffer (200 mM tris/HCl pH 6.8, 20 % glycerol, 10 % SDS, 0.05 % bromophenol blue) in a ratio of 1:1 and directly applied to the gel. After electrophoresis at 150 V for approximately 2 h, SDS was removed from the gel by shaking in 2.5 % triton X-100 for 30 min at RT, a short washing period in water and successive washing in incubation buffer for 30 min. After incubation in McIlvaine´s buffer, pH 4.0, the gel was stained with 0.5 % alcian blue in 7 % acetic acid for 1 h and destained in 7 % acetic acid until the regions of hyaluronan digest were visible. The gel was counterstained with Coomassie Brilliant Blue G-250 (Serva, Heidelberg, Germany).

4.2.9. Activation of platelets

For platelet activation PRP was prepared as described above. After centrifugation, the resulting platelet pellet was re-suspended in hepes-buffer pH 7.4 (137 mM NaCl; 2.7 mM KCl; 10 mM hepes; 1.7 mM $MgCl_2$; 25 mM glucose; 0.05 % BSA) containing 2 U/mL apyrase (Sigma-Aldrich, Munich, Germany) and 200 µM $CaCl_2$. Platelets were incubated at 37 °C for 10 min before centrifuging at 1000 g for 15 min. After carefully re-suspending the pellet in buffer 1 mM $CaCl_2$ (100 mM stock solution), 1 U/mL thrombin (Boehringer, Mannheim, Germany, 5 U/mL stock solution in Hepes-buffer) and 10 µg/mL collagen (MP Biomedicals, Heidelberg, Germany, 250 µg/mL stock solution) were added. The clot was washed with hepes-buffer and used for investigations.

4.2.10. Ca^{2+} assay for measuring platelet activation

For measuring platelet activation, the increase of intracellular Ca^{2+} after addition of mediators of platelet function was observed. Washed platelet suspensions in loading buffer (145 mM NaCl, 5 mM KCl, 10 mM Hepes, 1 mM $MgSO_4$, 10 mM glucose, 0.1 % BSA, pH 7.4), containing 2 U/mL apyrase and 200 µM $CaCl_2$, were loaded with fura-2/AM according to the following protocol. 1 µM fura-2/AM (Invitrogen, Karlsruhe, Germany, 1 mM stock solution in anhydrous DMSO) and 5 µL of Pluronic® F-127 (Calbiochem-Novabiochem Corporation, La Joila, Canada, 20 % stock solution in DMSO) were added to 1 mL of cell suspension. After 45 min of incubation in the dark at room temperature, 12 µL of ACD were added to the suspension. The cells were centrifuged at 700 g for 20 min at room temperature and re-suspended in the same volume of loading buffer containing 2 U/mL apyrase. The resulting suspension was incubated for another 30 min in the dark to ensure complete intracellular cleavage of the acetoxymethyl (AM) ester groups. Platelets were washed and re-suspended in loading buffer. 1 mL of the platelet suspension was diluted in a cuvette with 0.98 mL loading buffer and 20 µL of 100 mM $CaCl_2$. Measurements were performed in a LS 50 B spectrofluorimeter (PerkinElmer, Überlingen, Germany) under continuous stirring at 25 °C at low speed. Instrumental settings were: λ_{ex}: 340 and 380 nm alternating with slit 10 nm and λ_{em}: 510 nm with slit 10 nm. The baseline was recorded for approximately 20 s before challenging the loaded cells by thrombin (Böhringer, Mannheim, Germany), collagen (MP Biomedicals, Solon, USA) and the thrombin receptor activator peptide SFLLRN (Bachem AG, Bubendorf, Switzerland), respectively. The PAR_1 antagonist peptide YFLLRNP (Bachem AG, Bubendorf,

Switzerland) was incubated with the cells for 15 min in the dark at room temperature prior to measurement. For the calculation of intracellular Ca^{2+} the Grynkiewcz equation was used (Grynkiewicz et al., 1985):

$$[Ca^{2+}] = K_D \cdot \frac{(R - R_{min})}{(R_{max} - R)} \cdot SFB$$

Eq. 4.1

with K_D being the dissociation constant of fura-2-Ca^{2+} (225 nM), R the ratio of fluorescence intensity at 510 nm after excitation at 340 and 380 nm, R_{max} the fluorescence ratio at saturating Ca^{2+} concentration, determined after adding 10 µL of digitonin (2 % in water, Sigma-Aldrich, Munich, Germany), which causes lysis of the cells and saturation of the dye with the Ca^{2+}-ions present in the mixture in the cuvette, R_{min} the fluorescence ratio of Ca^{2+}-free dye, determined after addition of 50 µL of EGTA (600 mM in 1M Tris/HCl buffer, pH 8.7) to the lysed cells and SFB a correction factor, which accounts for the ratio of fluorescence intensity at 510 nm after excitation at 380 nm of the Ca^{2+}-free and Ca^{2+}-saturated dye.

4.3. Results and discussion

4.3.1. SDS-Page and Western Blot analysis of Hyal-2 in human platelets

In order to verify the findings of de la Motte et al. (de la Motte et al., 2009), who stated that Hyal-2 is the only hyaluronidase in platelets, Western Blot analysis was performed. Using a primary anti-Hyal-2 antibody, two immunoreactive bands with apparent molecular weights of 54 and 44 kDa, respectively, were detected (**Fig. 4.1**, left). Purified recombinant human Hyal-1 expressed in DS-2 cells (Hofinger et al., 2007) (rhHyal-1) was utilized as a control to exclude crossreactivity of the antibody. rhHyal-1 was detected with anti Hyal-1 serum, kindly provided by Prof. Dr. Robert Stern, UCSF (**Fig. 4.1**, right).

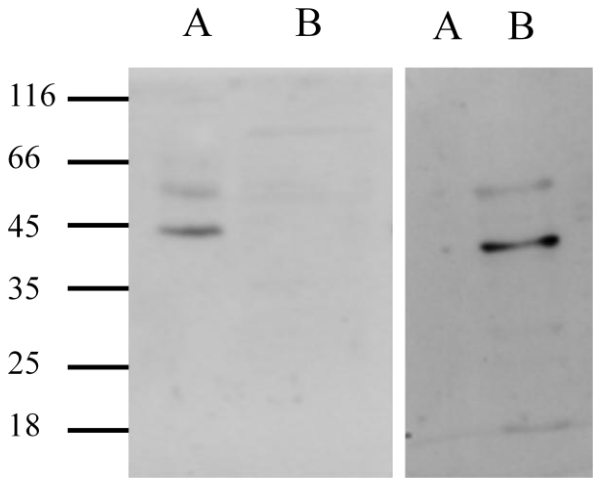

Fig. 4.1: Western blot analysis of Hyal-2 (left) and Hyal-1(right) in human platelets (lane A). rhHyal-1 (lane B) was used as negative (for anti-Hyal-2) and positive (for anti-Hyal-1) control, respectively

In accordance with the literature, Hyal-2 was detected as the only hyaluronidase in human platelets with no evidence for Hyal-1. The antibody against Hyal-2 did not show cross-reactivity with Hyal-1 and vice versa.

4.3.2. 2-D gel electrophoresis

For the determination of the properties of Hyal-2 in human platelet membrane preparations, 2-D electrophoresis was performed. In the following Western blot analysis two spots with a molecular weight of 54 kDa, corresponding to the calculated mass of Hyal-2, were detected. The pI of the two isoforms was 7.9 and 8.2, respectively. Lectin blotting showed that both isoforms exist as glycosylated proteins (**Fig. 4.2**).

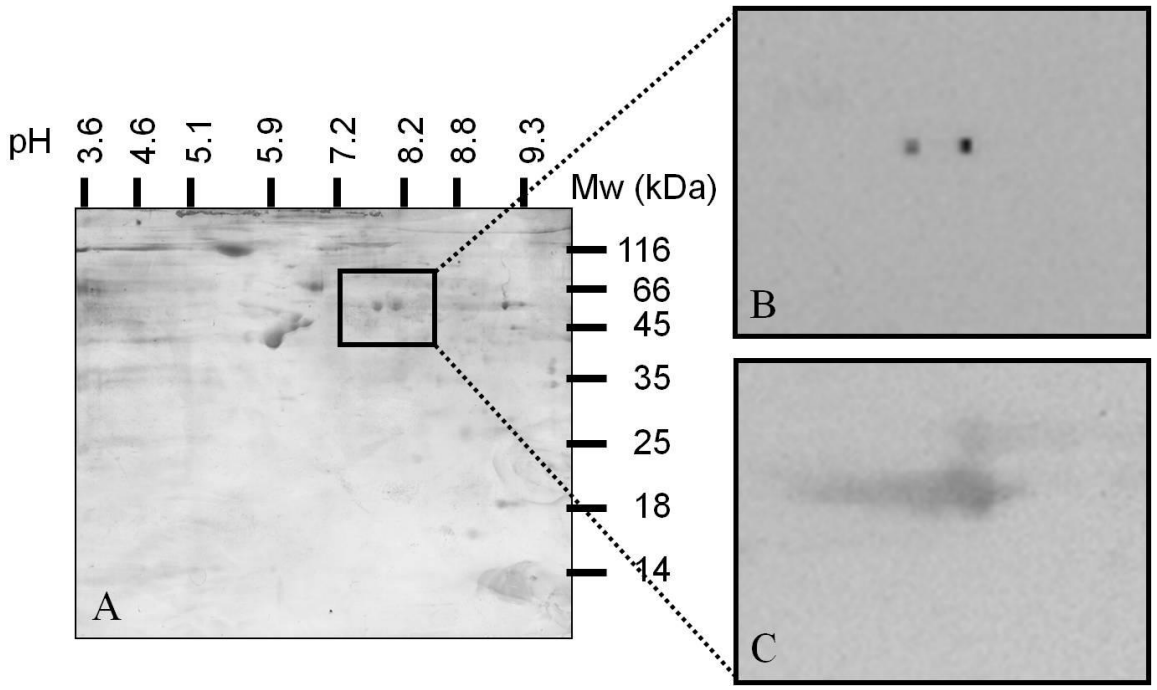

Fig. 4.2: 2-D electrophoresis of human platelet membrane preparations. A) Silver staining, B) Western blot analysis. Anti-Hyal-2 polyclonal antibody was used as primary antibody, HRP-conjugated anti-rabbit-IgG as secondary antibody and detection was achieved by ECL, C) Lectin blot analysis. HRP-conjugated lectin from *Helix pomatia* was used as antibody and detection was achieved by ECL.

In contrast to the one-dimensional Western Blot analysis, there was no protein with a molecular weight of 44 kDa detected in the 2-D analysis. This result supports the suggestion that during one-dimensional SDS-PAGE sample preparation protein degradation takes place, as there is no heating of the samples during 2-D electrophoresis.

4.3.3. Detection of enzymatic activity of Hyal-2 in non-activated human platelets by viscosimetry

The determination of the decrease in viscosity during degradation of hyaluronan is the most sensitive method to investigate hyaluronidase activity (Hofinger, 2007). Therefore, a viscosimetric assay was established to find HA degrading activity in human platelets.

The optimal pH for Hyal-2 activity is discussed very controversially in literature. Therefore, firstly, mixtures containing HA from *S. zooepidemicus* and washed human platelets were incubated for 48 h under acidic (pH 4.0, and pH 5.0) and neutral (pH 7.0) conditions to determine the appropriate pH value for further investigations. At pH 4.0 the incubation mixtures containing human platelets showed a stronger decrease in viscosity compared to the negative control without platelets. At pH 5.0 and pH 7.0 there was no difference between the negative control and platelet containing incubation mixtures, thus

no HA degrading activity was detectable (**Fig. 4.3**). Therefore, all following experiments were performed under acidic conditions.

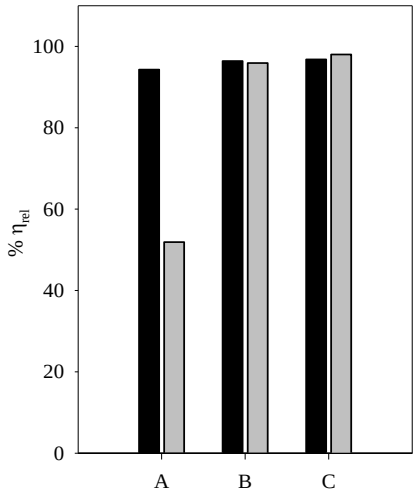

Fig. 4.3: Viscosimetry of HA digestion mixtures with human platelets incubated at 37 °C for 24 h at different pH values (grey bars). The HA was of microbial origin (*S. zooepidemicus*). The black bars represent reference HA mixtures incubated at 37 °C for 24 h. A) pH 4.0, B) pH 5.0, C) pH 7.0

The hyaluronan degrading activity of isolated and washed human platelets was compared to that of rhHyal-1 (0.42 mU/mL). The low activity of rhHyal-1 was chosen, because contamination by traces of plasma Hyal-1 in the platelet preparations could not be excluded at that time. Hyaluronidase levels in human serum from healthy volunteers range from 3 mU/mL (Natowicz and Wang, 1996) to 9 mU/mL (Laudat et al., 2000). Platelet associated hyaluronidase activity became obvious within 24 h, but at a much slower rate than that of rhHyal-1 (**Fig. 4.4**, **A**). Enzymatic activity was also compared to that of a human platelet preparation, which was inactivated by heating at 100 °C for 15 min, as viscosity always decreased to a minimal extent, even without enzyme. The decrease in viscosity generated by human platelets differed significantly from that observed for inactivated platelets ($p = 0.007$).

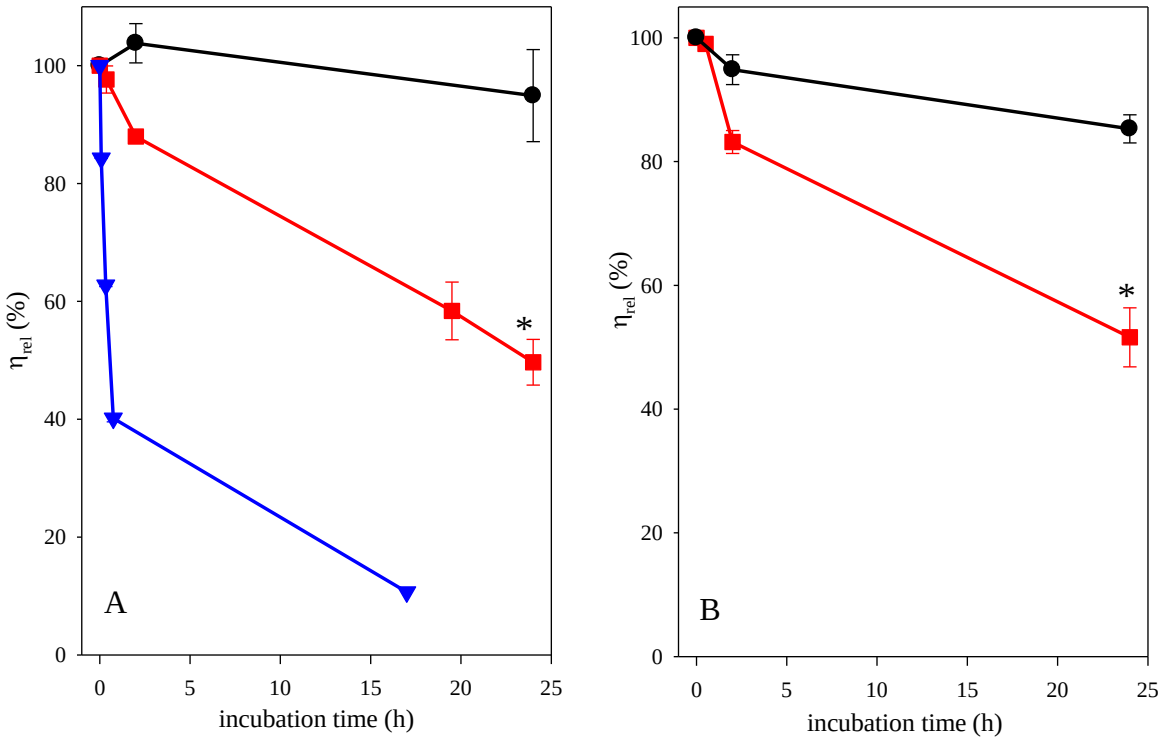

Fig. 4.4: Viscosimetric analyses of hyaluronidase activity. A: human platelets (squares) compared to 0.42 mU/mL rhHyal-1(triangles) and heat-inactivated platelets (circles), respectively. B: Human platelet membrane preparation (squares) compared to heat-inactivated membranes (circles). Error bars represent SEM of 3 independent experiments. The used hyaluronan was from *S zooepidemicus*.

Hyal-2 has been suggested to be a GPI-anchored protein on the cell-membrane (Rai et al., 2001). Consequently, viscosimetric analysis of Hyal-2 activity was also performed with human platelet membrane preparations. In comparison to the substrate mixture incubated with inactivated membranes, viscosity decreased significantly ($p = 0.003$) within 24 h (**Fig. 4.4**, **B**)

These results prove that Hyal-2 is catalytically active in human platelets and that it is present in platelet membrane preparations. The enzyme displays highest activity at pH 4. Therefore, Hyal-2 should be located in an acidic microenvironment to be active under physiological conditions. As Hyal-2 is associated with specialized microdomains in the plasma membrane, so-called lipid rafts (Andre et al., 2011), the interaction of CD44 with the Na^+-H^+-exchanger NHE1 in the presence of HA could play an important role. Bourgignon et al. detected complexed CD44 and NHE1 in lipid rafts after treatment of MDA-MB-231 cells with hyaluronan, but no association without HA-treatment. The authors suggested that HA recruits signaling complexes, including NHE1 and RhoA-

activated Rho kinase (ROK) into lipid rafts of the cells used (Bourguignon et al., 2004). This could also happen in platelets, which express rather high amounts of NHE1 (Rutherford et al., 1997). For platelet-associated Hyal-2 activity the hyaluronan receptor CD44 also could play an important role. CD44 is able to mediate the adhesion of platelets to HA (Koshiishi et al., 1994). Therefore the HA receptor could bring membrane bound Hyal-2 close to its substrate in the extracellular matrix. We also confirmed the expression of CD44 in human platelet membrane preparations with a molecular weight of approximately 85 kDa, which correlates well with the calculated mass of isoform 1 (81.5 kDa) (**Fig. 4.5**). The second immunoreactive band is of a molecular mass of about 170 kDa, which is approximately double the mass of a CD44 monomer. HA is an extremely multivalent ligand and therefore clustering of monomeric receptors into a multimeric complex could increase the avidity to such a ligand (Perschl et al., 1995; Sleeman et al., 1996).

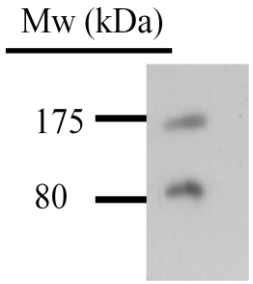

Fig. 4.5: Presence of CD-44 in human platelet membranes determined by Western blotting. Anti-CD44 monoclonal antibody was used as primary antibody, HRP-conjugated anti-rabbit IgG as secondary antibody and detection was achieved by ECL

4.3.4. Dependency of substrate degradation by platelet-derived Hyal-2 on the source of HA

By analogy with the investigation of the recombinant enzyme, the activity of platelet-associated Hyal-2 was determined with hyaluronan from different sources. We used the kinetic viscosimetric assay to reveal differences in the degradation of HA from *S. zooepidemicus*, HA from human umbilical cord and from rooster comb, respectively. Actually, the results were in agreement with those for the recombinant enzyme (**Fig. 4.6**). Hyaluronan from microbial origin was degraded slower and to an apparently lesser extent than HA from vertebrate sources (**Tab. 4.2**).

Tab. 4.2: Decrease in η_{rel} (%) per h using different sources of hyaluronan. Platelet derived Hyal-2 compared to rhHyal-2.

source of HA	*S. zooepidemicus*	human umbilical cord	rooster comb
human platelets	2.0	3.1	2.7
rhHyal-2	1.7	3.1	n. d.

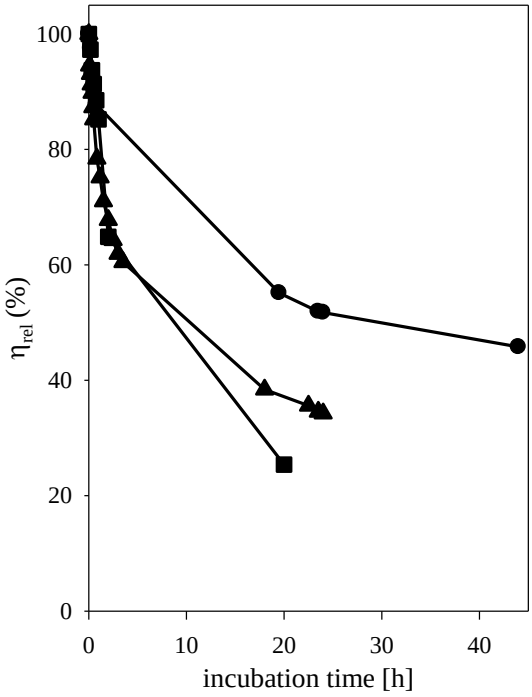

Fig. 4.6: Viscosimetric analyses of enzymatic activity of platelet-derived Hyal-2 using hyaluronan from different sources: HA of microbial origin (circles), HA from human umbilical cord (squares) and HA from rooster comb (triangles).

4.3.5. Gel permeation chromatography for determination of hyaluronan fragments generated by platelet-associated Hyal-2

To determine the size distribution of the generated hyaluronan fragments, gel permeation chromatography was performed. The incubation mixtures of hyaluronan with human platelets, rhHyal-1 and bovine testicular hyaluronidase (BTH, Neopermease®) were separated with a BioSep-SEC-S 4000 column. As there were hardly any differences between the chromatograms (**Fig. 4.7**), this approach was discontinued.

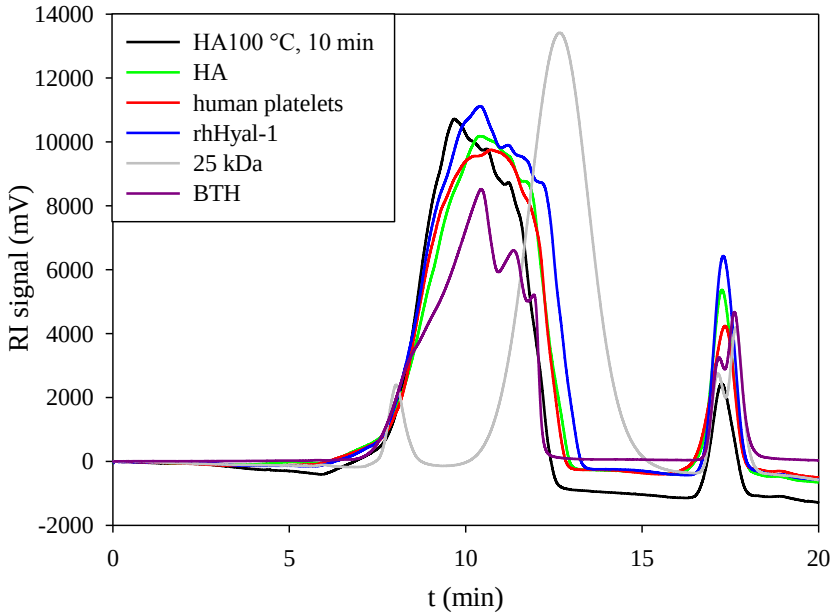

Fig. 4.7: Gel permeation chromatography of hyaluronan incubation mixtures with human platelets, rhHyal-1 and BTH, respectively

4.3.6. Determination of enzymatic activity of Hyal-2 in non-activated human platelets by electrophoresis

In order to verify the results from the viscosimetric analyses by an additional method and to get a hint regarding the HA fragment size resulting from degradation by Hyal-2, electrophoretic investigations were performed. Platelet mediated hyaluronan degradation was compared to the action of rhHyal-1 and BTH, respectively, and the approximate size of the generated fragments was determined by comparing the migration of the fragments with those of sulphated polystyrenes of known sizes. **Fig. 4.8** shows a typical gel and the corresponding densitometric scans. As expected, rhHyal-1 and BTH degrade HA into fragments smaller than 17 kDa, whereas fragments generated by human platelets appear to have a *minimal* size of 17 kDa after incubation for 48 h. This finding correlates with the results of Lepperdinger et al., who found a size limit of 20 kDa or 50 disaccharides (Lepperdinger et al., 2001; Lepperdinger et al., 1998). Surprisingly, when incubations were performed with isolated platelet membrane fractions, HA degradation appears to result in fragments of a smaller size (**Fig. 4.9**).

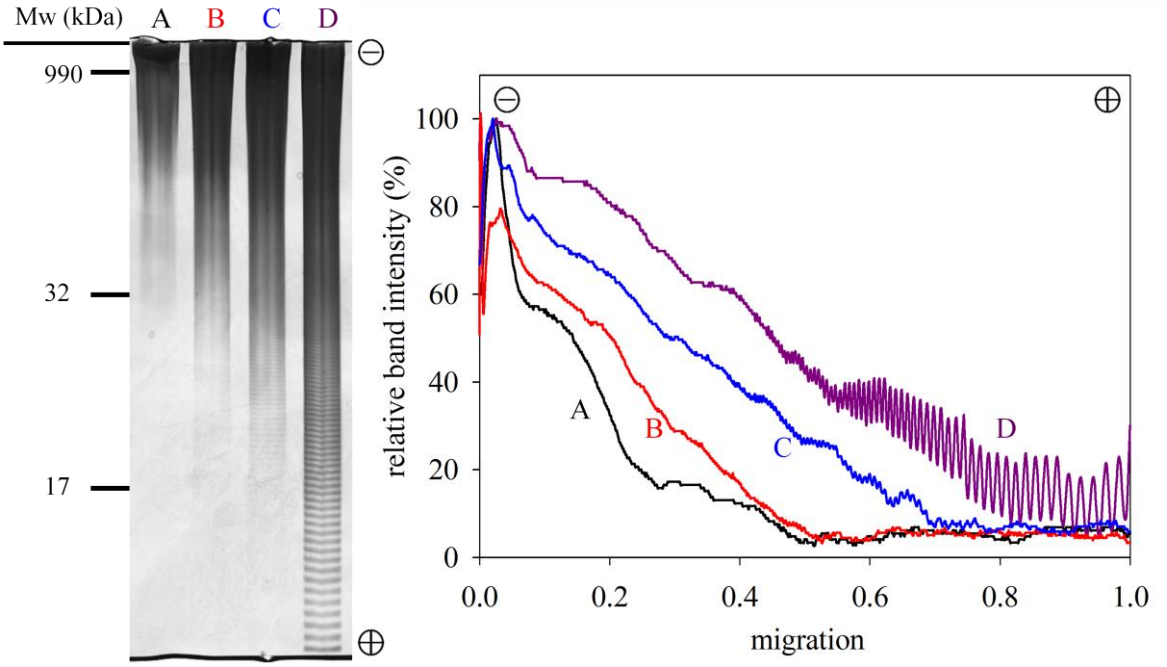

Fig. 4.8: PAGE and corresponding densitometric scans of hyaluronan (lane A) incubated with human platelets at 37 °C for 48 h (lane B), 0.0042 U/mL rhHyal-1 at 37 °C for 2 h (lane C) and 10 IE/mL BTH at 37 °C for 2 h (lane D)

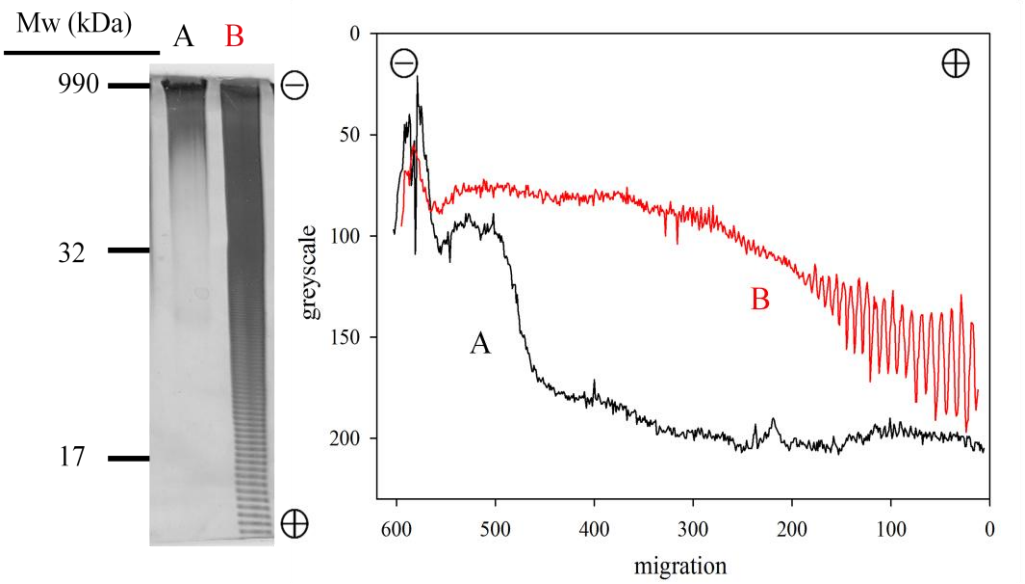

Fig. 4.9: PAGE and corresponding densitometric scans of hyaluronan (lane A) incubated with human platelet membranes at 37 °C for 48 h (lane B)

4.3.7. Zymography

The Western Blot analysis of human platelets revealed two immunoreactive bands of different molecular mass. The two proteins were investigated for hyaluronidase activity using SDS substrate-PAGE with hyaluronan immobilized in the separating gel.

Zymography revealed that only the 54 kDa protein exhibited hyaluronan degrading activity. Enzymatic activity was compared to that of 2.5 mU/mL rhHyal-1 which also displays one active protein band with a molecular mass of 55 kDa (**Fig. 4.10**).

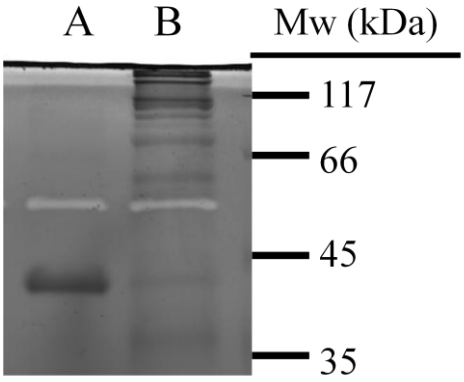

Fig. 4.10: Substrate gel analysis of 0.5 mg/mL human platelets (lane B) compared to 2.5 mU/mL rhHyal-1 (lane A), counterstained with coomassie

This result supports the suggestion that during SDS-PAGE sample preparation degradation of the protein takes place. The resulting protein fragment is not able to display enzymatic activity anymore.

4.3.8. Activation of human platelets

As platelets change their shape, form aggregates and secret their granule contents during activation, the question arose, if Hyal-2 activity changes along with platelet activation. For this reason platelets were stimulated with different platelet activation mediators and intracellular Ca^{2+}-levels were measured to control activation. Platelet activation was achieved by adding 1 U/mL thrombin, 50 µM ADP and 33.5 µM of the thrombin receptor activator peptide 6 (SFLLRN), respectively.

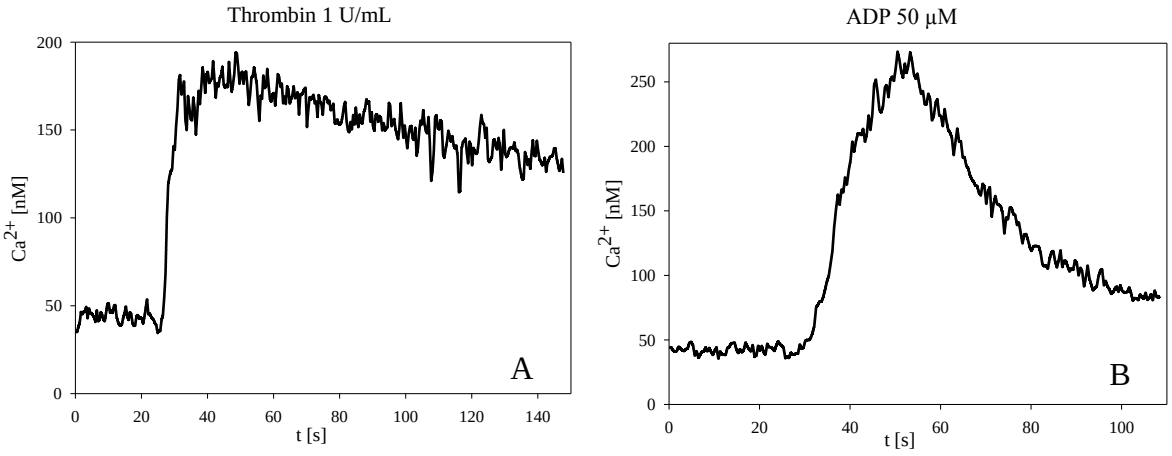

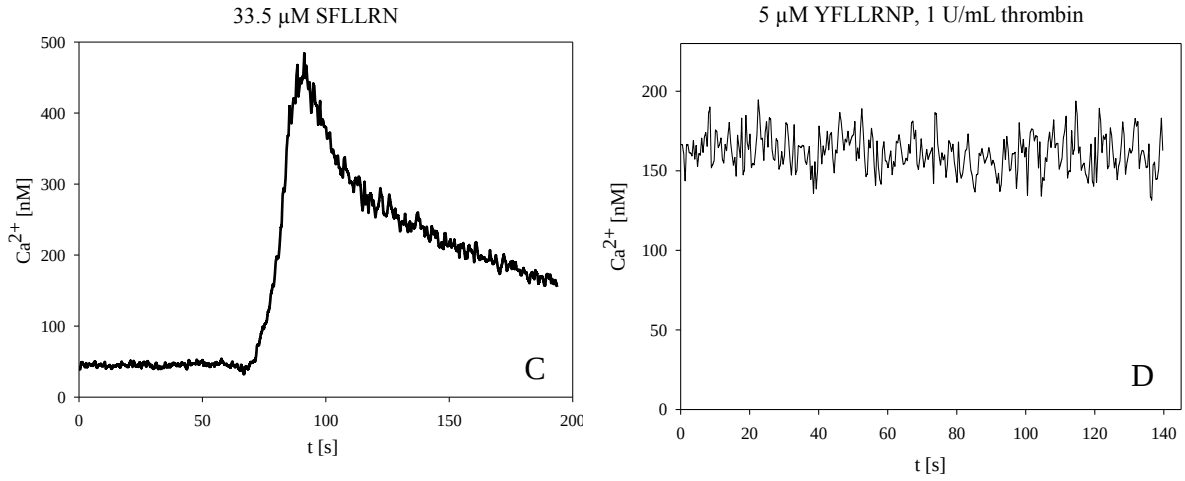

Fig. 4.11: Ca^{2+}-mobilization in human platelets by adding: A: 1 U/mL thrombin, B: 50 µM ADP and C: 33.5 µM SFLLRN, respectively. D: Blocking of thrombin mediated PAR_1 activation was achieved by 15 min preincubation with 5 µM YFLLRNP

Thrombin signalling in platelets has been proposed to be mediated by proteinase activated receptors 1 and 4 ($PAR_{1, 4}$). Therefore, a PAR_1-agonistic peptide (SFLLRN) was used to control Ca^{2+}-mobilization mediated by PAR_1. Preincubation of the platelets with a PAR_1 blocking peptide (YFLLRNP) showed that addition of thrombin did not trigger Ca^{2+}-mobilization anymore (**Fig. 4.11**). Thus, in human platelets the thrombin triggered increase in intracellular Ca^{2+} was the result of PAR_1 activation.

4.3.9. Hyaluronan degradation by Hyal-2 in activated human platelets

Viscosimetric measurements could not be performed with activated platelets because the resulting platelet clot would lead to a plug in the capillary of the used viscosimeter. Thus, only electrophoretic investigations were carried out. Incubation mixtures containing hyaluronan from *S. zooepidemicus* and activated or non-activated human platelets were used and compared to the migration pattern of HA fragments generated by rhHyal-1. In **Fig. 4.12** the migration pattern of the samples are shown.

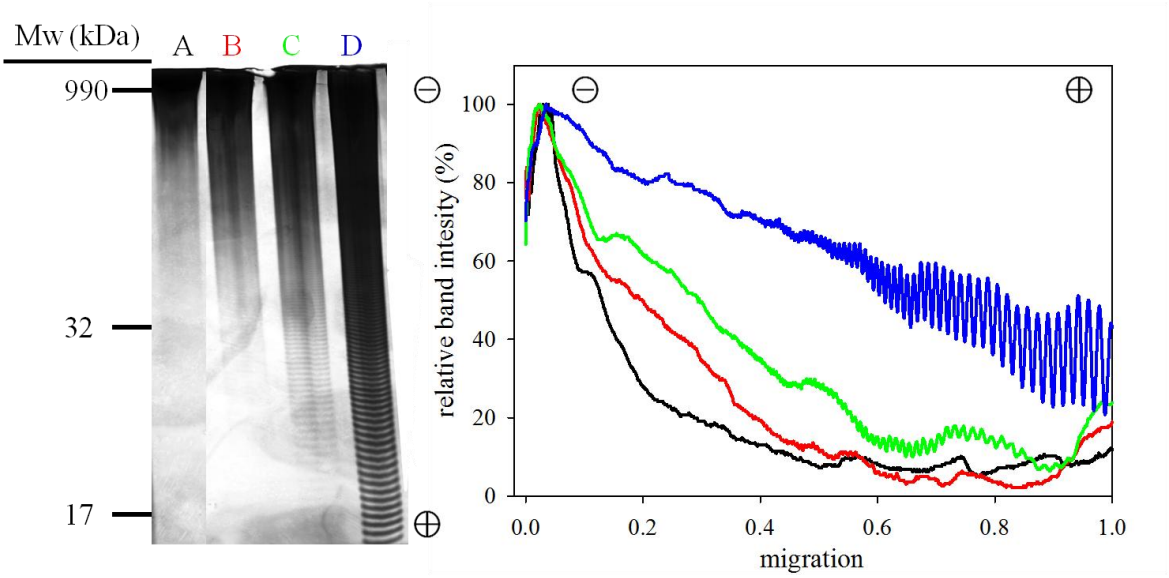

Fig. 4.12: PAGE and corresponding densitometric scan of hyaluronan from *S. zooepidemicus* (lane A) incubated with activated human platelets (lane B), non-activated human platelets (lane C). Incubation conditions were: 37 °C, 72 h. Migration patterns were compared to HA fragments generated by 0.0042 U/mL rhHyal-1 (lane D). Incubation conditions: 37 °C, 24 h

Apparently, there is a difference in the migration patterns of HA fragments generated by activated or non-activated platelets. It seems that activated human platelets are also able to degrade hyaluronan, but to a lesser extent than non-activated platelets. Although the protein content could not be reliably determined, because collagen was used for platelet activation, platelet numbers in the incubation mixtures were the same.

Another explanation for the different activities could be that Hyal-2 might be concentrated in platelet microparticles [1] (PMPs), which are produced and released during platelet activation (Warren and Vales, 1972; Wolf, 1967), especially after activation with strong agonists like thrombin and collagen (Nomura, 2001), which were used in this study.

4.3.10. Detection of enzymatic activity of Hyal-2 in murine platelets by viscosimetry

As contamination of platelet preparations with plasma Hyal-1 cannot be excluded, platelet preparations from Hyal-2 knock-out (KO) mice (Jadin et al., 2008) were used to assess the effectiveness of Hyal-1 removal by extensive washing. Hyal-2 KO mice displayed moderate thrombocytopenia (443 ± 106 vs. 1175 ± 126 x 103/µL). This was taken into account in further investigations by diluting platelet preparations from wildtype (WT) mice accordingly. Dilution was controlled by determination of the protein content in the samples with the BCA assay. **Fig. 4.13** shows that viscosimetric measurements with wildtype

[1] Prof. Dr. B. Flamion, Namur (Belgium), personal communication

platelets resulted in a significantly lower viscosity (P = 0.026) after an incubation time of 72 h in comparison to incubation mixtures containing Hyal-2 KO platelets. Plasma from Hyal-2 KO mice was investigated to confirm functional Hyal-1 expression in these animals.

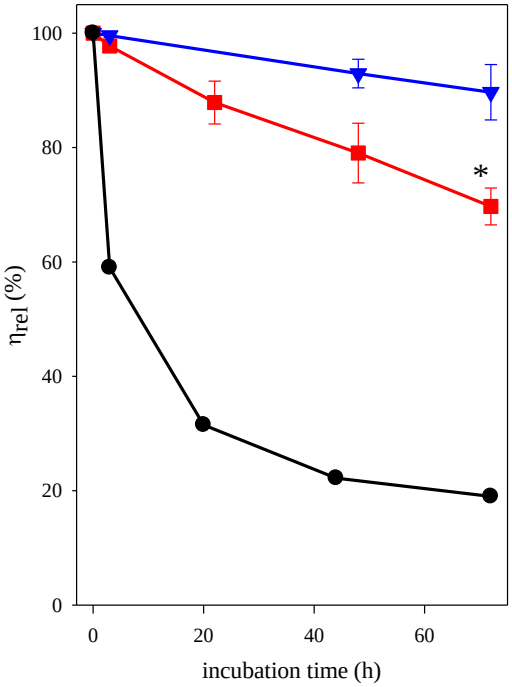

Fig. 4.13: Viscosimetric analysis of enzymatic activity in murine wildtype platelets (squares) compared to Hyal-2 KO platelets (triangles) and plasma Hyal-1 from Hyal-2 KO mice (circles). Error bars represent SEM of 3 independent experiments.

4.3.11. Detection of hyaluronan fragments generated by murine platelet-derived Hyal-2 using electrophoresis

Polyacrylamide gel electrophoresis with subsequent combined alcian blue silver staining was performed to visualize differences in hyaluronan fragmentation by wildtype and Hyal-2 KO platelets, respectively. Plasma Hyal-1 from Hyal-2 KO mice served as positive control. As negative control an incubation mixture without platelets or plasma, incubated as long as the fragmentation samples, was used. **Fig. 4.14** clearly shows the differences in the fragmentation pattern between the respective samples. There was no difference in the migration pattern between HA incubated alone and HA treated with platelets from Hyal-2 KO mice. Wildtype platelets are able to degrade hyaluronan to an approximate size of 17 kDa, which is also consistent with the findings of Lepperdinger et al. (Lepperdinger et al., 2001; Lepperdinger et al., 1998). Hyal-2 KO mice functionally express Hyal-1, which is present in plasma and degrades HA into small oligosaccharides.

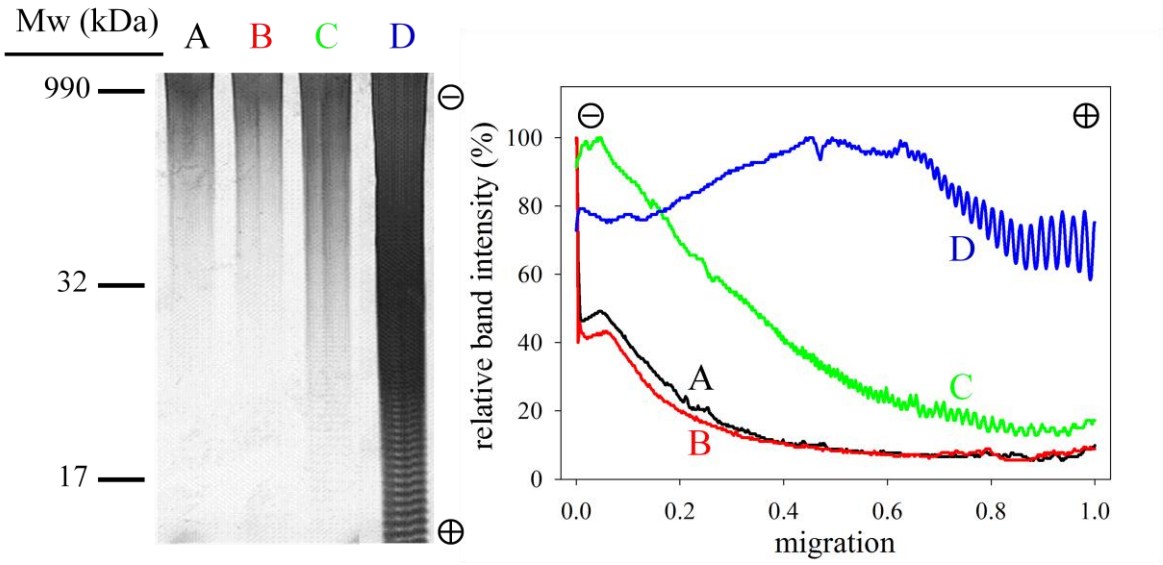

Fig. 4.14: PAGE and corresponding densitometric scans of hyaluronan from umbilical cord (lane A) incubated with Hyal-2 KO platelets (lane B), platelets from wildtype mice (lane C) and plasma from Hyal-2 KO mice (lane D), respectively. Incubation conditions were: 37 °C, 72 h.

4.3.12. Hyaluronan degradation by Hyal-2 derived from activated murine platelets

By analogy with activated human platelets only an electrophoretic assay was performed in case of activated murine platelets. There was a slight difference in the migration pattern of non-activated and activated wildtype platelets. Non-activated platelets apparently degrade HA to smaller fragments than activated ones (**Fig. 4.15**). This observation is consistent with the results obtained from activated human platelets and supports the speculation about Hyal-2 being released in PMPs during activation. But this suggestion has to be investigated in more detail by isolating PMPs after platelet activation and detecting Hyal-2 in the microparticles.

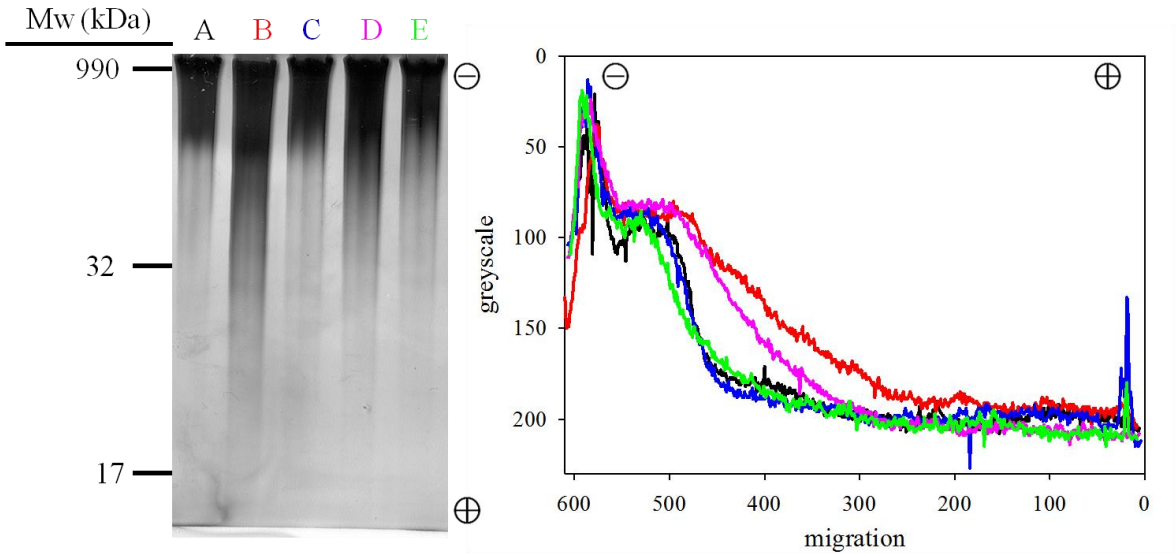

Fig. 4.15: PAGE and corresponding densitometric scans of hyaluronan from umbilical cord (lane A) incubated with non-activated wildtype platelets (lane B), activated wildtype platelets (lane D), non-activated Hyal-2 KO platelets (lane C) and activated KO platelets (lane E). Incubation conditions were: 37 °C, 72 h.

4.4. Summary and conclusion

As de la Motte et al. reported that Hyal-2 is the only hyaluronidase expressed in platelets with no evidence for Hyal-1 (de la Motte et al., 2009), platelets were chosen as source for Hyal-2. Due to the controversial discussion with respect to Hyal-2 activity (Bourguignon et al., 2004; de la Motte et al., 2009; Harada and Takahashi, 2007; Lepperdinger et al., 1998; Vigdorovich et al., 2007; Vigdorovich et al., 2005) we investigated non-activated human and murine platelets particularly with regard to HA degrading activity. Hyaluronidase-2 expressed in human platelets appears to consist of two glycosylated isoforms with different pI values.

The significant decrease in HA viscosity, particularly at the beginning of the degradation reaction (Hoechstetter, 2005) as well as the high sensitivity of the assay favors the use of viscosimetry for the detection of Hyal-2 activity. Human platelet-rich plasma preparations were extensively washed to isolate platelets and remove residual plasma Hyal-1. Incubations of HA with washed non-activated platelets showed a significantly higher decrease in viscosity compared to HA incubations with heat-inactivated platelets at acidic pH. The results obtained from investigations with human platelets were consistent with those obtained from investigations with rhHyal-2. Enzymatic activity depended on the

source of hyaluronan used; HA from microbial origin was degraded slower and to a lesser extent than HA from vertebrate origin.

To get reliable data, additionally murine platelet preparations were investigated. Particularly interesting was the comparison between HA degrading activity of wildtype platelets and Hyal-2 knock out platelets. We can exclude false positive results by the action of residual plasma Hyal-1 as only the HA incubations containing wildtype platelets, corrected for platelet counts, showed a decrease in viscosity within 72 h.

Furthermore, activated platelet preparations were used to determine if there is a difference in hyaluronan degrading activity between activated and non-activated platelets. The obtained results led us to the suggestion, that Hyal-2 might be released in platelet microparticles during activation, because the generated fragments from HA incubation with activated platelets seemed to be greater in the performed electrophoretic assay, compared to those from incubations with non-activated platelets. This could be observed with both types of platelets, human and murine. Hyal-2 is associated with lipid rafts in the plasma membrane (Andre et al., 2011) and PMPs are produced after platelet activation by e.g. thrombin and collagen, they contain several components of the platelet membrane (Nomura, 2001), so Hyal-2 could be concentrated in the microparticles. This speculation needs to be verified in further investigations using isolated PMPs.

Previously, platelet membranes were demonstrated to be able to induce airway smooth muscle cell (ASMC) proliferation (Svensson Holm et al., 2011) and very recently, the influence of HA on platelet-induced ASMC proliferation was investigated. The presence of platelets causes a significant increase in the proliferation of ASMC after 24 h of coincubation and this could be reduced by adding a CD44 blocking antibody. Additionally, ASMC were found to synthesize considerable amounts of HA and it was concluded that the interaction between ASMC derived HA, platelets and CD44 causes enhanced proliferation (Svensson Holm et al., 2012). Thus, we propose, that platelet-derived Hyal-2 degrades hyaluronan synthesized by ASMC to fragments that can stimulate proliferation, which can be mediated by a signaling pathway through CD44 like described by Slevin et al. (Slevin et al., 2007). A hypothetical model is shown in **Fig. 4.16**. Such interactions could also take place with other proliferating cells.

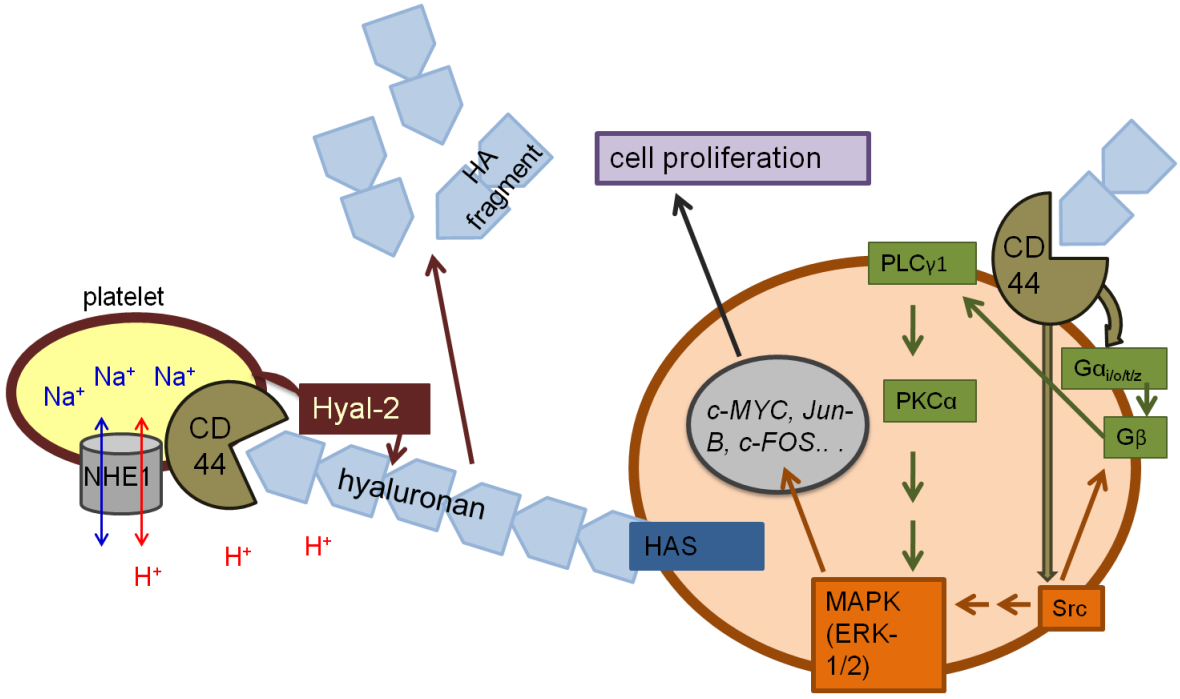

Fig. 4.16: Possible interaction of platelets with ASMC and CD44 cell signalling pathway modified from Slevin et al. (Slevin et al., 2007). Hyaluronan synthase produces hyaluronan, which is bound by CD44 on the platelet membrane. NHE1 supplies acidic microenvironment (Bourguignon et al., 2004) necessary for platelet-derived Hyal-2 activity. Hyaluronan fragments generated by Hyal-2 bind to CD44 on ASMC membrane and trigger complex cell signalling pathway that leads to cell proliferation.

4.5. References

Andre, B., Duterme, C., Van Moer, K., Mertens-Strijthagen, J., Jadot, M., Flamion, B., 2011. Hyal2 is a glycosylphosphatidylinositol-anchored, lipid raft-associated hyaluronidase. Biochem. Biophys. Res. Commun. 411, 175-179.

Bourguignon, L.Y., Singleton, P.A., Diedrich, F., Stern, R., Gilad, E., 2004. CD44 interaction with Na+-H+ exchanger (NHE1) creates acidic microenvironments leading to hyaluronidase-2 and cathepsin B activation and breast tumor cell invasion. J. Biol. Chem. 279, 26991-27007.

Bradford, M.M., 1976. A rapid and sensitive method for the quantitation of microgram quantities of protein utilizing the principle of protein-dye binding. Anal. Biochem. 72, 248-254.

Cherr, G.N., Meyers, S.A., Yudin, A.I., VandeVoort, C.A., Myles, D.G., Primakoff, P., Overstreet, J.W., 1996. The PH-20 protein in cynomolgus macaque spermatozoa: identification of two different forms exhibiting hyaluronidase activity. Dev. Biol. 175, 142-153.

Danese, S., Scaldaferri, F., Papa, A., Pola, R., Sans, M., Gasbarrini, G., Pola, P., Gasbarrini, A., 2004. Platelets: new players in the mucosal scenario of inflammatory bowel disease. Eur. Rev. Med. Pharmacol. Sci. 8, 193-198.

de la Motte, C., Nigro, J., Vasanji, A., Rho, H., Kessler, S., Bandyopadhyay, S., Danese, S., Fiocchi, C., Stern, R., 2009. Platelet-derived hyaluronidase 2 cleaves hyaluronan into fragments that trigger monocyte-mediated production of proinflammatory cytokines. Am. J. Pathol. 174, 2254-2264.

de la Motte, C.A., Hascall, V.C., Drazba, J., Bandyopadhyay, S.K., Strong, S.A., 2003. Mononuclear leukocytes bind to specific hyaluronan structures on colon mucosal smooth muscle cells treated with polyinosinic acid: Polycytidylic acid - Inter-alpha-trypsin inhibitor is crucial to structure and function. Am. J. Pathol. 163, 121-133.

Fiszer-Szafarz, B., Litynska, A., Zou, L., 2000. Human hyaluronidases: electrophoretic multiple forms in somatic tissues and body fluids. Evidence for conserved hyaluronidase potential N-glycosylation sites in different mammalian species. J. Biochem. Biophys. Methods 45, 103-116.

Grynkiewicz, G., Poenie, M., Tsien, R.Y., 1985. A new generation of Ca2+ indicators with greatly improved fluorescence properties. J. Biol. Chem. 260, 3440-3450.

Harada, H., Takahashi, M., 2007. CD44-dependent intracellular and extracellular catabolism of hyaluronic acid by hyaluronidase-1 and-2. J. Biol. Chem. 282, 5597-5607.

Harrison, P., 2005. Platelet function analysis. Blood Rev. 19, 111-123.

Hoechstetter, J., 2005. Characterisation of bovine testicular hyaluronidase and a hyaluronate lyase from Streptococcus agalactiae, Doctoral thesis, University of Regensburg.

Hofinger, E., 2007. Recombinant expression, purification and characterization of human hyaluronidases, Doctoral thesis, University of Regensburg.

Hofinger, E.S.A., Spickenreither, M., Oschmann, J., Bernhardt, G., Rudolph, R., Buschauer, A., 2007. Recombinant human hyaluronidase Hyal-1: insect cells versus Escherichia coli as expression system and identification of low molecular weight inhibitors. Glycobiology 17, 444-453.

Horstman, L., Jy, W., Ahn, Y., Zivadinov, R., Maghzi, A., Etemadifar, M., Steven Alexander, J., Minagar, A., 2010. Role of platelets in neuroinflammation: a wide-angle perspective. J. Neuroinflammation 7, 10.

Irving, P., Rampton, D., 2007. Platelet-leucocyte aggregation in IBD. Am. J. Hematol. 82, 686.

Jadin, L., Wu, X.L., Ding, H., Frost, G.I., Onclinx, C., Triggs-Raine, B., Flamion, B., 2008. Skeletal and hematological anomalies in HYAL2-deficient mice: a second type of mucopolysaccharidosis IX? FASEB J. 22, 4316-4326.

Koshiishi, I., Shizari, M., Underhill, C.B., 1994. Cd44 Can Mediate the Adhesion of Platelets to Hyaluronan. Blood 84, 390-396.

Laudat, A., Guechot, J., Lecourbe, K., Damade, R., Palluel, A.M., 2000. Hyaluronidase activity in serum of patients with monoclonal gammapathy. Clin. Chim. Acta 301, 159-167.

Lepperdinger, G., Mullegger, J., Kreil, G., 2001. Hyal2 - less active, but more versatile? Matrix Biol. 20, 509-514.

Lepperdinger, G., Strobl, B., Kreil, G., 1998. HYAL2, a human gene expressed in many cells, encodes a lysosomal hyaluronidase with a novel type of specificity. J. Biol. Chem. 273, 22466-22470.

Lindemann, S., Kramer, B., Daub, K., Stellos, K., Gawaz, M., 2007. Molecular pathways used by platelets to initiate and accelerate atherogenesis. Curr. Opin. Lipidol. 18, 566-573.

Natowicz, M.R., Wang, Y., 1996. Human serum hyaluronidase: Characterization of a clinical assay. Clin. Chim. Acta 245, 1-6.

Nomura, S., 2001. Function and clinical significance of platelet-derived microparticles. Int. J. Hematol. 74, 397-404.

Perschl, A., Lesley, J., English, N., Trowbridge, I., Hyman, R., 1995. Role of CD44 cytoplasmic domain in hyaluronan binding. Eur. J. Immunol. 25, 495-501.

Poole, A.R., Dieppe, P., 1994. Biological markers in rheumatoid arthritis. Semin. Arthritis Rheum. 23, 17-31.

Rai, S.K., Duh, F.M., Vigdorovich, V., Danilkovitch-Miagkova, A., Lerman, M.I., Miller, A.D., 2001. Candidate tumor suppressor HYAL2 is a glycosylphosphatidylinositol (GPI)-anchored cell-surface receptor for jaagsiekte sheep retrovirus, the envelope protein of which mediates oncogenic transformation. Proc. Natl. Acad. Sci. U. S. A. 98, 4443-4448.

Rutherford, P., Pizzonia, J., AbuAlfa, A., Biemesderfer, D., Reilly, R., Aronson, P., 1997. Sodium-hydrogen exchange isoform expression in blood cells: Implications for studies in diabetes mellitus. Experimental and Clinical Endocrinology & Diabetes 105, 13-16.

Shen, J., Ran, Z.H., Zhang, Y., Cai, Q., Yin, H.M., Zhou, X.T., Xiao, S.D., 2009. Biomarkers of altered coagulation and fibrinolysis as measures of disease activity in active inflammatory bowel disease: a gender-stratified, cohort analysis. Thromb. Res. 123, 604-611.

Sleeman, J., Rudy, W., Hofmann, M., Moll, J., Herrlich, P., Ponta, H., 1996. Regulated clustering of variant CD44 proteins increases their hyaluronate binding capacity. The Journal of Cell Biology 135, 1139-1150.

Slevin, M., Krupinski, J., Gaffney, J., Matou, S., West, D., Delisser, H., Savani, R.C., Kumar, S., 2007. Hyaluronan-mediated angiogenesis in vascular disease: uncovering RHAMM and CD44 receptor signaling pathways. Matrix Biol. 26, 58-68.

Svensson Holm, A.-C.B., Bengtsson, T., Grenegård, M., Lindström, E.G., Hyaluronic acid influence on platelet-induced airway smooth muscle cell proliferation. Exp. Cell Res.

Svensson Holm, A.-C.B., Bengtsson, T., Grenegård, M., Lindström, E.G., 2011. Platelet membranes induce airway smooth muscle cell proliferation. Platelets 22, 43-53.

Svensson Holm, A.-C.B., Bengtsson, T., Grenegård, M., Lindström, E.G., 2012. Hyaluronic acid influence on platelet-induced airway smooth muscle cell proliferation. Exp. Cell Res. 318, 632-640.

Vigdorovich, V., Miller, A.D., Strong, R.K., 2007. Ability of hyaluronidase 2 to degrade extracellular hyaluronan is not required for its function as a receptor for jaagsiekte sheep retrovirus. J. Virol. 81, 3124-3129.

Vigdorovich, V., Strong, R.K., Miller, A.D., 2005. Expression and characterization of a soluble, active form of the jaagsiekte sheep retrovirus receptor, Hyal2 (vol 79, pg 79, 2005). J. Virol. 79, 3228-3228.

Warren, B.A., Vales, O., 1972. The release of vesicles from platelets following adhesion to vessel walls in vitro. Br. J. Exp. Pathol. 53, 206-215.

Wolf, P., 1967. The nature and significance of platelet products in human plasma. Br. J. Haematol. 13, 269-288.

Chapter 5

Determination of Hyal-2 activity in red blood cells

5.1. Introduction

Red blood cells, also called erythrocytes, are derived from hematopoietic stem cells in the bone marrow and are anucleated biconcave disc shaped cells in their mature form. The cells are highly specialized and well adapted for their primary function of transporting oxygen from the lungs to all of the body tissues. The red blood cell is enclosed in a thin membrane that is composed of chemically complex lipids, proteins, and carbohydrates in a highly organized structure.

Erythrocytes express several adhesion molecules on their surface, like ICAM-4, CD44 and CD47 (Spring and Parsons, 2000), but they are generally considered to be nonadhesive to endothelial surfaces. However, in several pathologic conditions, adhesion of erythrocytes to the vascular endothelium is increased. For example, red blood cells in sickle cell disease and erythrocytes infected with *Plasmodium falciparum* have an increased binding to host endothelial cells and sequester in postcapillary venules, likely contributing to the fetal complication of cerebral malaria (Hebbel, 1991; Pasloske and Howard, 1994). As a hyaluronan receptor CD44 could contribute to red blood cell binding to the ECM.

Red blood cells were also found to tether to and roll on HA under shear conditions and this interaction was demonstrated to be mediated by CD44 (Kerfoot et al., 2008).

To our knowledge, there are no studies dealing with hyaluronidase activity in red blood cells, so far. Thus, we investigated human and murine red blood cells and their ghost membranes with respect to Hyal-1 and Hyal-2 expression and performed enzymatic activity assays in analogy to platelets described in Chapter 4.

5.2. Materials and methods

5.2.1. Isolation of human and murine red blood cells

Blood was collected and centrifuged as described in Chapter 4. After careful removal of the buffy coat, the red blood cell (RBC) fraction was washed five times with 0.9 % NaCl solution by centrifuging at 1000 g for 15 min.

5.2.2. Determination of RBC number in murine blood

The number of RBC in murine blood was determined using a Neubauer counting chamber. Therefore washed RBC were diluted 200-fold with Hayem´s solution (0.25 % $HgCl_2$, 2.5 % Na_2SO_4, 0.5 % NaCl) using a RBC pipette. After careful mixing, and discarding a few drops, a small volume of the RBC dilution was introduced under the coverslip, which was placed on the counting chamber. Cells were allowed to settle for 5 min before counting.

5.2.3. Preparation of erythrocyte ghost membranes

500 µL of washed, packed RBC´s were suspended in 10 mL of ice-cold 5 mM phosphate buffer (pH 8.0) and centrifuged at 9000 g for 20 min at 4 °C. The hemolytic fraction was discarded and the operation was repeated at least 5 times until the supernatant appeared colorless. Centrifugation was then increased to 20000 g and washing was repeated until the ghost membranes appeared yellow-whitish. Membranes were re-suspended in 1 mL of buffer stored at -80 °C until use.

5.2.4. SDS-PAGE and Western Blot analysis

Electrophoresis and immunodetection of Hyal-2 in RBC membranes was performed as described in Chapter 3. Primary antibodies for Western Blot analysis were: rabbit polyclonal anti-Hyal-2 (Abcam, Cambridge, UK) and mouse monoclonal anti-Hyal-1 (1D10) (Santa Cruz Biotechnology Inc., Santa Cruz, USA). Secondary antibodies were donkey anti-rabbit IgG-HRP (Santa Cruz Biotechnology Inc.) and goat anti-mouse IgG-HRP (Fc specific) (Sigma-Aldrich, Munich, Germany), respectively.

5.2.5. Viscosimetry and PAGE for determination of Hyal-2 activity in RBC

Hyaluronidase assays were the same as in Chapter 3. 100 µL of washed, packed RBC, 1 mL of RBC membrane preparation and 50 µL of plasma were used for incubations, respectively.

5.3. Results and discussion

5.3.1. Identification of Hyal-2 in RBCs and RBC membranes by immunodetection

By analogy with platelets, RBC´s and RBC membranes were investigated with respect to Hyal-2 expression by immunodetection using an anti-Hyal-2 and an anti-Hyal-1 primary antibody, respectively.

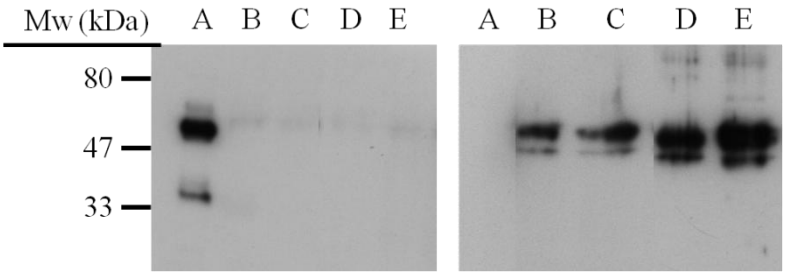

Fig. 5.1: Immunodetection of Hyal-1 (left) and Hyal-2 (right) in murine RBC (lane B), murine RBC membranes (lane C) and human RBC (lane D). rhHyal-1 (lane A) and rhHyal-2 (lane E) served as positive controls. Primary antibodies were polyclonal anti-Hyal-2 and monoclonal anti-Hyal-1. Secondary antibodies were HRP-conjugated and detection was achieved by ECL.

As in platelets, Hyal-2 is the only hyaluronidase expressed in human and murine RBC, respectively. Western Blot analysis showed two immunoreactive bands with a molecular mass of approximately 60 and 45 kDa (**Fig. 5.1**).

There was evidence for Hyal-1 expression neither in RBC membranes, nor in whole, washed RBC´s. Hence, RBC´s were investigated with respect to hyaluronidase activity.

5.3.2. Hyaluronidase activity assays of Hyal-2 in RBC

At first, a viscosimetric assay using whole washed murine RBC´s as sample was performed. Surprisingly, relative viscosity decreased dramatically after an incubation time of 20 h. The decrease in viscosity in the presence of 100 µL of RBC´s was even stronger in comparison to incubation mixtures containing 50 µL of murine plasma. PAGE with combined alcian blue silver staining revealed that fragments generated by RBC´s were smaller than 15 kDa, the determination of the fragment size was not possible (**Fig. 5.2**).

Although washed RBC preparations were able to degrade hyaluronan, we suppose that the observed enzymatic activity was due to contamination with Hyal-1 from residual plasma in the preparation. RBC´s are used to visualize HA-rich pericellular coats; this would not be possible, if RBS´s displayed such a high hyaluronidase activity (Clarris and Fraser, 1968; Knudson and Toole, 1985). Erythrocytes are very sensitive and should not be centrifuged at high speed to avoid severe damage. This explains why, despite careful separation, traces of plasma including Hyal-1 could not be completely removed.

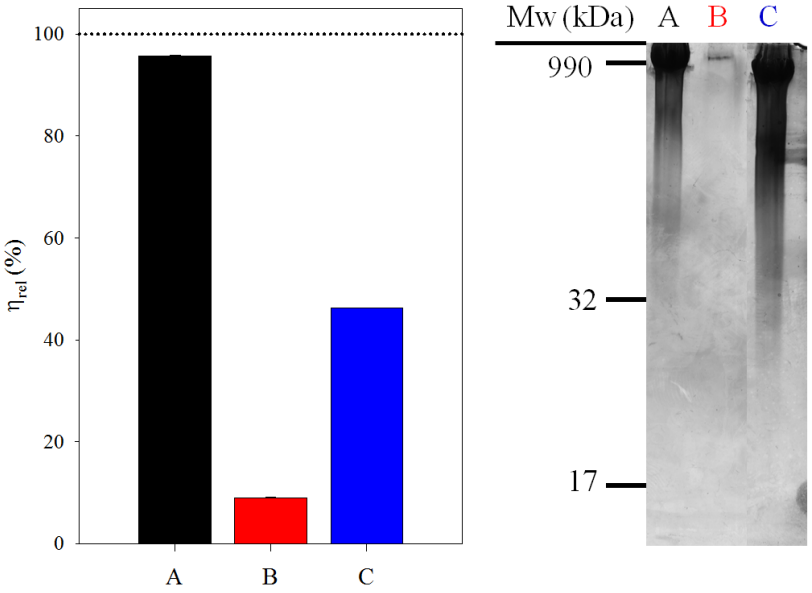

Fig. 5.2: Viscosimetric and electrophoretic analyses of incubation mixtures containing HA from *S. zooepidemicus*. A: control without sample at t = 20 h, B: 100 µL of murine RBCs at t = 20 h, C: 50 µL of murine plasma at t = 20 h.

5.3.3. Hyaluronidase activity assay of Hyal-2 in RBC membranes

Because of the surprising results of the viscosimetric investigations using whole erythrocytes, RBC membranes, which also contain Hyal-2, were investigated with respect to enzymatic activity. RBC membranes from wildtype and Hyal-2 KO mice were used for comparison. Prior to membrane preparation, RBC count was determined and equal amounts were used. Incubations were performed at different pH values considering potential differences in the pH dependency of Hyal-2 in RBC membranes and Hyal-2 in platelet membranes. As becomes obvious from **Fig. 5.3** there were no marked differences in the degradation pattern. HA and murine RBC membranes were incubated for 72 h at different pH values. Comparable results were obtained, when using human RBC membranes (data not shown).

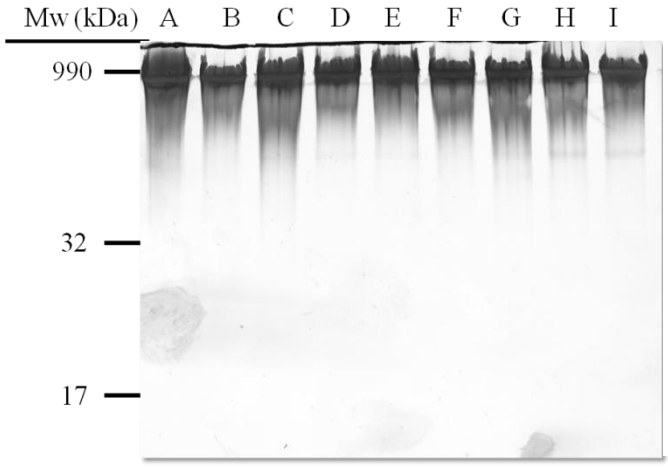

Fig. 5.3: PAGE with combined alcian blue silver staining for determination of Hyal-2 activity in murine RBC membranes. Investigations were performed with HA from rooster comb (lane A) incubated with membranes from wildtype (lanes B – E) and Hyal-2 KO RBC´s (lanes F – I) at pH 4.0 (lanes B, F), pH 5.0 (lanes C, G), pH 6.0 (lanes D, H) and pH 7.0 (lanes E, I), respectively. Incubation conditions were: 37 °C, 72 h.

The results from the electrophoretic analysis obtained with RBC membranes support the suggestion that the activities obtained with whole RBC´s were due to residual plasma Hyal-1 in the sample.

5.4. Summary and conclusion

By analogy with platelets, red blood cells only express Hyal-2 with no evidence for Hyal-1 as determined by immunodetection. Thus, enzymatic Hyal-2 activity was investigated with RBC´s and RBC membranes, respectively, using viscosimetric and electrophoretic methods.

Viscosimetric measurements with whole RBS´s showed a surprisingly high HA degrading activity, which was considered as residual plasma Hyal-1 activity due to insufficient washing of the highly sensitive erythrocytes. Therefore, RBC ghost membranes were prepared and incubated with HA at different pH-values, to exclude, that possible Hyal-2 activity in RBC membranes is different compared to platelet preparations.

The performed electrophoretic assay revealed no hyaluronan degrading activity derived from RBC membranes at any pH tested, indicating that the results obtained with whole RBC´s were really due to Hyal-1.

These results support speculations that either RBC associated Hyal-2 is not involved in hyaluronan degradation, but has other functions in the erythrocytes. Alternatively, there exists a not yet characterized inhibitor, which may be inactivated to switch onHyal-2 activity under certain physiological conditions

5.5. References

Clarris, B.J., Fraser, J.R.E., 1968. On the pericellular zone of some mammalian cells in vitro. Exp. Cell Res. 49, 181-193.

Hebbel, R.P., 1991. Beyond hemoglobin polymerization: the red blood cell membrane and sickle disease pathophysiology. Blood 77, 214-237.

Kerfoot, S.M., McRae, K., Lam, F., McAvoy, E.F., Clark, S., Brain, M., Lalor, P.F., Adams, D.H., Kubes, P., 2008. A novel mechanism of erythrocyte capture from circulation in humans. Exp. Hematol. 36, 111-118.

Knudson, C.B., Toole, B.P., 1985. Changes in the Pericellular Matrix during Differentiation of Limb Bud Mesoderm. Dev. Biol. 112, 308-318.

Pasloske, B.L., Howard, R.J., 1994. Malaria, the red cell, and the endothelium. Annu. Rev. Med. 45, 283-295.

Spring, F.A., Parsons, S.F., 2000. Erythroid cell adhesion molecules. Transfus. Med. Rev. 14, 351-363.

Chapter 6

Investigations on the effect of hyaluronan digestion mixtures on the proliferation of human endothelial cells

6.1. Introduction

Many physiological and pathophysiological processes including wound healing, tissue repair, tumor growth and vascular diseases are associated with angiogenesis (Folkman, 1995). Moreover, hyaluronan and HA oligosaccharides have been demonstrated to play a role in the proliferation of several different cell types and in angiogenesis. Mostly, HA induced cell proliferation was correlated with the expression of CD44 on the cell surface.

The involvement of HA in angiogenesis was first suggested by West et al., who observed that degraded HA products with a length of 4 – 25 disaccharide units stimulated wound healing *in vivo* (West et al., 1985). Later, it was reported that semi-purified HA fragments consisting of 3 – 16 disaccharide units were able to stimulate proliferation and migration of endothelial cells, while non-degraded HA showed the opposite effect (West and Kumar, 1989). Trochon et al. studied the effect of a monoclonal CD44 antibody on two different endothelial cell lines and concluded that the cell surface receptor CD44 is involved in endothelial cell proliferation (Trochon et al., 1996).

Furthermore, hyaluronan was shown to induce proliferation of human melanoma cells, thereby CD44 was the principle mediator of this effect (Ahrens et al., 2001).The interaction of HA and CD44 enhanced the proliferation of biliary epithelial cells (BEC), which was determined by treating immortalized mouse intrahepatic BEC with HA and antagonizing the effects with an anti-CD44 antibody (He et al., 2008). The proliferation of undifferentiated progenitor cells was also enhanced through HA mediated CD44 signalling (Hamann et al., 1995). David-Raoudi et al. demonstrated increased proliferation of human dermal fibroblasts by addition of HA fragments containing 6 and 440 disaccharide units. The strongest effect occurred at a concentration of 10 – 50 µg/mL. The authors suggested an implication of CD44, although the involvement of other receptors was not ruled out (David-Raoudi et al., 2008).

The aim of this study was to investigate possible effects of HA fragments generated by human platelet-derived Hyal-2 on the proliferation of human endothelial cells. Additionally, the effect of HA digests prepared with BTH and rhHyal-1 were investigated, and high molecular weight HA and a HA oligosaccharide preparation with HA fragments < 10 kDa were used as controls. The expression of two HA receptors, namely CD44 and RHAMM, was determined by Western Blot and flow cytometric analyses.

6.2. Materials and methods

6.2.1. Cell culture conditions and storage

Immortalized human microvascular endothelial cells (HMEC-1, kindly provided by Prof. Dr. J. Heilmann) were grown in 75-cm² culture flasks (Sarstedt, Nürnbrecht, Germany) in Dulbecco´s Modified Eagle Medium (DMEM, Sigma-Aldrich, Munich, Germany) containing 15 % fetal calf serum (FCS, Biochrom, Berlin, Germany) and 2 mM L-glutamine (Biochrom, Berlin, Germany). The cells were cultured in a water-saturated atmosphere of 95 % air and 5 % CO_2 at 37 °C and were serially passaged following trypsination using trypsin (0.05 %)/EDTA (0.02 %) solution. For a detailed characterization of the cell see Ades et al. (Ades et al., 1992).

For long term storage, confluent cells were detached from the bottom of the culture flask by trypsination, followed by trypsin inactivation of adding fresh medium, containing serum. Cells were counted in a Casy® 1 TTC cell counter (Schärfe Systems, Reutlingen, Germany), then centrifuged at 1000 g for 5 min and re-suspended in freezing medium (DMEM, 15 % FCS, 2 mM L-glutamine, 10 % DMSO) to a final cell density of $1 \cdot 10^6$ cells/mL. The suspension was split into aliquots of 1 mL and cooled down slowly for the storage in liquid nitrogen. For revival an aliquot of frozen cells was quickly thawed and diluted with 25 mL of fresh medium. After attachment of the cells to the bottom of the culture flask, medium was exchanged with fresh medium to remove residual DMSO.

6.2.2. Preparation of cell lysates for SDS-PAGE/Western Blot

Confluent cells in a 75-cm² culture flask were trypsinized and washed 3 times with PBS (800 g, 5 min). The pellet was re-suspended in 5 x the pellet volume of PBS, frozen in liquid nitrogen and thawed at room temperature. The freezing and thawing cycle was repeated 10 times to completely disrupt the cells. The protein content of the lysates was determined by the Bradford assay. For SDS-PAGE/Western Blot, 10 µg of protein per band were applied to the gel.

6.2.3. SDS-PAGE and Western Blot analysis

Electrophoresis and Western Blot analysis were performed as described in Chapter 3. The primary antibodies were anti human CD44 rabbit monoclonal antibody (1:5000) and anti human CD168/RHAMM rabbit monoclonal antibody (1:5000) (both from Epitomics Inc.,

Burlingame, USA). As secondary antibody, donkey anti-rabbit IgG-HRP (Santa Cruz Biotechnology, Santa Cruz, USA) was used.

6.2.4. Hyaluronan receptor detection by flow cytometry

For further characterization of the hyaluronan receptor expression in the used cell line, a flow cytometric assay (FACS) was performed. Confluent HMEC-1 cells were trypsinized, suspended in PBS and centrifuged at 500 g for 5 min. After re-suspension in PBS, containing 10 % FCS and cell counting, a cell density of $1 – 2 \cdot 10^6$ /mL was adjusted with PBS/FCS. The cell suspension was split into aliquots of 500 µL and the primary antibody was added to an appropriate dilution (CD44: 1:30, RHAMM: 1:500). Following 1 h of incubation, cells were washed 3 times with PBS (400 g, 5 min, 4 °C) and then re-suspended in a solution of 3 % BSA in PBS, containing the secondary antibody at a dilution of 1:250 (goat-anti-rabbit IgG, phycoerythrin conjugated from Rockland Inc., Gilbertsville, USA). After 1 h of incubation in the dark, cells were washed again twice with PBS, re-suspended in 500 µL of 3 % BSA/ PBS and measured in a FacsCalibur™ (Becton Dickinson, Heidelberg Germany). Instrument settings were: FSC: E-1, SSC: 350, Fl-2, flow high. Raw data were averaged with the WinMDI 2.9 software and then exported to SigmaPlot™ 11.0.

6.2.5. Preparation of different hyaluronan digestion mixtures

Hyaluronan digestion mixtures were prepared by incubation of HA from rooster comb (Sigma-Aldrich, Munich, Germany) with BTH, rhHyal-1 and human platelet membrane preparation, respectively. Incubation mixtures contained 8 mL of McIlvaine´s buffer (pH 4.0 for rhHyal-1 and platelets, pH 5 for BTH), 2 mL of BSA solution (0.2 mg/mL), 2 mL of HA solution (5 mg/mL) and 3 mL of enzyme sample. Final enzymatic activities for rhHyal-1 and BTH were 0.28 U and 0.033 U, respectively. The mixtures were incubated at 37 °C for 48 h, then dialyzed against 0.1 M ammonium acetate using a SpectraPor MWCO 500 membrane and lyophilized. Characterization of the HA digestions was achieved by polyacrylamide gel electrophoresis as described in Chapter 3 for longer HA fragments but with 15 % PAA gels and by High Performance Anion Exchange Chromatography with pulsed amperometric detection (HPAEC-PAD)[2] for fragments of smaller chain length.

[2] M. Rothenhöfer, personal communication

6.2.6. Crystal violet assay for proliferation studies

For endothelial cell proliferation studies, the crystal violet assay was performed as described by Bernhardt et al. (Bernhardt et al., 1992). 100 µL of cell suspension were seeded in 96-well flat-bottomed microtiter plates (Greiner, Frickenhausen, Germany) at a density of about 15 cells/ microscopic field (magnification: 320 x). The plates were incubated at 37 °C (water-saturated atmosphere, 5 % CO_2) for 24 h before adding the HA digests. Therefor the lyophilisates were solved in water to a concentration of 10 mg/mL and sterile filtered, mixed with fresh medium and 100 µL were added to the cells. Final concentrations of the hyaluronan digests were: 5, 10, 30, 50 and 100 µg/mL. As controls high molecular weight HA (nHA) from rooster comb and HA oligosaccharides with an average molecular weight < 10 kDa (o-HA, Hyalo-Oligo® was a kind gift from Kewpie Corporation, Tokyo, Japan) were used. On every plate two rows served as growth controls where no HA was added and one row (n = 8) was used per HA concentration.

After various periods of incubation, the culture medium was shaken off the plates and the cells were fixed with a 1 % solution of glutardialdehyde in PBS and stored at 4 °C. At the end of the experiment all plates were stained with a 0.02 % aqueous solution of crystal violet simultaneously. After washing the plates with water and dissolving bound stain with 180 µL/well of 70 % ethanol, absorbance was measured at 580 nm using a Tecan Genios Pro microtiter plate reader (Tecan, Crailsheim, Germany) with XFluor Genios Pro software version V.4.55.

Results are presented as plots of absorbance versus time of incubation using SigmaPlot version 11.0.

6.3. Results and discussion

6.3.1. Expression of the hyaluronan receptors CD44 and RHAMM by HMEC-1 cells

6.3.1.1. Western Blot analysis

Western Blot analysis of HMEC-1 lysate for CD44 and RHAMM revealed that only RHAMM is expressed. A MCF-7 cell lysate served as positive control for RHAMM immunodetection (Product data sheet from Epitomics). For CD44 control, HT-29 cells were used, because these cells were previously shown to express the receptor isoform CD44 E (Dougherty et al., 1994). However, the used primary antibody was possibly

unsuitable for the detection of CD44 isoforms, both in endothelial and HT-29 cells, because no bands were detectable in the Western Blot (data not shown).

The other hyaluronan receptor RHAMM was detected as a single band, with a molecular weight of approximately 84 kDa, which was found in cell lysates of both, MCF-7 and HMEC-1 (**Fig. 6.1**). The experimentally determined molecular mass is in good agreement with the calculated mass of 84.1 kDa for RHAMM Class A.

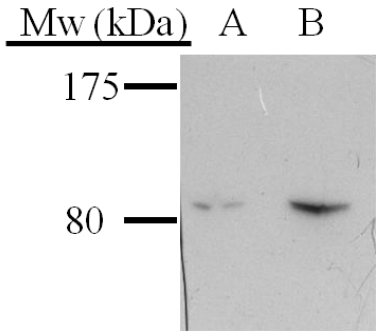

Fig. 6.1: Immunodetection of RHAMM in MCF-7 (lane A) and HMEC-1 (lane B) cell lysates. RHAMM monoclonal antibody was used as primary antibody, donkey-anti-rabbit IgG, peroxidase conjugated was used as secondary antibody and detection was achieved by ECL.

6.3.1.2. Determination of CD44 and RHAMM in endothelial cells by flow cytometry

In addition to the Western Blot analysis of the HA receptors, an indirect flow cytometric assay was performed. In analogy to Western Blot analysis, only RHAMM expression could be demonstrated as shown in **Fig. 6.2**. As negative controls the autofluorescence of the cells and possible binding of the secondary antibody alone were used. The secondary antibody alone did not bind to the HMEC-1 cells, thus the shift in fluorescence intensity after incubating with RHAMM antibody is due to binding of the primary antibody to the HA receptor. We were not able to show CD44 expression in HMEC-1 cells, neither by Western Blot analysis, nor in the FACS assay, whereas other authors reported on CD44 expression on the surface of these cells (Trochon et al., 1996; Xu et al., 1994). CD44 expression was suggested to be involved in endothelial cell proliferation, migration and angiogenesis (Savani et al., 2001; Trochon et al., 1996).

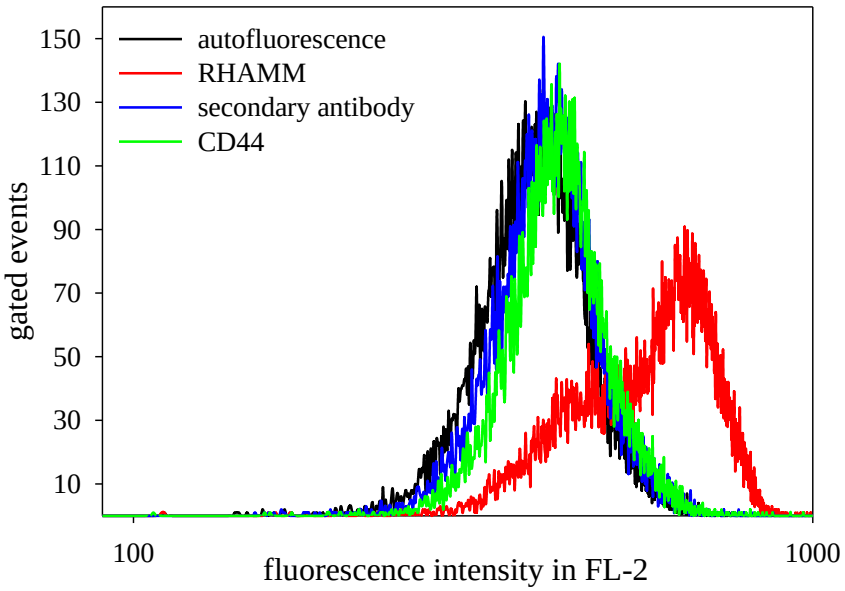

Fig. 6.2: Flow cytometric analysis of hyaluronan receptors in human endothelial cells. Primary antibodies were monoclonal antibodies against CD44 and RHAMM, respectively. The secondary antibody was phycoerythrin-conjugated goat-anti-rabbit IgG.

6.3.2. Characterization of the different hyaluronan digests

The lyophilized hyaluronan digests were analyzed with respect to the sizes of the fragments generated through enzymatic cleavage by the different hyaluronidases. Fragments with a higher molecular weight were analyzed by polyacrylamide gel electrophoresis. In **Fig. 6.3** the gel and the corresponding densitometric scan are depicted. Digestion of HA by human platelet membranes ended with fragments of approximately 10 kDa in size. rhHyal-1 degraded HA from rooster comb to fragments smaller than 20 kDa, but the smallest digestion products could not be determined with electrophoresis, because the detection limit with 15 % PAA gels was about 10 kDa. Hence, degradation products from rhHyal-1 activity had to be determined with another analytical method.

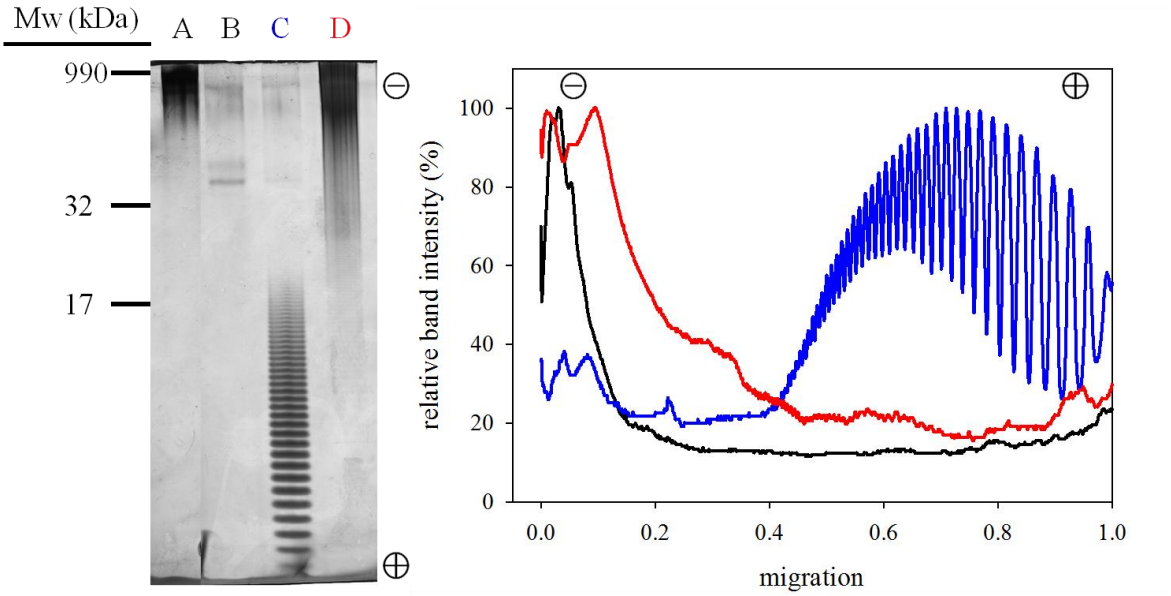

Fig. 6.3: Polyacrylamide gel electrophoresis and corresponding densitometric scans of lyophilized HA digests resulting from incubations of HA from rooster comb (lane A) with 0.03 U BTH (lane B), 0.28 U rhHyal-1 (lane C) and 0.2 mg proteins from human platelet membranes (lane D)

Obviously, BTH degrades HA to fragments, which are smaller than the detection limit of the electrophoretic method. Therefore a method developed by M. Rothenhöfer in our workgroup, HPAEC-PAD, was used to assess the sizes of low molecular weight fragments generated by BTH and rhHyal-1, respectively. The main product of HA degradation by BTH was the tetrasaccharide (n_2) (**Fig. 6.4 A**), which has already been identified as the major and smallest hydrolysis product by means of ion-spray mass spectrometry (Takagaki et al., 1994) and capillary zone electrophoresis (CZE) (Hofinger et al., 2007). For rhHyal-1 the reaction products vary between the tetrasaccharide (n_2) (**Fig. 6.4 B**) and HA fragments of molecular weights up to ~ 20 kDa.

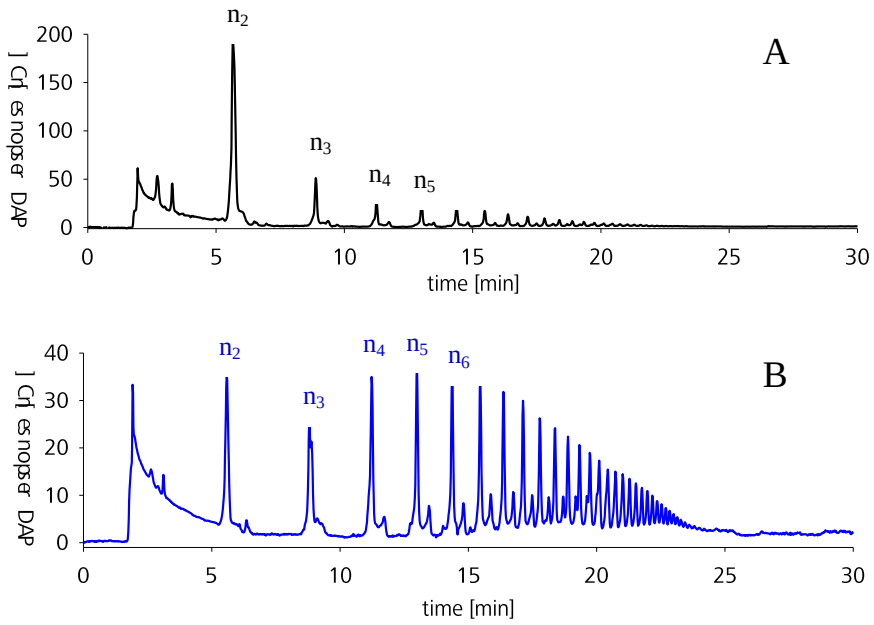

Fig. 6.4: HPAEC-PAD[3] of lyophilized HA digests resulting from incubation of HA from rooster comb with BTH (A) and rhHyal-1 (B), respectively. n represents 1 HA disaccharide unit, e.g. the tetrasaccharide is named n_2.

6.3.3. Investigations of the effect of HA digests on the proliferation of human endothelial cells

To investigate, if there is any effect on the proliferation of human microvascular endothelial cells by adding the different hyaluronan digests, a proliferation assay in the 96-well plate format was performed. Experiments were run over 162 h of incubation and cell densities in the wells were measured by crystal violet staining.

As illustrated by **Fig. 6.5**, we could hardly detect any effect on endothelial cell proliferation, neither by n-HA, nor by hyaluronan digests containing fragments of sizes suggested to be involved in cell signalling or angiogenesis. Possibly, these results correlate with the absence of CD44 on the surface of the used cells, as Lokeshwar et al. and Trochon et al. showed that blocking of CD44 with antibodies resulted in inhibited endothelial cell proliferation (Lokeshwar et al., 1996; Trochon et al., 1996). Savani et al. additionally investigated the effect of a RHAMM antibody and found that the CD44- but not the RHAMM antibody was able to inhibit EC proliferation (Savani et al., 2001). Only the HA digest resulting from incubation with human platelet membranes showed a slight dose-dependent inhibition of cell proliferation. This effect may be due to remaining platelet membrane components in the HA digest preparation.

[3] M. Rothenhöfer, personal communication

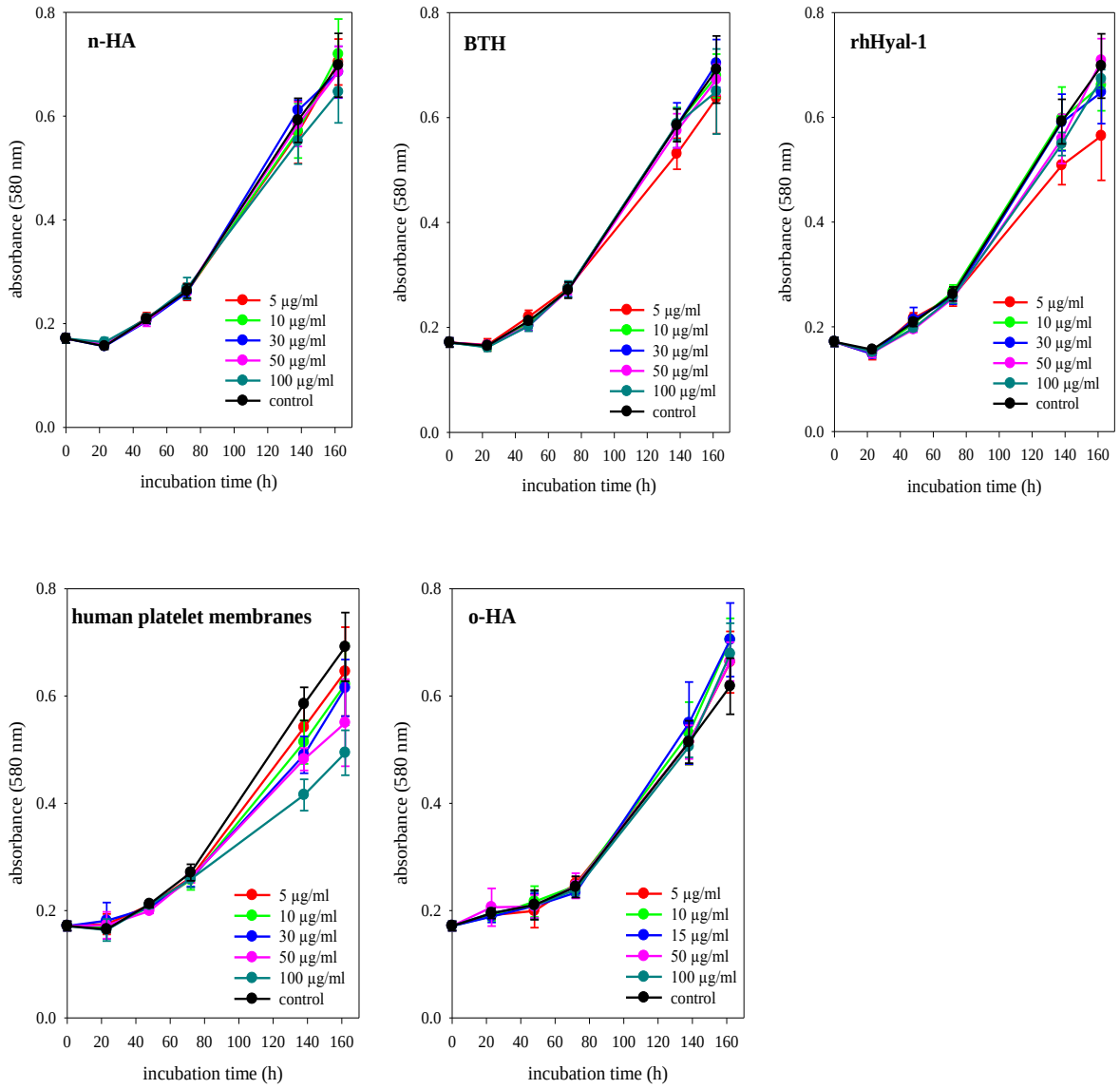

Fig. 6.5: Proliferation curves of human endothelial cells after addition of different concentrations of digests of high molecular weight HA (n-HA) from rooster comb with BTH, rhHyal-1 and human platelet membranes. Proliferation curves after addition of different concentrations of HA oligosaccharides (o-HA, molecular mass < 10 kDa) served as second control. Growth curves were determined with a kinetic microassay based on crystal violet staining.

6.4. Summary and conclusion

Different lyophilized hyaluronan digests were prepared in order to investigate their effect on human microvascular endothelial cell proliferation by a kinetic proliferation assay based on crystal violet staining. The fragments produced by BTH, rhHyal-1 and human platelet-derived Hyal-2 were characterized with respect to their size distribution by polyacrylamide gel electrophoresis with combined alcian blue silver staining and HPAEC-PAD, respectively. The main product of BTH degradation was the tetrasaccharide. This is

in accordance with previously reported results (Hofinger et al., 2007; Takagaki et al., 1994). Fragments generated by rhHyal-1 varied between the tetrasaccharide and oligosaccharides with molecular weights of ~ 20 kDa. Degradation of HA by incubation with human platelet membrane preparations containing Hyal-2 gave fragments of molecular weights > 10 kDa or 25 disaccharide units. Fragments which have been suggested to induce cell proliferation and angiogenesis were detectable in all lyophilized HA digests. High molecular weight HA and a HA preparation with a molecular weight of < 10 kDa were used as controls.

To determine the expression of the hyaluronan receptors CD44 and RHAMM, immunodetection methods were applied. Only RHAMM expression could be verified in the used HMEC-1 cells. There was no evidence for CD44, although this receptor was reported to be present in HMEC-1 by Trochon et al. and Xu et al. (Trochon et al., 1996; Xu et al., 1994). This indicates that either the antibody used in this study was not suitable to detect the CD44 isoform in the cells, or the cells did not express the HA receptor. The latter is supported by the results from the proliferation assay.

We could hardly determine any effect on HMEC-1 proliferation by adding the different HA digests at any concentration over an incubation period of 162 h. The absence of an effect can be explained by the lack of CD44 expression on the surface of the HMEC-1 cells, as the interaction between HA fragments and CD44 seems to be essential for inducing proliferation (Nandi et al., 2000; Savani et al., 2001; Slevin et al., 1998; Trochon et al., 1996). On the contrary, Gao et al. proposed that a RHAMM mediated signal pathway and not CD44 is responsible for stimulation of proliferation by HA oligosaccharides (Gao et al., 2008). As these authors used a porcine iliac vascular endothelial cell line, species-dependent differences in o-HA mediated cell proliferation cannot be ruled out, but this suggestion needs to be verified by further investigations.

6.5. References

Ades, E.W., Candal, F.J., Swerlick, R.A., George, V.G., Summers, S., Bosse, D.C., Lawley, T.J., 1992. HMEC-1: establishment of an immortalized human microvascular endothelial cell line. J. Invest. Dermatol. 99, 683-690.

Ahrens, T., Assmann, V., Fieber, C., Termeer, C., Herrlich, P., Hofmann, M., Simon, J.C., 2001. CD44 is the principal mediator of hyaluronic-acid-induced melanoma cell proliferation. J. Invest. Dermatol. 116, 93-101.

Bernhardt, G., Reile, H., Birnbock, H., Spruss, T., Schoenenberger, H., 1992. Standardized Kinetic Microassay to Quantify Differential Chemosensitivity on the Basis of Proliferative Activity. J. Cancer Res. Clin. Oncol. 118, 35-43.

David-Raoudi, M., Tranchepain, F., Deschrevel, B., Vincent, J.-C., Bogdanowicz, P., Boumediene, K., Pujol, J.-P., 2008. Differential effects of hyaluronan and its fragments on fibroblasts: Relation to wound healing. Wound Repair Regen. 16, 274-287.

Dougherty, G.J., Cooper, D.L., Memory, J.F., Chiu, R.K., 1994. Ligand binding specificity of alternatively spliced CD44 isoforms. Recognition and binding of hyaluronan by CD44R1. J. Biol. Chem. 269, 9074-9078.

Folkman, J., 1995. Angiogenesis in cancer, vascular, rheumatoid and other disease. Nat. Med. 1, 27-31.

Gao, F., Yang, C.X., Mo, W., Liu, Y.W., He, Y.Q., 2008. Hyaluronan oligosaccharides are potential stimulators to angiogenesis via RHAMM mediated signal pathway in wound healing. Clin. Invest. Med. 31, E106-116.

Hamann, K.J., Dowling, T.L., Neeley, S.P., Grant, J.A., Leff, A.R., 1995. Hyaluronic acid enhances cell proliferation during eosinopoiesis through the CD44 surface antigen. J. Immunol. 154, 4073-4080.

He, Y., Wu, G.D., Sadahiro, T., Noh, S.I., Wang, H., Talavera, D., Vierling, J.M., Klein, A.S., 2008. Interaction of CD44 and hyaluronic acid enhances biliary epithelial proliferation in cholestatic livers. Am. J. Physiol. Gastrointest. Liver Physiol. 295, G305-312.

Hofinger, E.S.A., Bernhardt, G., Buschauer, A., 2007. Kinetics of Hyal-1 and PH-20 hyaluronidases: Comparison of minimal substrates and analysis of the transglycosylation reaction. Glycobiology 17, 963-971.

Lokeshwar, V.B., Iida, N., Bourguignon, L.Y., 1996. The cell adhesion molecule, GP116, is a new CD44 variant (ex14/v10) involved in hyaluronic acid binding and endothelial cell proliferation. J. Biol. Chem. 271, 23853-23864.

Nandi, A., Estess, P., Siegelman, M.H., 2000. Hyaluronan anchoring and regulation on the surface of vascular endothelial cells is mediated through the functionally active form of CD44. J. Biol. Chem. 275, 14939-14948.

Savani, R.C., Cao, G., Pooler, P.M., Zaman, A., Zhou, Z., DeLisser, H.M., 2001. Differential involvement of the hyaluronan (HA) receptors CD44 and receptor for HA-mediated motility in endothelial cell function and angiogenesis. J. Biol. Chem. 276, 36770-36778.

Slevin, M., Krupinski, J., Kumar, S., Gaffney, J., 1998. Angiogenic oligosaccharides of hyaluronan induce protein tyrosine kinase activity in endothelial cells and activate a cytoplasmic signal transduction pathway resulting in proliferation. Lab. Invest. 78, 987-1003.

Takagaki, K., Nakamura, T., Izumi, J., Saitoh, H., Endo, M., Kojima, K., Kato, I., Majima, M., 1994. Characterization of hydrolysis and transglycosylation by testicular hyaluronidase using ion-spray mass spectrometry. Biochemistry (Mosc.) 33, 6503-6507.

Trochon, V., Mabilat, C., Bertrand, P., Legrand, Y., Smadja-Joffe, F., Soria, C., Delpech, B., Lu, H., 1996. Evidence of involvement of CD44 in endothelial cell proliferation, migration and angiogenesis in vitro. Int. J. Cancer 66, 664-668.

West, D.C., Hampson, I.N., Arnold, F., Kumar, S., 1985. Angiogenesis induced by degradation products of hyaluronic acid. Science 228, 1324-1326.

West, D.C., Kumar, S., 1989. The effect of hyaluronate and its oligosaccharides on endothelial cell proliferation and monolayer integrity. Exp. Cell Res. 183, 179-196.

Xu, Y., Swerlick, R.A., Sepp, N., Bosse, D., Ades, E.W., Lawley, T.J., 1994. Characterization of expression and modulation of cell adhesion molecules on an immortalized human dermal microvascular endothelial cell line (HMEC-1). J. Invest. Dermatol. 102, 833-837.

Chapter 7

Purification of *Streptococcus pneumoniae* hyaluronate lyase and screening for possible small molecule inhibitors

7.1. Introduction

Streptococcus pneumoniae is a bacterial respiratory pathogen and an important cause of many diseases like pneumonia, meningitis, otitis media and sinusitis (Boulnois, 1992). The gram-positive, alpha-hemolytic bacterium is a common mucosal resident in the nasopharynx, especially in young children (Marchisio et al., 2002). Recent studies show a worrying increase in drug resistant strains of *S. pneumoniae* (DRSP) (Nuermberger and Bishai, 2004). Hence, new selective antibiotics or vaccines would be useful tools in the treatment of DRSP infections.

The bacterium produces several virulence factors, such as the capsule, pneumococcal surface proteins A and C, pneumolysin and hyaluronate lyase (*Spn*Hyl). The bacterial hyaluronidase could serve as a target for new "antibacterial" agents (Kadioglu et al., 2008) to inhibit the spreading of the bacteria in the tissue and to enhance the efficacy of co-administered antibiotics.

*Spn*Hyl acts as a spreading factor for the bacterium by cleaving hyaluronan in the extracellular matrix of connective tissues in the host through an enzymatic ß-elimination process. In *S. pneumoniae* cultures, the enzyme was detected in both the culture medium and the cell-associated fractions. This suggests that a portion of *Spn*Hyl is released by the bacterium during infection to facilitate bacterial invasion (Berry et al., 1994). After successful crystallization and X-ray analyses by Jedrzejas et al. (Jedrzejas et al., 1998a; Jedrzejas et al., 1998b), recent structural studies deal with the mechanism of hyaluronan degradation by *Spn*Hyl. The enzyme structure contains two domains: one built mostly from helices, which form the catalytic domain with a cleft responsible for HA binding and degradation, and the C-terminal domain consisting almost entirely of ß-sheets (Li et al., 2000; Ponnuraj and Jedrzejas, 2000). The knowledge of the structure and the suggested mechanism of action of the enzyme render the application of computer-aided methods in search of possible inhibitors. However, there are just a few rather weak inhibitors of *Spn*Hyl known so far, such as L-ascorbic acid 6-hexadecanoate with an IC_{50} value of 100 µM (Botzki et al., 2004) or a 2-phenylindole (1-decyl-2-(4-sulfamoyloxyphenyl)-1*H*-indol-6-yl sulfamate) with an IC_{50}-value of > 100 µM (Rigden et al., 2006) (**Fig. 7.1**). These molecules are non-selective and not drug-like. Thus, in cooperation with Origenis GmbH (Martinsried, Germany) new more drug-like molecules were designed, synthesized in a multi-component reaction approach and screened for inhibitory activity on purified

*Spn*Hyl and hyaluronate lyase from *S. agalactiae* (*Sag*Hyal$_{4755}$), respectively. Both enzymes show a sequence identity of 53 % (Rigden et al., 2006).

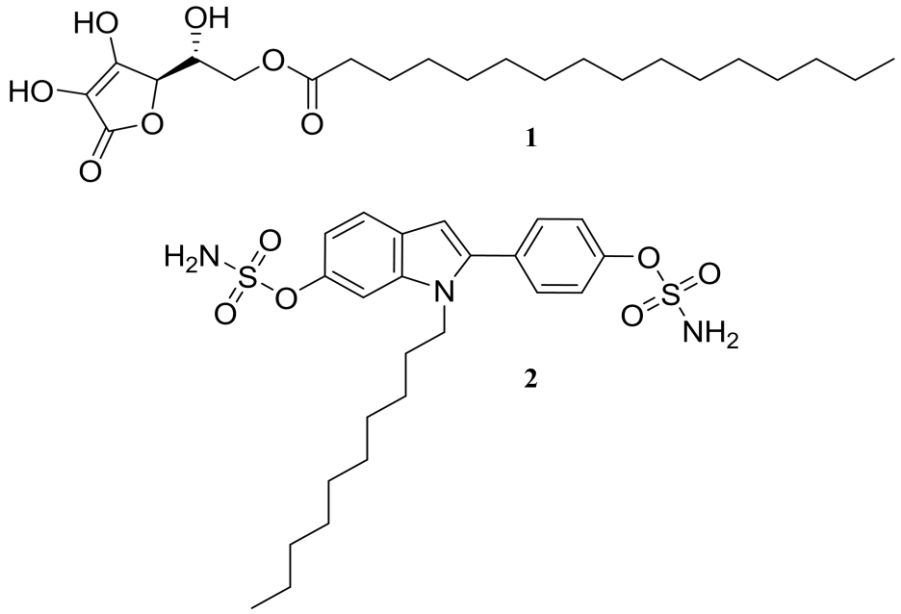

Fig. 7.1: Structures of known inhibitors of *Spn*Hyl. **1**: L-ascorbic acid 6-hexadecanoate; **2**: 1-decyl-2-(4-sulfamoyloxyphenyl)-1*H*-indol-6-yl sulfamate

7.2. Materials and methods

7.2.1. Small scale expression of *S. pneumoniae* hyaluronate lyase

*Spn*Hyl-6-His was expressed in *E. coli* strain BL21 (DE3) as described before (Jedrzejas et al., 1998b). In brief, a transformed *E. coli* cell colony was inoculated into 200 mL of LB medium supplemented with 100 µg/mL ampicillin and incubated at 37 °C on an incubator-shaker overnight. The protein was then induced by addition of isopropyl-*ß-D*-1-thiogalactopyranoside (IPTG, Sigma-Aldrich, Munich, Germany) and growth was continued for another 3 h. The cells were harvested by centrifugation at 6000 rpm at 4 °C for 10 min. The resulting cell pellet was re-suspended in McIlvaine´s buffer pH 5.0, supplemented with 20 % of glycerol and frozen at -80 °C. After thawing on ice, the suspension was again centrifuged and the pellet re-suspended in McIlvaine´s buffer pH 6.0. The sample was sonicated for 5 x 20 s with 1 min intervals on ice and the resulting cell lysate was centrifuged at 15000 rpm at 4 °C for 30 min. The supernatant was then used for activity measurements, SDS-PAGE and Western Blot analysis.

7.2.2. SDS-PAGE and Western Blot analysis

Gel electrophoresis and Western Blot analysis were performed as described in Chapter 3. As primary antibody anti-6-His (Sigma-Aldrich, Munich, Germany) at a dilution of 1:5000 was used. The secondary antibody was goat anti-mouse IgG (Fc specific), peroxidase-conjugated (Sigma-Aldrich, Munich, Germany) at a dilution of 1:1000.

7.2.3. Purification of *Spn*Hyl with Ni-Sepharose™ 6 FF

Ca. 10 g of frozen cell pellets from large scale expression performed by Christian Textor from our laboratories in cooperation with the Institute of Biotechnology (Prof. Dr. R. Rudolph) at the Martin-Luther University Halle-Wittenberg (Germany), were thawed on ice and centrifuged at 6000 rpm at 4 °C for 10 min. The pellet was re-suspended in 50 mL of binding buffer (20 mM Na_2HPO_4, 0.5 M NaCl, 20 mM imidazole, pH 7.4), supplemented with an EDTA-free protease inhibitor cocktail (Sigma-Aldrich, Munich, Germany) following sonication as described in **7.2.1**. The cell lysate was centrifuged at 15000 rpm at 4 °C for 30 min and the supernatant was used for purification with Ni Sepharose™ 6 FF (GE Healthcare, Munich, Germany).

For purification Ni Sepharose was washed with 5 x Sepharose volume of water by gentle shaking for 15 min. Ni Sepharose was then sedimented by centrifugation at 1000 g for 5 min, the supernatant was discarded. The washing and centrifugation procedure was repeated with 5 x Sepharose volume of binding buffer. After discarding the supernatant a 50 % slurry was made by adding an appropriate volume of binding buffer to the Ni Sepharose. This slurry was used for sample binding. One slurry volume of cell lysate was added and binding of *Spn*Hyl-6-His was allowed for 1 h under gentle shaking at room temperature. Afterwards the suspension was centrifuged at 1000 g for 5 min and the supernatant was again discarded. The sedimented Ni Sepharose was washed 3 times with 5 x volume of binding buffer and the supernatants were collected. The following elution steps were performed by adding 3 times 2 x Sepharose volume elution buffer (20 mM Na_2HPO_4, 0.5 M NaCl, 0.5 M imidazole, pH 7.4) and collecting the supernatants. All samples resulting from the washing and elution steps were analyzed by SDS-PAGE. The elution fractions were desalted with PD-10 columns (purchased from Sigma-Aldrich, Munich, Germany); their protein content was determined by the method of Bradford (Bradford, 1976) using the Bio-Rad protein assay (Bio-Rad, Munich, Germany) following the manufacturer´s instructions for the standard microtiter plate assay and hyaluronidase activity was determined with the colorimetric assay (see below).

7.2.4. Colorimetric hyaluronidase activity assay

Hyaluronidase activity was determined by a colorimetric assay (Morgan-Elson reaction) as described elsewhere in detail (Muckenschnabel et al., 1998). Thereby N-acetyl-D-glucosamine (NAG) (Sigma-Aldrich, Munich, Germany) at the reducing end of sugars generated from hyaluronan was determined according to the method of Reissig et al. (Reissig et al., 1955). Enzymatic activity was quantified by comparing the absorbance of the samples with the absorbance of standards containing known amounts of NAG, which were treated exactly like the samples. According to the International Union of Biochemistry 1 unit (U) of hyaluronidase is defined as the enzymatic activity catalyzing the liberation of 1 µmol NAG at the reducing ends of sugars per min under specified conditions.

The incubation mixtures contained 200 µL of McIlvaine´s buffer pH 6.0, 50 µL of H_2O, 50 µL of BSA solution (0.2 mg/mL), 50 µL of hyaluronan solution (5 mg/mL) and 50 µL

of elution fraction. The samples were incubated at 37 °C for 30 min followed by adding 110 µL of alkaline borate solution and heating at 100 °C for 4.5 min to stop the enzymatic reaction. After cooling on ice for 2 min, 1.25 mL of p-dimethylaminobenzaldehyde were added and the color was allowed to develop for 20 min at 37 °C. The absorbance of the samples and standards was measured at 586 nm using a Cary 100 UV-Vis spectrophotometer (Varian, Darmstadt, Germany).

7.2.5. Turbidimetric hyaluronidase activity assay for screening

The turbidimetric hyaluronidase assay was performed according to Di Ferrante (Di Ferrante, 1956) with modifications for the 96 well plate format.

The incubation mixtures contained 30 µL of McIlvaine´s buffer pH 5.0, 8 µL of BSA solution (0.2 mg/mL), 8 µL of HA solution (2 mg/mL), 9 µL of H_2O, 10 µL of inhibitor solution (1.5 mM in 30 % DMSO) and 10 µL of enzyme solution (10 IE in 0.2 mg/mL BSA solution) per well. Reference wells contained the corresponding solvent instead of the inhibitor solution and for the preparation of reference A 0.2 mg/mL BSA solution was used instead of enzyme. As some compounds from the multi-component reactions were colored, blank wells were prepared for every compound to exclude false positive values. Blank wells contained H_2O instead of HA in the reaction mixture and BSA instead of enzyme. Vcpal served as reference inhibitor. After incubation of the MTPs at 37 °C for 1 h, 200 µL of 2.5 % cetyltrimethylammonium bromide (CTAB) solution (2.5 % CTAB in 0.5 N NaOH) were added to each well to precipitate residual high molecular weight hyaluronan. Turbidity was allowed to develop for 20 min at RT. The optical density was then measured at 580 nm using a Tecan Genios Pro microtiter plate reader (Tecan, Crailsheim, Germany) with XFluor Genios Pro software version V.4.55. The values of the blank wells were subtracted from the OD values of samples and references before calculating relative activity of *Spn*Hyl in presence of inhibitor using the following equation:

$$A_{Spn\mathrm{Hyl}}(\%) = 100 * \frac{(OD_{RefA} - OD_{sample})}{(OD_{RefA} - OD_{RefB})}$$

Eq. 7.1

The values for relative enzyme activity given in the result section are mean values ± SEM (standard error of the mean) of duplicates.

For determination of the IC_{50} value, the residual enzymatic activities after incubation with various concentrations of inhibitor were plotted against the logarithm of the inhibitor concentration. The IC_{50} value was calculated by curve fitting of experimental data with SigmaPlot 11.0 (simple ligand binding, sigmoidal dose response).

7.3. Results and discussion

7.3.1. Small scale expression of S. pneumoniae hyaluronate lyase

Expression of *Spn*Hyl was accomplished in BL21 cells and isolation of the protein was performed as described in the materials and method section. Enzymatic hyaluronidase activity in the unpurified sample was investigated using the turbidimetric assay and it was measureable after 15 min of incubation. Thereafter, expression of *Spn*Hyl was verified by SDS-PAGE and Western Blot analysis. SDS-PAGE of 10 µg of unpurified protein revealed a prominent protein band at 84 kDa, which closely corresponds to the expected molecular weight of 83 kDa (Jedrzejas et al., 1998b). This protein band was then shown to be *Spn*Hyl-6-His in the Western Blot analysis using an anti-6-His primary antibody (**Fig. 7.2**).

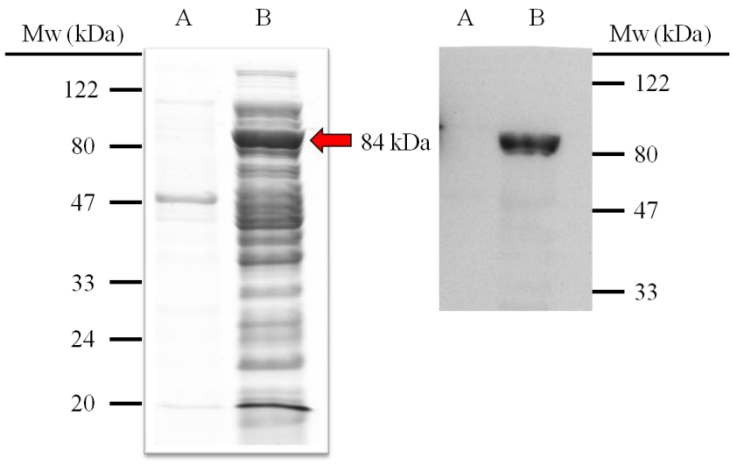

Fig. 7.2: SDS-PAGE (left) and Western Blot (right) analysis of isolated unpurified protein from small scale *Spn*Hyl expression experiment (lane B). Non-transfected BL21 cells served as negative control (lane A). SDS-PAGE was stained with Coomassie brilliant blue, primary antibody for Western Blotting was an anti-6-His antibody; secondary antibody was a HRP-conjugated goat-anti-mouse antibody. Immunodetection was achieved with ECL.

7.3.2. Purification and characterization of *Spn*Hyl after large scale expression

After the successful expression of enzymatically active *Spn*Hyl in the small scale format, the protein expression was scaled up[4]. The supernatant of the lysed cells was purified using Ni-Sepharose and the resulting elution fractions were analyzed with respect to protein content, purity and enzymatic activity. As shown in **Fig. 7.3**, elution fraction II appeared to have a satisfying purity, so the screening of small molecule inhibitors was performed using only elution fraction II after determination of its specific activity.

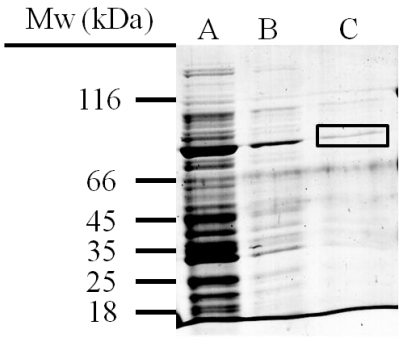

Fig. 7.3: Purification of *Spn*Hyl from large scale expression. Lane A: unpurified supernatant from cell lysis; lane B: elution fraction I; lane C: elution fraction II. 20 µL of sample were applied to the SDS-gel and staining was accomplished with Coomassie brilliant blue.

After purification and desalting, the protein content of the elution fractions was determined using the method of Bradford (Bradford, 1976) in the microtiter plate format. Elution fractions I and II contained 13.5 and 5.5 µg/mL protein, respectively. Enzymatic activity was then measured using the colorimetric hyaluronidase assay and specific activity in U/mg was calculated by dividing enzymatic activity and protein content (**Tab. 7.1**).

Tab. 7.1: enzymatic and specific activity of *Spn*Hyl in the elution fractions as determined with the colorimetric assay. Results are presented as mean ± SEM from two independent experiments.

elution fraction	enzymatic activity (mU/mL)	specific activity (U/mg)
I	63.5 ± 3.9	4.7 ± 0.3
II	21.3 ± 1.7	3.9 ± 0.3

7.3.3. Screening of small molecules for inhibition of *Spn*Hyl

The 96-deep-well plates from the multicomponent reaction approach were provided by C. Textor from our workgroup. Each substance was tested in duplicates at an assumed final concentration of 200 µM for inhibition of *Spn*Hyl at a final enzymatic activity of 0.1 mU.

[4] C. Textor, personal communication

After performing the turbidimetric assay, deep-well plates were controlled for the presence of the desired molecules by means of mass spectrometry, and screening hits were summarized. Results of each plate shown in Fig. 7.4 are from two independent experiments ± SEM. Residual *Spn*Hyl activity after incubation with the generated molecules were compared to the results obtained with *Sag*Hyal$_{4755}$ for estimating the selectivity. A screening hit was defined as generated molecule with an inhibitory activity of ≥ 50 %.

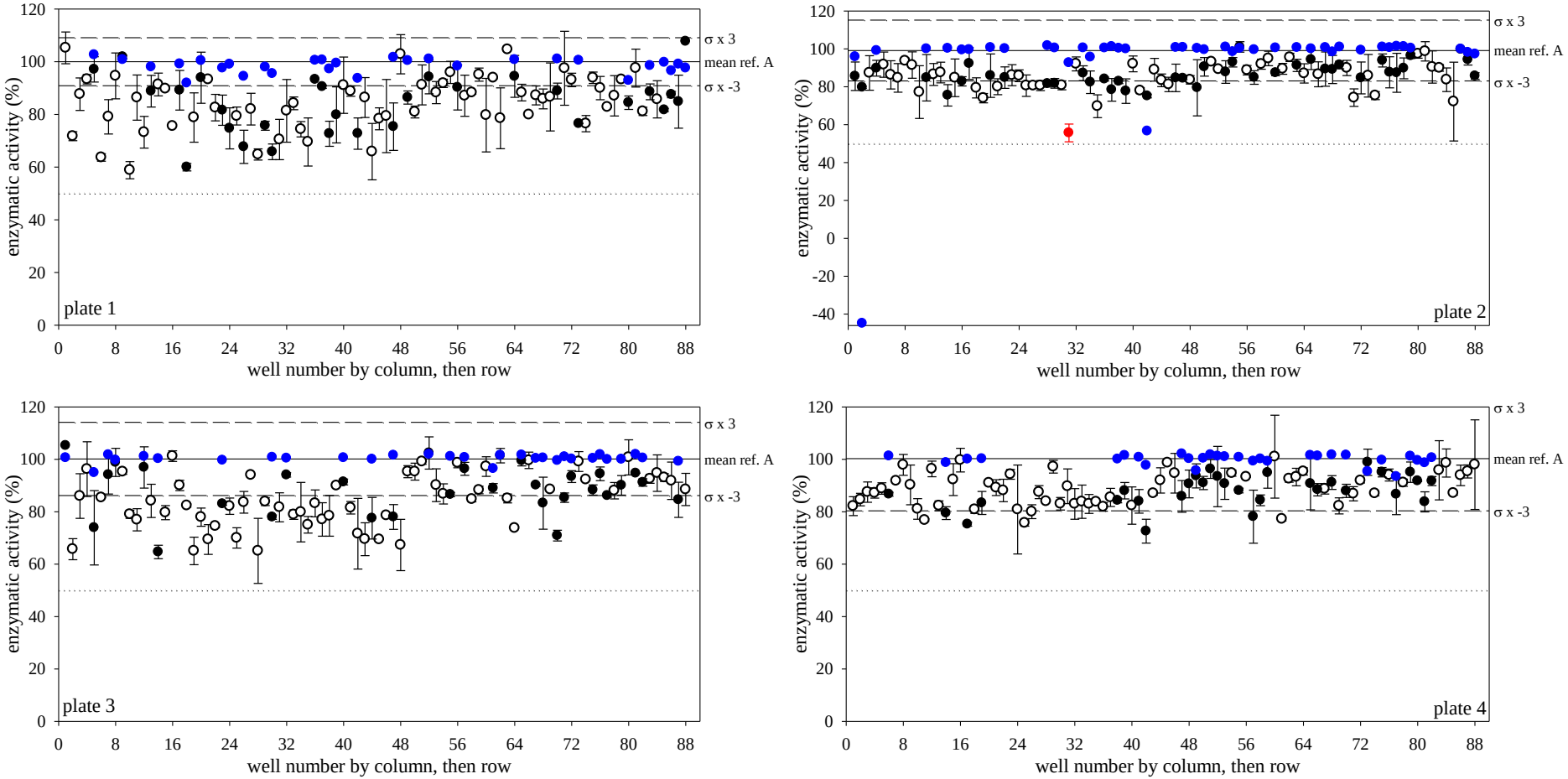
enzymatic activity (%)
well number by column, then row
σ x 3
mean ref. A
σ x -3
plate 1
plate 2
plate 3
plate 4

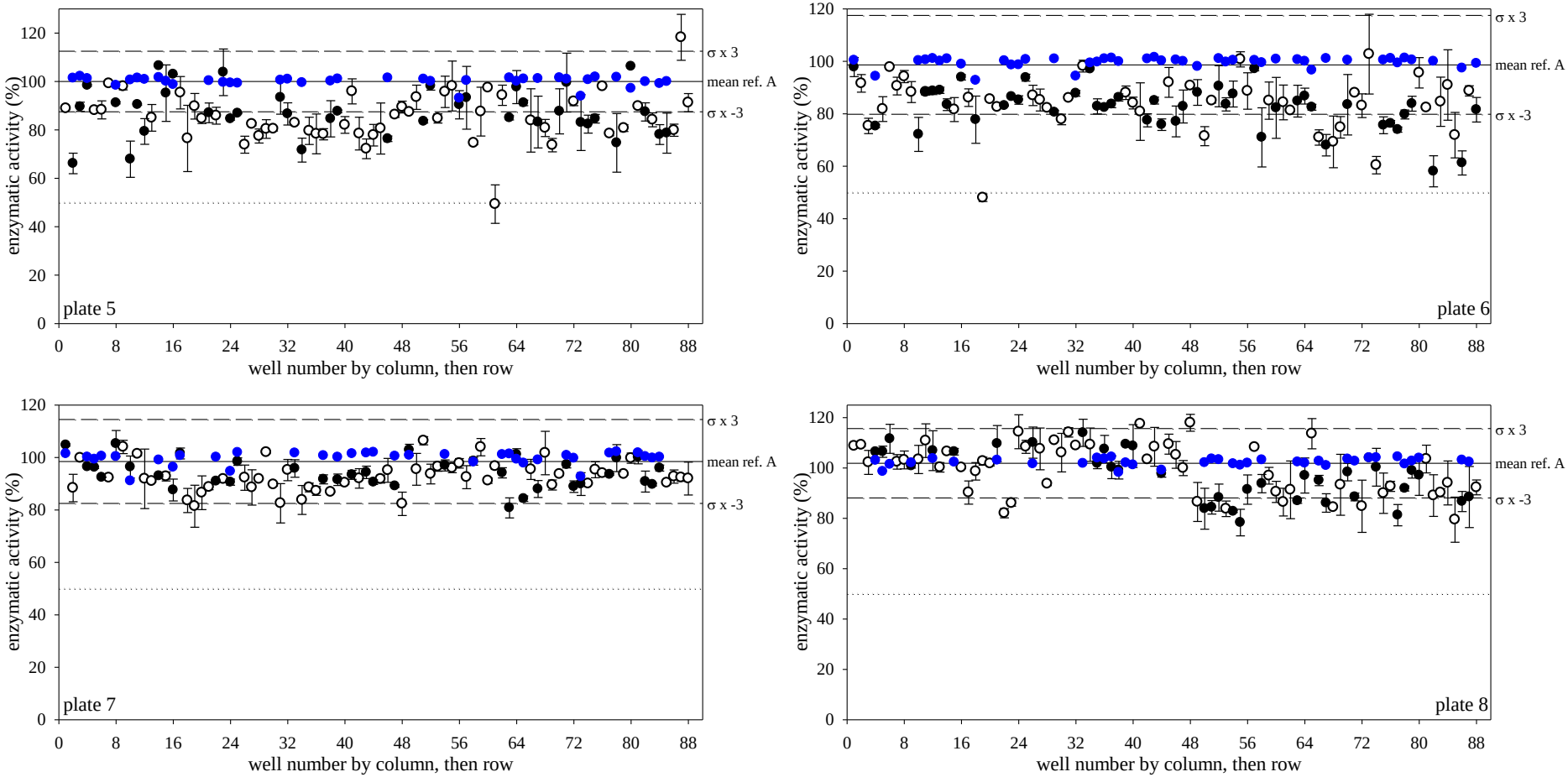
enzymatic activity (%)
well number by column, then row
σ x 3
mean ref. A
σ x -3
plate 5
plate 6
plate 7
plate 8

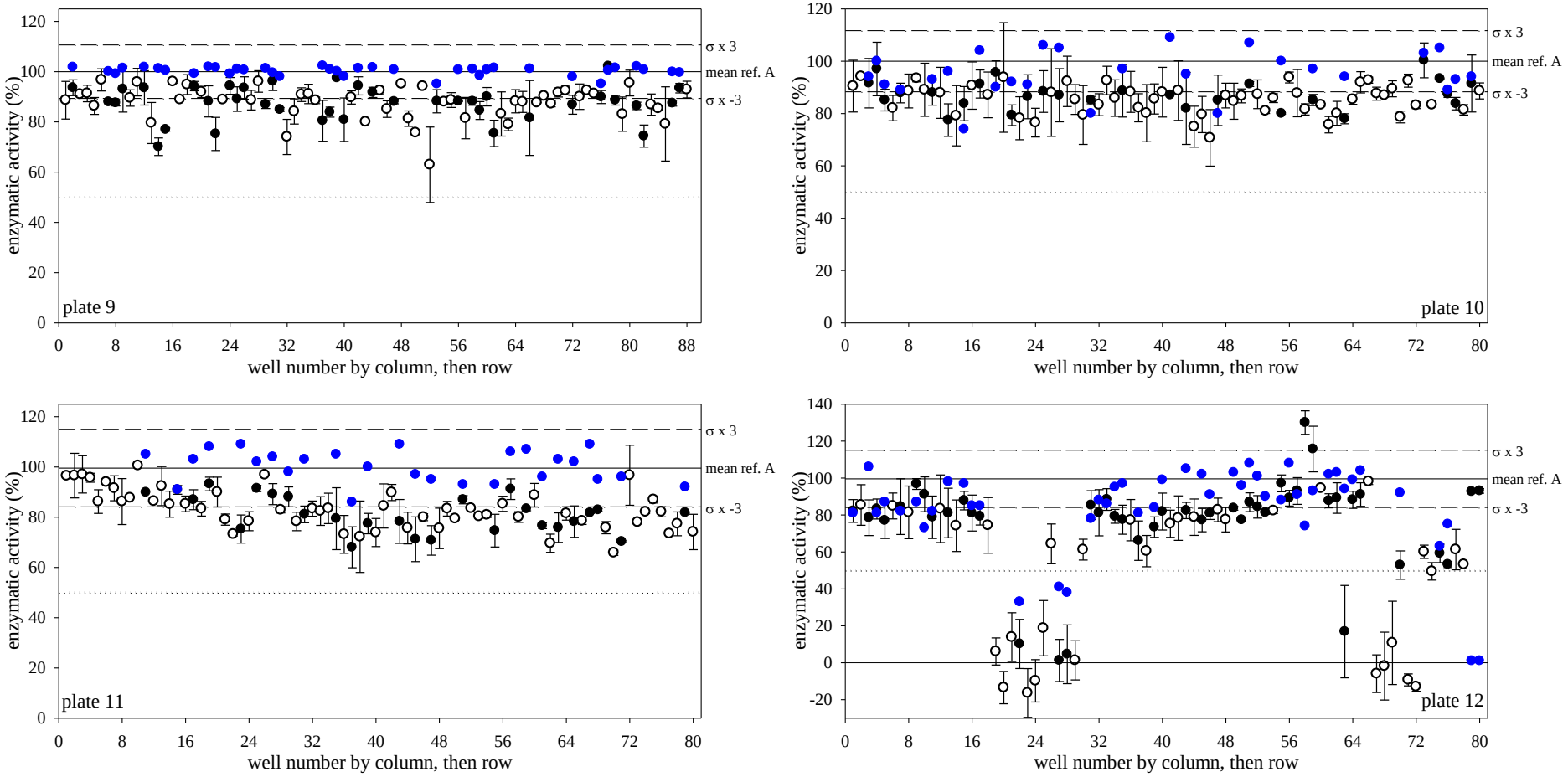
plate 9
plate 10
plate 11
plate 12
σ x 3
mean ref. A
σ x -3
enzymatic activity (%)
well number by column, then row

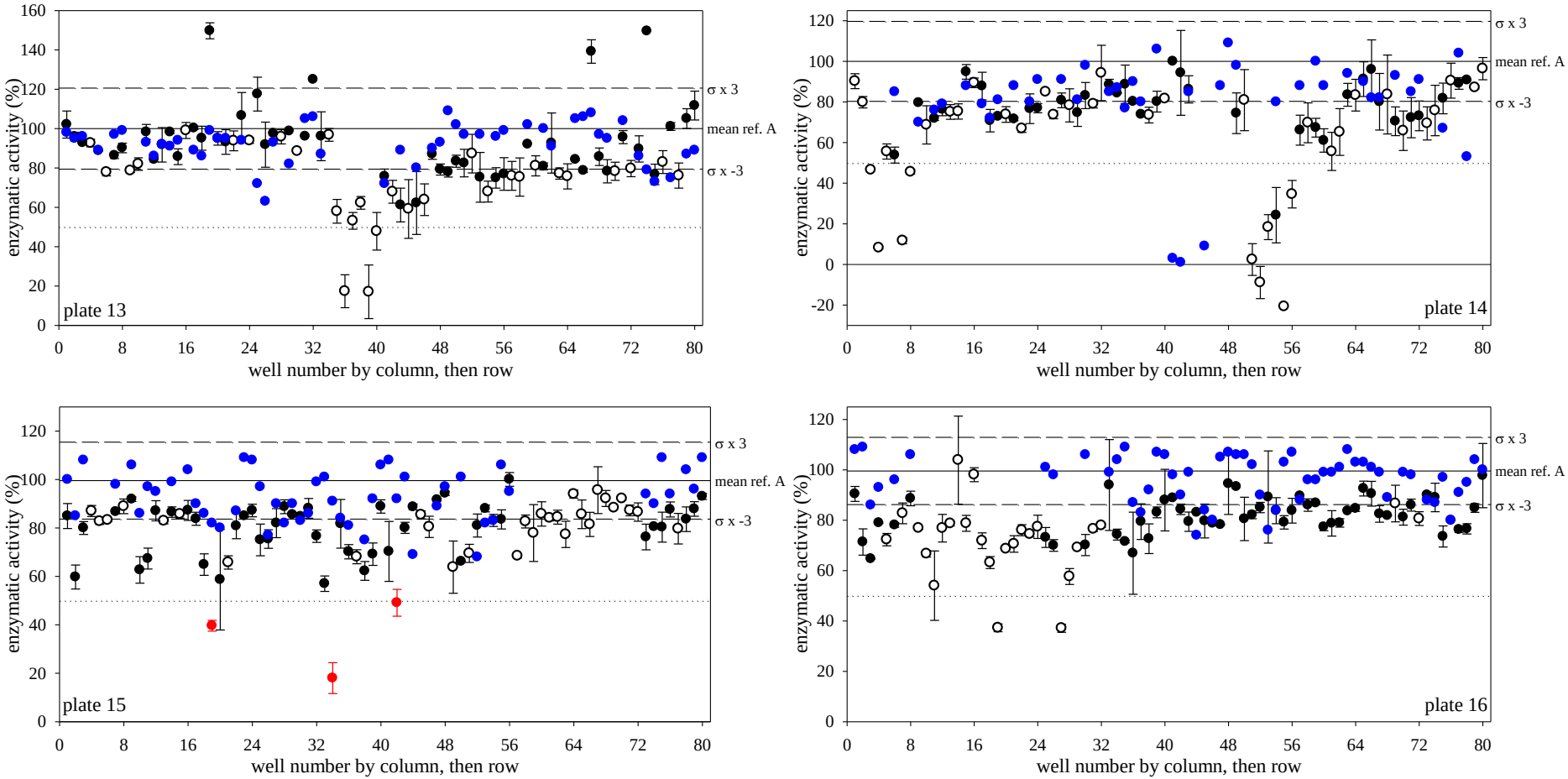

Fig. 7.4: Results of screening for inhibition of *Spn*Hyl by small molecules from a multicomponent synthesis approach. Each chart corresponds to one 96-deep-well plate. ○ wells in which the target compounds could not be detected; ● wells in which the desired product was generated as confirmed by mass spectrometry; ● screening hits; ● results of the screening for inhibition of *Sag*Hyal$_{4755}$, wells with generated product

Four molecules out of a total of 1352 screened molecules were identified as "hits", corresponding to a hit rate of 0.3 %. The structures of the screening hits are depicted in **Fig. 7.5**.

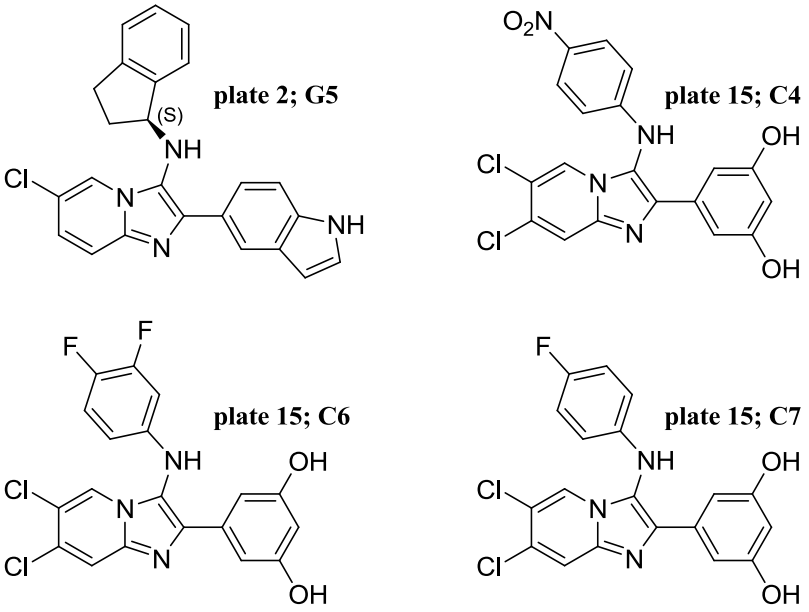

Fig. 7.5: Structures of the four screening hits with the highest inhibitory activity against *Spn*Hyl.

All identified compounds are imidazopyridines with rather space-filling substituents in positions 2 and 3.

In **Tab. 7.2** the inhibitory activities of the identified hits on *Spn*Hyl are summarized and compared to the activities on *Sag*Hyal$_{4755}$. All compounds proved to inhibit *Spn*Hyl activity to a higher extent, indicating possible selectivity for this bacterial enzyme.

Tab. 7.2: Inhibitory activities of the identified hits on *Spn*Hyl at an assumed concentration of 200 µM. Presented values are means ± SEM of duplicates. Activities were compared to inhibition of *Sag*Hyal$_{4755}$[5].

Compound	Inhibition of *Spn*Hyl (%) ± SEM (assumed concentration: 200 µM)	Inhibitory activity on *Sag*Hyal$_{4755}$ (%) (assumed concentration: 200 µM)
Plate 2; G5	45 ± 5	8
Plate 15, C4	60 ± 2	18
Plate 15, C6	82 ± 6	9
Plate 15, C7	51 ± 5	8

[5] C. Textor, personal communication

After the screening for small molecule inhibitors, a purified 2-phenylindole[6] (**Fig. 7.6**) (UR-CT-619) bearing space-filling substituents in 1- and 2-position and structurally resembling the identified hits, was tested for inhibition of *Spn*Hyl activity.

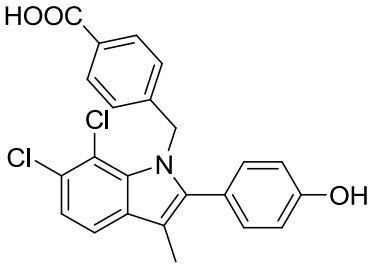

Fig. 7.6: Structure of the purified compound tested for inhibitory activity on SpnHyl, UR-CT-619

The compound was tested in the turbidimetric assay at different concentrations in triplicate and the IC_{50} value was determined as described in the material and methods section (**Fig. 7.7**).

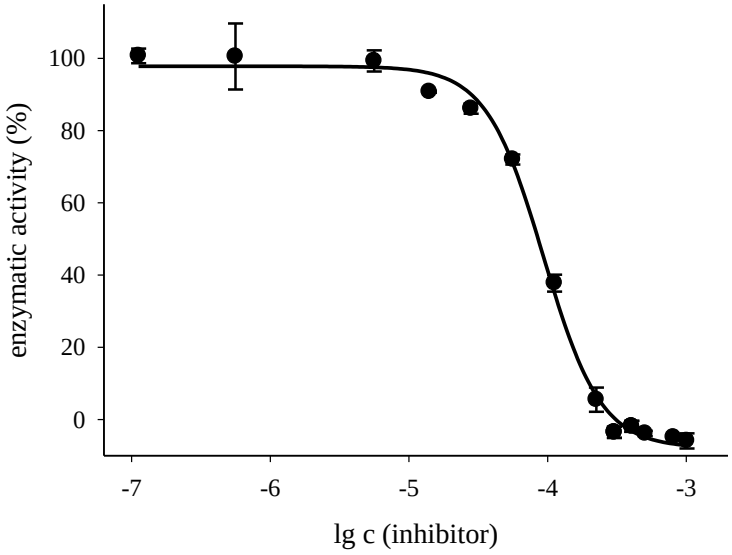

Fig. 7.7: Graph for determination of the IC_{50} value for UR-CT-619. Presented data are mean values ± SEM of triplicates.

An IC_{50} value of 93 µM ± 1.05 was determined for inhibition of *Spn*Hyl. To our knowledge this is the most potent drug-like small molecule inhibitor of *Spn*Hyl designed so far. Interestingly, UR-CT-619 is even more potent as an inhibitor of *Sag*$Hyal_{4755}$[7]. By contrast the imidazopyridines identified as hits showed selectivity towards *Spn*Hyl. Therefore, these compounds have to be re-synthesized for more detailed studies on bacterial hyaluronidases to substantiate the results. We suspect that the apparent selectivity for *Spn*Hyl is due to the missing carboxylic group in the identified molecules.

[6] provided by C. Textor from our workgroup
[7] C. Textor, Personal communication

7.4. Summary and conclusion

*Spn*Hyl-6-His was successfully expressed in *E. coli* strain BL21 cells and purified by means of a Ni-Sepharose. The enzyme was then used in a screening approach to identify small molecules as inhibitors of *Spn*Hyl. The compounds were synthesized by multicomponent reactions in the microtiter plate format. After having tested 1352 potential inhibitors in a turbidimetric 96-well microtiter plate assay, the deep-well-plates were analyzed for the presence of the desired molecules and screening hits were identified. The screening revealed 4 hits with inhibitory activities on *Spn*Hyl of ≥ 50 %. The most potent compound was identified in well C6 on plate 15, showing 82 % inhibition of *Spn*Hyl at an assumed final concentration of 200 µM. All identified compounds possess a similar structure based on an imidazopyridine scaffold with rather space-filling substituents in positions 2 and 3. Moreover these hits have promising drug-like properties, fulfilling Lipinski´s rule of five.

In order to substantiate the screening results, UR-CT-619, a 2-phenylindole having a rather similar structure compared to the identified hits was tested for inhibition of *Spn*Hyl. With the turbidimetric assay, an IC_{50} value of 93 µM was determined and therefore UR-CT-619 was identified as the most potent *Spn*Hyl inhibitor reported so far.

The inhibitory effects of the generated molecules on *Spn*Hyl were compared to those on another bacterial hyaluronidase, *Sag*$Hyal_{4755}$. UR-CT-619 was shown to be even more potent as an inhibitor of *Sag*$Hyal_{4755}$, whereas all previously identified screening hits showed selectivity towards *Spn*Hyl. We therefore suggest that a carboxylic group, as present in UR-CT-619, is important for inhibition of *Sag*$Hyal_{4755}$ compared to *Spn*Hyl. Additional studies with purified hit compounds have to be performed to proof inhibition of *Spn*Hyl and to explore the structure-activity relationships.

Provided that the screening hits will be confirmed as potent inhibitors of *Spn*Hyl, optimized compounds might be useful to perform proof-of-concept studies on the potential value of hyaluronidase inhibitors as antibacterial agents. The inhibition of the spread of pathogenic *Streptococci*, particularly in the early stage of infections, may prevent the onset of bacterial disease. Moreover, the compounds could be valuable pharmacological tools in further understanding the role of the hyaluronate lyase for the bacterium.

7.5. References

Berry, A.M., Lock, R.A., Thomas, S.M., Rajan, D.P., Hansman, D., Paton, J.C., 1994. Cloning and nucleotide sequence of the Streptococcus pneumoniae hyaluronidase gene and purification of the enzyme from recombinant Escherichia coli. Infect. Immun. 62, 1101-1108.

Botzki, A., Rigden, D.J., Braun, S., Nukui, M., Salmen, S., Hoechstetter, J., Bernhardt, G., Dove, S., Jedrzejas, M.J., Buschauer, A., 2004. L-Ascorbic acid 6-hexadecanoate, a potent hyaluronidase inhibitor. X-ray structure and molecular modeling of enzyme-inhibitor complexes, J. Biol. Chem., 2004/08/24 ed, pp. 45990-45997.

Boulnois, G.J., 1992. Pneumococcal proteins and the pathogenesis of disease caused by Streptococcus pneumoniae. J. Gen. Microbiol. 138, 249-259.

Bradford, M.M., 1976. A rapid and sensitive method for the quantitation of microgram quantities of protein utilizing the principle of protein-dye binding. Anal. Biochem. 72, 248-254.

Di Ferrante, N., 1956. Turbidimetric Measurement of Acid Mucopoly-Saccharides and Hyaluronidase Activity. J. Biol. Chem. 220, 303-306.

Jedrzejas, M.J., Chantalat, L., Mewbourne, R.B., 1998a. Crystallization and preliminary X-ray analysis of Streptococcus pneumoniae hyaluronate lyase. J. Struct. Biol. 121, 73-75.

Jedrzejas, M.J., Mewbourne, R.B., Chantalat, L., McPherson, D.T., 1998b. Expression and purification of Streptococcus pneumoniae hyaluronate lyase from Escherichia coli. Protein Expr. Purif. 13, 83-89.

Kadioglu, A., Weiser, J.N., Paton, J.C., Andrew, P.W., 2008. The role of Streptococcus pneumoniae virulence factors in host respiratory colonization and disease. Nat. Rev. Microbiol. 6, 288-301.

Li, S., Kelly, S.J., Lamani, E., Ferraroni, M., Jedrzejas, M.J., 2000. Structural basis of hyaluronan degradation by Streptococcus pneumoniae hyaluronate lyase. EMBO J. 19, 1228-1240.

Marchisio, P., Esposito, S., Schito, G.C., Marchese, A., Cavagna, R., Principi, N., 2002. Nasopharyngeal carriage of Streptococcus pneumoniae in healthy children: implications for the use of heptavalent pneumococcal conjugate vaccine. Emerg. Infect. Dis. 8, 479-484.

Muckenschnabel, I., Bernhardt, C., Spruss, T., Dietl, B., Buschauer, A., 1998. Quantitation of hyaluronidases by the Morgan-Elson reaction: comparison of the enzyme activities in the plasma of tumor patients and healthy volunteers. Cancer Lett. 131, 13-20.

Nuermberger, E.L., Bishai, W.R., 2004. Antibiotic resistance in Streptococcus pneumoniae: what does the future hold? Clin. Infect. Dis. 38 Suppl 4, S363-371.

Ponnuraj, K., Jedrzejas, M.J., 2000. Mechanism of hyaluronan binding and degradation: structure of Streptococcus pneumoniae hyaluronate lyase in complex with hyaluronic acid disaccharide at 1.7 A resolution. J. Mol. Biol. 299, 885-895.

Reissig, J.L., Storminger, J.L., Leloir, L.F., 1955. A modified colorimetric method for the estimation of N-acetylamino sugars. J. Biol. Chem. 217, 959-966.

Rigden, D.J., Botzki, A., Nukui, M., Mewbourne, R.B., Lamani, E., Braun, S., von Angerer, E., Bernhardt, G., Dove, S., Buschauer, A., Jedrzejas, M.J., 2006. Design of new

benzoxazole-2-thione-derived inhibitors of Streptococcus pneumoniae hyaluronan lyase: structure of a complex with a 2-phenylindole. Glycobiology 16, 757-765.

Chapter 8

Summary

Hyaluronan (hyaluronic acid, HA) and its degradation products, generated by hyaluronidases, are known to be involved in cell signaling, cell migration, inflammation and tumor invasion. But the role of hyaluronidases in physiological and pathological processes is relatively unclear, due to insufficient information on enzymatic properties and the lack of specific inhibitors as pharmacological tools. Especially hyaluronidase-2 (Hyal-2) has been a matter of debate with respect to the degradation of hyaluronan. Therefore, the aim of this thesis was to investigate the catalytical Hyal-2 activity of a recombinant human enzyme and in blood cells.

Recombinant human Hyal-2, expressed in DS-2 insect cells, elaborated by Edith Hofinger, was successfully purified to investigate enzymatic activity using two different methods. Viscosimetry was previously shown to be the most sensitive among the classical hyaluronidase assays. The isolated rhHyal-2 proved to be able to degrade hyaluronan within 24 h under acidic conditions (pH = 4.0). Surprisingly, a preference for HA from vertebrate sources (human umbilical cord, rooster comb) over HA of microbial origin was observed. The former was degraded faster and to an apparently higher extent than HA from *S. zooepidemicus*. By means of polyacrylamide gel electrophoresis followed by a combined alcian blue, silver staining protocol it became possible to estimate the size of the HA fragments generated by the action of rhHyal-2. The results obtained with this method correlated well with data from viscosimetric measurements. HA fragments, formed by the degradation of HA from vertebrate sources (< 15 kDa) were definitely smaller in size than those produced by degradation of HA from *S. zooepidemicus* (~ 20 kDa).

Inspired by results published by Carol de la Motte et al., human and murine blood platelets were chosen to investigate native Hyal-2. Hyal-2 is the only hyaluronidase present in platelets, with no evidence for other hyaluronidase isoforms. Extensively washed platelets and platelet membrane preparations were analyzed with respect to hyaluronidase activity at different pH values using HA from different sources. Hyaluronan degrading activity could only be detected at acidic pH of 4.0. By analogy with rhHyal-2, HA from vertebrates was the preferred substrate of platelet-associated Hyal-2. In order to unambiguously exclude that, despite extensive washing of the samples, the observed hyaluronidase activity in platelets is due to traces of plasma Hyal-1, platelets from Hyal-2 knock-out (KO) mice were analyzed exactly in the same way as wildtype platelets. Thereby, Hyal-2 activity was definitely proven in platelets, as there was no HA digestion after incubation with KO platelets.

Additionally, red blood cells (RBCs) were investigated. The presence of Hyal-2 and the absence of Hyal-1 were confirmed by Western Blot analysis, and erythrocytes and ghost membrane preparations were analyzed for Hyal-2 activity. Although HA degradation in the presence of RBCs was high, the enzymatic activity resulted from residual plasma Hyal-1. There was no hydrolytic activity upon incubation (72 h) of HA with ghost membrane preparations at any pH tested. The biological relevance of the relatively high expression of Hyal-2 in RBCs, detected immunologically, needs to be further investigated either with regard to the existence of a putative co-receptor or an endogenous inhibitor, associated with Hyal-2 in the RBC membranes.

To gain more insight into the role of HA fragments and to explore, if platelets are capable of generating biologically active HA oligosaccharides, the proliferation of endothelial cells (EC) was examined after addition of HA digests. However, there was no effect on cell proliferation. As there was no evidence for expression of the HA receptor CD44 by these cells, it can be speculated that the presence of functional CD44 is essential for enhanced cell proliferation mediated by binding HA fragments.

Hyaluronidases are also considered virulence factors of microorganism, including several pathogenic strains of *Streptococci*. Inhibitors of such hyaluronate lyases could serve as pharmacological tools or might be used as adjuvant in the chemotherapy of drug-resistant bacteria. In a screening approach, out of 1352 molecules, obtained from multicomponent synthesis, 4 imidazopyridines were identified as inhibitors of a bacterial lyase (*Spn*Hyl). At an estimated concentration of 200 µM, the most potent compound showed 82 % inhibition of *Spn*Hyl, when incubated with the reaction mixture. In addition, a structurally related conventionally synthesized 2-phenylindole (UR-CT-619), proved to be the most potent inhibitor of *Spn*Hyl known so far.

Appendix

In vitro investigations on lobaplatin against triple-negative human breast cancer cells

1 Introduction

Breast cancer comprises a collection of heterogeneous disease entities. Consequently, both, preclinical and clinical research target specific subgroups of breast cancer with the aim to reveal subgroup-specific therapies. Examples include the targeting of estrogen receptor (ER)-driven breast cancers using tamoxifen or the subgroup driven by the human epidermal growth factor receptor 2 (HER2), which is targeted by trastuzumab (Widakowich et al., 2007). However, these newer targeting strategies are of no benefit for a significant group of women (15 % of all types of breast cancer), who have breast cancers that fail to express ERs and progesterone receptors (PRs) and that do not overexpress HER2. This type of cancer is in the so-called receptor-negative or triple-negative (TN) category. Because of the absence of specific treatment options, triple-negative cancers are managed with standard treatment associated with a high rate of local and systemic relapse.

Histologically and transcriptionally, TN breast cancers have many similarities to breast cancer susceptibility gene 1 (BRCA1) associated breast cancers, which suggests that dysfunction in BRCA1 or related pathways occurs in this subset of cancers (Cleator et al., 2007). A lack of BRCA1 results in DNA repair by non-conservative, potentially mutagenic mechanisms, and therefore, leads to genomic instability and cancer predisposition (Turner et al., 2004). There is increasing evidence that BCRA1 related cancers confer sensitivity to particular systemic agents such as platinum-based drugs (e.g. cisplatin), which bring about interstrand cross-links (Byrski et al., 2009).

Due to severe toxic side effects and the development of resistance against cisplatin, new analogues have been developed. One of these is lobaplatin (**Fig. 1**), a platinum drug of the third generation. In previous *in vitro* studies, lobaplatin exhibited activity against various cancer cell lines with an incomplete cross-resistance to cisplatin (McKeage, 2001). In phase I and II clinical trials, lobaplatin displayed no nephro-, neuro- or ototoxicity, but the dose limiting toxicity was short-lasting thrombocytopenia, which is manageable (Gietema et al., 1995). In the following *in vitro* studies, the efficacy of lobaplatin against triple-negative breast cancer cells was investigated.

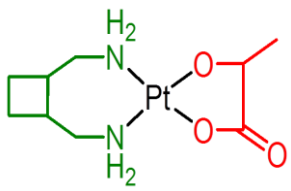

Fig. 1: Structure of the third-generation platinum drug lobaplatin, containing stably coordinated 1,2-bis(aminomethyl)cyclo-butane and lactic acid as leaving group.

2 Materials and methods

2.1 Platinum drugs

Lobaplatin was kindly provided by Aeterna Zentaris (Frankfurt, Germany), cisplatin, carboplatin, doxorubicin, tamoxifen, vinblastin and fulvestrant were purchased from Sigma-Aldrich (Munich, Germany).

2.2 Cell lines and culture conditions

Five human breast cancer cell lines were investigated.. MCF-7, T-47-D and MDA-MB-231 were obtained from the American Type Culture Collection (ATCC; Rockville, USA), HCC-1937 and HCC-1809 were kindly provided by Dr. Jörg Engel, Frauenklinik, University of Würzburg. The triple-negative cell lines HCC-1937, HCC-1806 and the ER-negative MDA-MB-231 were cultured in RPMI-1640 medium (Sigma-Aldrich, Munich, Germany), containing 5 % FCS. The ER- and PR-positive cell line T-47-D was cultured in RPMI-1640 medium, supplemented with 5 % FCS and 10 µg/mL of insulin. The estrogen-sensitive cell line MCF-7 was maintained in RPMI-1640, supplemented with 5 % FCS and 1 nM estradiol. All cells were grown in a water saturated atmosphere (95 % air/5 % CO_2) and serially passaged following trypsination with 0.05 % trypsin/0.02 % EDTA (Roche Diagnostics, Mannheim, Germany).

2.3 Subcutaneous injection of HCC-1806 and -1937 cells and histology

Nude mice, housed under specified pathogen free (SPF) conditions in the central animal facility of the University of Regensburg, were used to establish and characterize subcutaneous HCC-1806 and -1937 tumors. The mice were kept in type III cages from TecniplastTM (Hohenpeißenberg, Germany) at a 12 hours light/dark cycle, 26 °C and 70 % relative humidity. Animals took food (Ssniff, Soest, Germany) and water (autoclaved tap water) ad libitum.

For subcutaneous tumor cell implantation, cells were detached from the culture flask with trypsin/EDTA and FCS-free RPMI 1640. After a subsequent washing step, cells were re-suspended with serum-free RPMI 1640 and $1 \cdot 10^7$ cells (100 - 150 µL cell suspension) were injected under the thoracic dermis of nude mice. Tumor progression as well as body

weight was monitored once weekly (all animals were individually identifiable due to tattooed pads).

Excised tumor tissue was fixed for at least three days in Bouin´s solution (300 mL aqueous saturated picric acid, 100 mL formaldehyde and 20 mL glacial acetic acid) and embedded in paraffin by a standard procedure (cf. section 2.3.9.1 in (Müller, 2007)). Sections of 6 µm were cut by a Leica RM2255 microtome (Leica, Bensheim, Germany), transferred to SuperFrost plus microscope slides followed by deparaffinization using xylene and re-hydration in a descending alcohol series. Subsequently, the samples were stained by the procedure of Masson-Goldner (MG). Masson-Goldner (Jerusalem's modification): Weigert's iron-haematein (45 s), rinsing (H_2O demin), running tap water (10 min), differentiation with 200 mL of H_2O demin + 20 mL of 2 M aq. hydrochloric acid (15 s), running tap water (10 min), rinsing (H_2O demin), 0.5 % aq. phosphotungstic acid (15 s), running H_2O demin (10 min), acid fuchsine-Ponceau (30 s), 1 % aq. acetic acid (3 × immersion), phosphoric acid-Orange G (10 s), 1% aq. acetic acid (3 × immersion), 0.2 % light green (3.5 min), 1 % aq. acetic acid (3 × immersion), 96% aq. ethanol (2 × 3 min), 100 % ethanol (2 × 3 min), 100 % xylene (3 min). Entellan (Merck) was used for covering.

2.4 Chemosensitivity assay based on crystal violet staining

The chemosensitivity assay was performed according to Bernhardt et al. (Bernhardt et al., 1992). In brief, 100 µL/well of cell suspension were seeded in transparent 96-well plates (Greiner, Frickenhausen, Germany) to a density of approximately 15 cells/microscopic field (magnification 320 x). After 24 h of incubation at 37 °C (water saturated atmosphere; 5 % CO_2), medium was carefully removed by suction and replaced by 200 µL of fresh medium containing various increasing concentrations of the platinum compounds. On every plate, two rows (16 wells) contained only solvent as control and two rows were used for the incubation with each concentration. Drugs were added as 1000-fold concentrated stock solutions. Approximately every 24 hours cells from a plate were fixed with glutardialdehyde (Merck, Darmstadt, Germany) and stored in a refrigerator. At the end of the experiment the cells were stained with 0.02 % crystal violet (Serva, Heidelberg, Germany) simultaneously. Plates were rinsed with water to remove excess dye, and cell-bound crystal violet was extracted with 70 % ethanol for three hours under shaking.

Subsequently, absorbance was measured at 578 nm using a Biotek 309 Autoreader (Tecnomara, Fernwald, Germany). Absorbance values were transformed into corrected T/C values expressing the net growth of the treated cells, relative to the growth of the solvent control; according to T/C_{corr} (%) = 100 · (T – C_0)/(C – C_0), where T is the absorbance of the treated cells, C the absorbance of the controls and C_0 the absorbance of the cells at the time, when drug was added. T/C_{corr} values at the various time points were plotted against the incubation time using SigmaPlot version 11.0. In **Fig. 2** a diagrammatic representation of typical data obtained with the crystal violet assay is depicted. The correction for the initial cell number allows discrimination between cytostatic and cytocidal drug action.

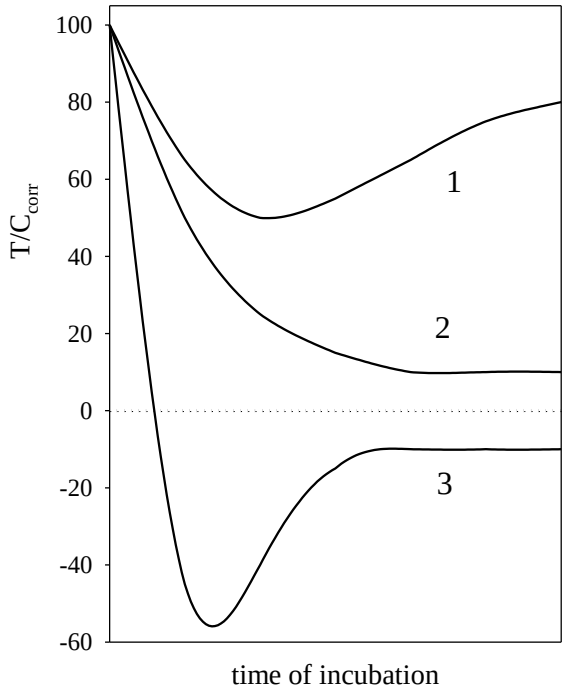

Fig. 2: Schematic diagram illustrating the in vitro response of cells to chemotherapeutics. 1: the population recovers after initial damage (cytotoxic drug effect), 2: cell proliferation is inhibited (cytostatic drug effect), 3: disintegration of the cells (cytocidal drug effect)

3 Results and discussion

3.1 Chemosensitivity of triple negative breast cancer cells

The potential activity of lobaplatin against triple-negative breast cancer was investigated. Cisplatin and carboplatin were used as standard platinum drugs to compare the chemosensitivities of the different breast cancer cell types using the kinetic crystal violet assay.

The human triple-negative breast cancer cell lines were about 10-fold more sensitive against the platinum drugs as the other cell lines tested. As expected, MDA-MB-231 cells turned out to be the most resistant against the platinum compounds. This cell line was previously shown to be insensitive against cisplatin (Bernhardt et al., 1992; Zhou et al., 2011) at therapeutically relevant concentrations.

In **Fig. 3** the results of the chemosensitivity assay are shown. For cisplatin and lobaplatin a cytotoxic effect against HCC-1806 and HCC-1937 was observed at a concentration of 0.3 µM, whereas in case of the other cell lines a concentration of 1–3 µM was needed (data not shown). These findings are consistent with the work of Sirohi et al., who revealed higher response rates to platinum based therapy for TN tumours compared to other types of breast cancer in a retrospective study (Sirohi et al., 2008). Carboplatin was found to be less potent than cisplatin and lobaplatin, respectively. In case of the human TN cell lines a concentration of 10 µM was required to obtain a cytotoxic effect. Apparently, the highest effects of the drugs became obvious with HCC-1937 cells, which were shown to have the BRCA1 mutation (Tomlinson et al., 1998).

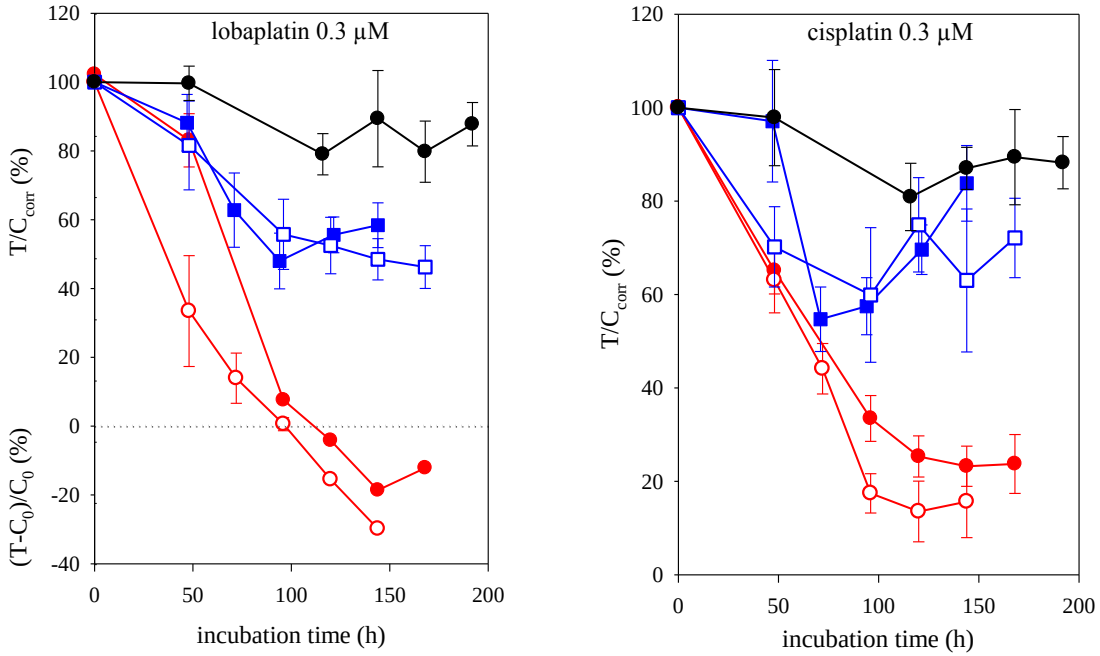

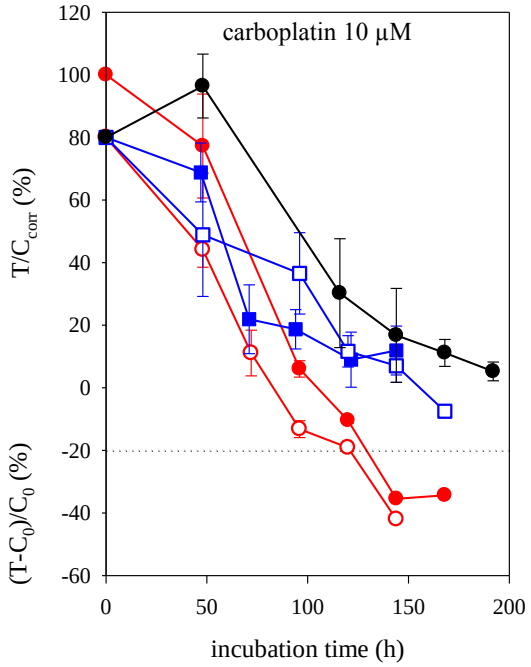

Fig. 2: *In vitro* treatment of various human breast cancer cell types with platinum drugs. Plots of corrected T/C values versus time determined in the kinetic crystal violet assay. ● MDA-MB-231, ■ MCF-7, □ T-47-D, ● HCC-1806, ○ HCC-1937

Additionally, the TN breast cancer cell types HCC-1806 and HCC-1937 were tested for their chemosensitivity against various other chemotherapeutics. With vinblastin and doxorubicin two classical cytostatic drugs were used. Furthermore, the classical antiestrogen tamoxifen and the estrogen receptor antagonist fulvestrant were used to demonstrate their ineffectiveness against TN cancers.

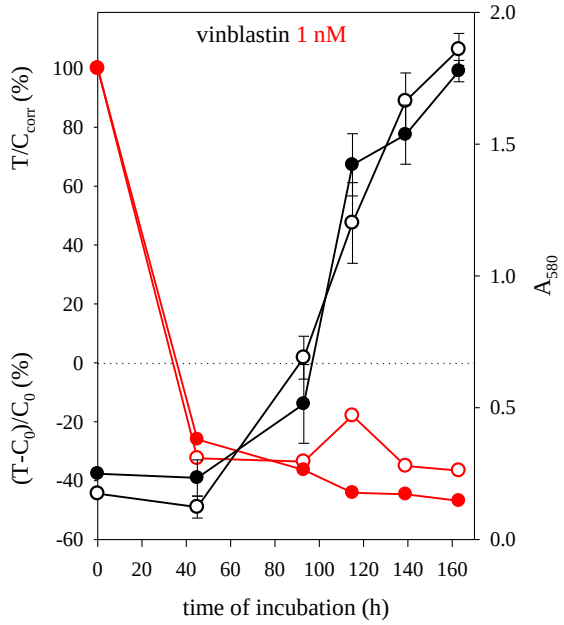

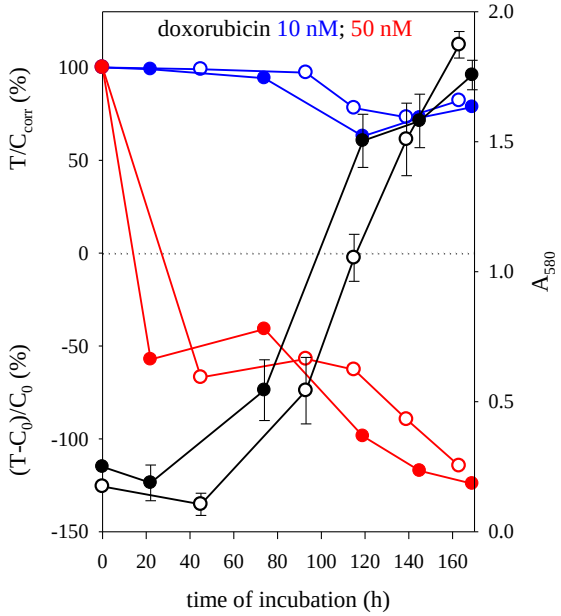

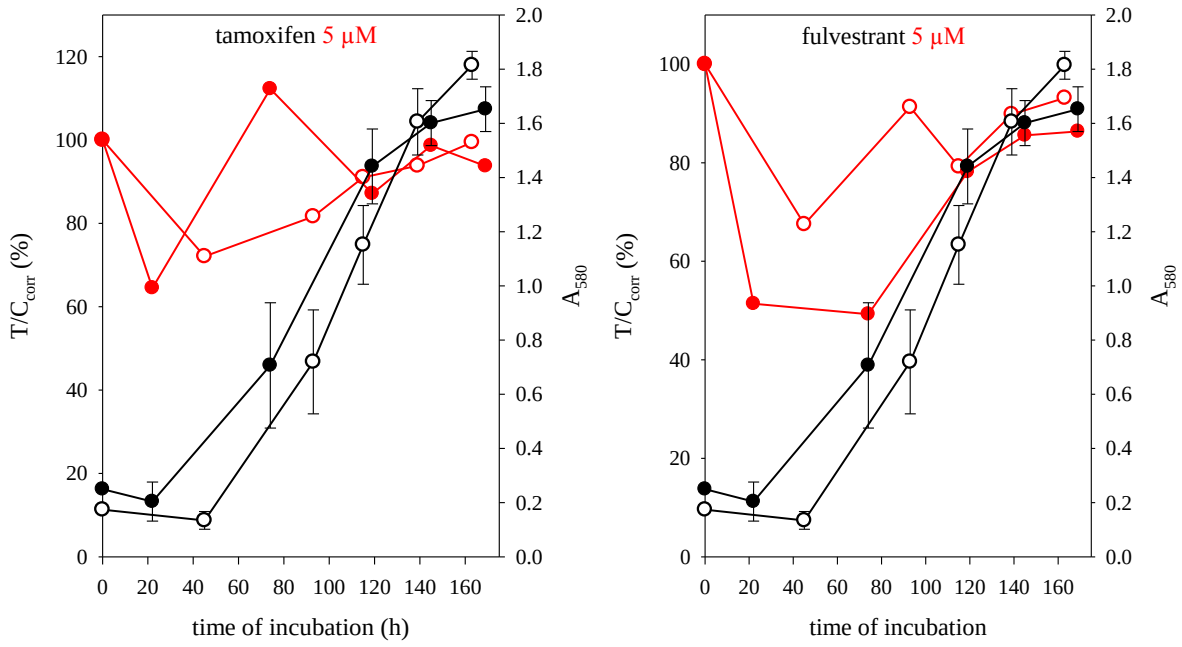

Fig. 4: *In vitro* treatment of TN breast cancer cell types with various cytostatic drugs. Plots of corrected T/C values versus time, determined in the kinetic crystal violet assay. ○ HCC-1937; ● HCC-1806; ○ growth curve solvent control HCC-1937; ● growth curve solvent control HCC-1806

3.2 Tumorigenicity and histology of HCC-1806 and HCC-1937 tumors

In order to evaluate the tumorigenicity of HCC-1806 and HCC-1937, the TN breast cancer cells were injected into nude mice and the growth of subcutaneous xenografts was determined once a week. As shown in **Fig. 4**, both cell types were highly tumorigenic.

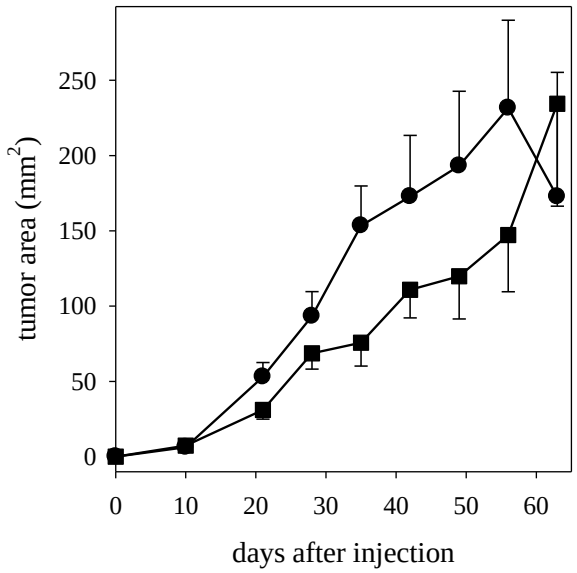

Fig. 4: *In vivo* growth curves of subcutaneous HCC-1806 (●) and HCC-1937 (■) xenografts. Data points are mean values ± SEM of 8 animals.

The subcutaneous solid xenografts formed by TN breast cancer cells were excised and characterized histologically. Both tumors showed poor differentiation, with cells containing prominent pleomorphic vesicular nucleoli. Typical for cancer cells there was an increased ratio of nucleus to cytoplasm. Furthermore, a high number of mitotic figures with abnormal mitotic spindles and fragments of condensed chromatin were observed. Both xenografts displayed a very low grade of tubule formation. In addition, the HCC-1937 tumor exhibited necrotic areas (**Fig. 5**). In summary, both anaplastic tumors are classified as grade 3 according to the breast cancer grading criteria of Elston and Ellis (Elston and Ellis, 1991).

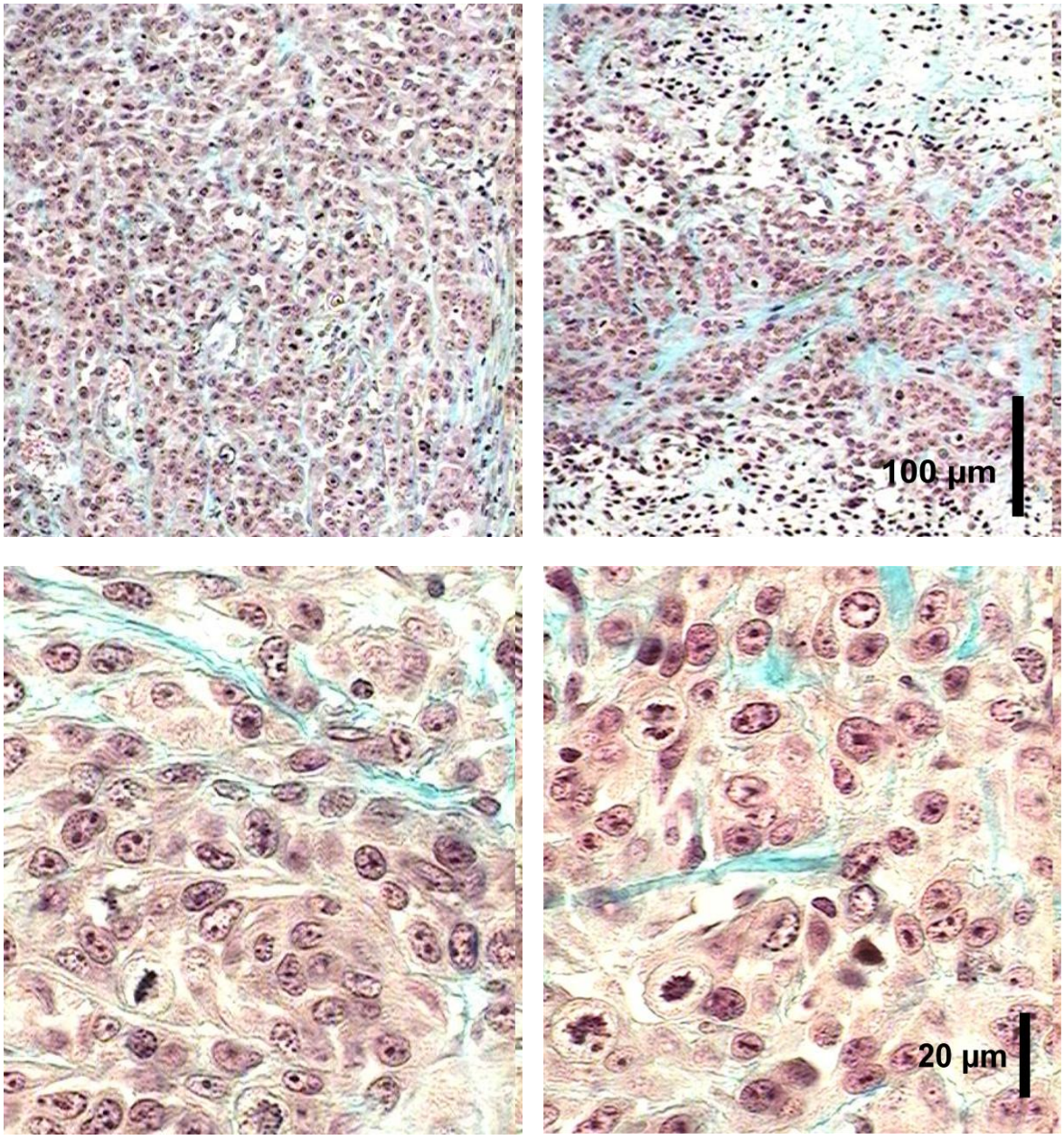

Fig. 5: Masson-Goldner staining of subcutaneous tumors originating from HCC-1806 (left) and HCC-1937 (right) cells

4 Summary

There is need for new anti-cancer drugs in the treatment of patients suffering from TN breast cancer phenotype, since no targeted therapy is available and because several studies have demonstrated that a poor prognosis is associated with the TN phenotype (Bauer et al., 2007; Sorlie et al., 2003; Tan et al., 2008). The role of platinum compounds was considered in TN tumors taking into account their mechanism of action and the potential DNA changes in these tumors, which are phenotypically and molecularly similar to tumors bearing the BRCA1 mutation. DNA repair defects may be adequate targets for alkylating agents. There are many ongoing trials in adjuvant, neoadjuvant and metastatic settings: carboplatin versus docetaxel (NCT00532727), gemcitabine plus cisplatin (NCT00601159), and gemcitabine plus oxaliplatin (NCT00674206) are some examples (Chacon and Costanzo, 2010).

In this study, cytotoxic activity of the third-generation platinum drug lobaplatin against triple-negative breast cancer cell types was compared to the standard platinum-based drugs cisplatin and carboplatin. Lobaplatin proved to be as effective as cisplatin in these *in vitro* studies against TN cancer cell lines.

In addition, the *in vivo* growth of TN tumors after injecting HCC-1806 and HCC-1937 cells into nude mice was monitored. Both cell types displayed a high tumorigenicity. Histological investigations revealed that both the TN tumors were anaplastic and could be classified as tumors of the highest grade 3.

5 References

Bauer, K.R., Brown, M., Cress, R.D., Parise, C.A., Caggiano, V., 2007. Descriptive analysis of estrogen receptor (ER)-negative, progesterone receptor (PR)-negative, and HER2-negative invasive breast cancer, the so-called triple-negative phenotype: a population-based study from the California cancer Registry. Cancer 109, 1721-1728.

Bernhardt, G., Reile, H., Birnbock, H., Spruss, T., Schoenenberger, H., 1992. Standardized Kinetic Microassay to Quantify Differential Chemosensitivity on the Basis of Proliferative Activity. J. Cancer Res. Clin. Oncol. 118, 35-43.

Byrski, T., Huzarski, T., Dent, R., Gronwald, J., Zuziak, D., Cybulski, C., Kladny, J., Gorski, B., Lubinski, J., Narod, S.A., 2009. Response to neoadjuvant therapy with cisplatin in BRCA1-positive breast cancer patients. Breast Cancer Res. Treat. 115, 359-363.

Chacon, R.D., Costanzo, M.V., 2010. Triple-negative breast cancer. Breast Cancer Res. 12 Suppl 2, S3.

Cleator, S., Heller, W., Coombes, R.C., 2007. Triple-negative breast cancer: therapeutic options. Lancet Oncol. 8, 235-244.

Elston, C.W., Ellis, I.O., 1991. Pathological Prognostic Factors in Breast-Cancer .1. The Value of Histological Grade in Breast-Cancer - Experience from a Large Study with Long-Term Follow-Up. Histopathology 19, 403-410.

Gietema, J.A., Veldhuis, G.J., Guchelaar, H.J., Willemse, P.H., Uges, D.R., Cats, A., Boonstra, H., van der Graaf, W.T., Sleijfer, D.T., de Vries, E.G., et al., 1995. Phase II and pharmacokinetic study of lobaplatin in patients with relapsed ovarian cancer. Br. J. Cancer 71, 1302-1307.

McKeage, M.J., 2001. Lobaplatin: a new antitumour platinum drug. Expert Opin. Investig. Drugs 10, 119-128.

Müller, C., 2007. New approaches to the therapy of glioblastoma: investigations on RNA interference, kinesin Eg5 and ABCB1/ABCG2 inhibition, Doctoral thesis, University of Regensburg.

Sirohi, B., Arnedos, M., Popat, S., Ashley, S., Nerurkar, A., Walsh, G., Johnston, S., Smith, I.E., 2008. Platinum-based chemotherapy in triple-negative breast cancer. Ann. Oncol. 19, 1847-1852.

Sorlie, T., Tibshirani, R., Parker, J., Hastie, T., Marron, J.S., Nobel, A., Deng, S., Johnsen, H., Pesich, R., Geisler, S., Demeter, J., Perou, C.M., Lonning, P.E., Brown, P.O., Borresen-Dale, A.L., Botstein, D., 2003. Repeated observation of breast tumor subtypes in independent gene expression data sets. Proc. Natl. Acad. Sci. U. S. A. 100, 8418-8423.

Tan, D.S., Marchio, C., Jones, R.L., Savage, K., Smith, I.E., Dowsett, M., Reis-Filho, J.S., 2008. Triple negative breast cancer: molecular profiling and prognostic impact in adjuvant anthracycline-treated patients. Breast Cancer Res. Treat. 111, 27-44.

Tomlinson, G.E., Chen, T.T., Stastny, V.A., Virmani, A.K., Spillman, M.A., Tonk, V., Blum, J.L., Schneider, N.R., Wistuba, II, Shay, J.W., Minna, J.D., Gazdar, A.F., 1998. Characterization of a breast cancer cell line derived from a germ-line BRCA1 mutation carrier. Cancer Res. 58, 3237-3242.

Turner, N., Tutt, A., Ashworth, A., 2004. Hallmarks of 'BRCAness' in sporadic cancers. Nat. Rev. Cancer 4, 814-819.

Widakowich, C., de Azambuja, E., Gil, T., Cardoso, F., Dinh, P., Awada, A., Piccart-Gebhart, M., 2007. Molecular targeted therapies in breast cancer: where are we now? Int. J. Biochem. Cell Biol. 39, 1375-1387.

Zhou, F.F., Yan, M., Guo, G.F., Wang, F., Qiu, H.J., Zheng, F.M., Zhang, Y., Liu, Q., Zhu, X.F., Xia, L.P., 2011. Knockdown of eIF4E suppresses cell growth and migration, enhances chemosensitivity and correlates with increase in Bax/Bcl-2 ratio in triple-negative breast cancer cells. Med. Oncol. 28, 1302-1307.

Ich erkläre hiermit an Eides statt, dass ich die vorliegende Arbeit ohne unzulässige Hilfe Dritter und ohne Benutzung anderer als der angegebenen Hilfsmittel angefertigt habe; die aus anderen Quellen direkt oder indirekt übernommenen Daten und Konzepte sind unter Angabe des Literaturzitats gekennzeichnet.

Regensburg,

Janina Hamberger